Cognitive Radio: Energy Sensing Analysis and Dynamic Spectrum Access modeling

by

Omar Altrad

M.Sc., New York Institute of Technology, 2008

B.Sc., Mutah University, 1996

A Thesis submitted in partial fulfillment
of the requirements for the degree of

Doctor of Philosophy

in the
School of Engineering Science
Faculty of Applied Sciences

SIMON FRASER UNIVERSITY
Fall 2013

APPROVAL

Name:	Omar Altrad
Degree:	Doctor of Philosophy
Title of Thesis:	Cognitive Radio: Energy Sensing Analysis and Dynamic Spectrum Access modeling
Examining Committee:	Dr. Carlo Menon Chair
	Dr. Jie Liang, Associate Professor, Senior Supervisor
	Dr. Sami Muhiadat, Assistant Professor, Supervisor
	Dr. Bozena Kaminska, Professor, SFU Examiner
	Dr. Walaa Hamouda, Associate Professor, Concordia University External Examiner
Date Approved:	November 25th, 2013

Partial Copyright Licence

Abstract

Efficient utilization of the spectrum has become a fundamental requirement in modern wireless networks, due mainly to spectrum scarcity and the ever-increasing demand for higher data rate applications and internet services. A particularly interesting proposal to meet this requirement is the cognitive radio (CR) system which can adapt its transmission parameters according to the environment. CRs, as will be shown in later chapters, are very efficient in maximizing spectrum utilization due to their inherent spectrum sensing capability.

The purpose of this dissertation is to investigate and analyze two main components of CR. First is the sensing or exploring component, which is the core of a CR device as it is the first stage to discover spectrum holes (SHs) in a spectrum band. For this component, a new algorithm to compute the detection probability in the case of odd degrees of freedom and a closed-form expression for the detection probability in Nakagami-m fading channels are presented, both for a local spectrum sensing scenario. For a cooperative scenario, the errors of CRs decisions which are caused by erroneous feedback channels are analyzed. In addition, the optimal number of CRs that are required to mitigate against such errors is derived. The second component is the access or exploiting component, i.e. how a CR device can exploit SHs efficiently. To study the second component, the interactions between the primary users (PUs) and secondary users (SUs) are modeled as a continuous time Markov chain (CTMC). Based on the CTMC model, the effect of two inevitable sensing errors (misdetection and false alarm) on the blocked call probability, the dropped call probability and system utilization is investigated for two access schemes. In the first scheme, the PUs are considered to access the system using a standard access policy. In the second scheme, the PUs use non-standard access policies. In both schemes, the overall (primary and secondary) system utilization is analyzed and compared under both perfect and imperfect sensing. The simulation results

obtained concur with the analytical ones and it is determined that spectrum utilization can be improved by choosing a suitable non-standard access policy.

"No matter how long it takes, definitely there is a happy end"

Omar Altrad

Acknowledgements

I would like to thank Prof. Sami Muhaidat for his direction and support. I am thankful for being benefited from the one who initiated the sparks of good ideas in my mind. He helped me with building up a strong foundation for my future scholarly career. I am really thankful for his supports. I would like to thank him for standing up for me and my future compassionately, looking for great opportunities for me.

I would like to thank Prof. Jie Liang for his kindness and support. He helped me a lot when I needed help. I would also like to thank my external examiner Prof. Walaa Hamouda, and the session chair for my defense Prof. Carlo Menon.

I also express my gratitude to the internal examiner Prof. Bozena Kaminska. I learned from her that I have to be organized, precise and smart to be a good academic scholar. I would like to thank her for standing up for me and my future compassionately.

I would like to thank all of my friends and colleagues in SFU and everywhere who supported me directly or indirectly during my PhD.

At last I would like to express my immense gratitude and respect to my mother, my lovely wife Nour, my daughters Rasha, Saja and Hala, and my sons Jawad and Hashem who, through their devotion and dedication, allowed me to continuously burn the midnight oil. A tedious project such as this could have never come to fruition without the support, understanding, and encouragement they provided me all during the preparation of this dissertation.

Contents

List of Figures

List of Symbols

X	random variable X
H_1	existence of a PU
H_0	absence od a PU
χ^2_N	central chi-squared distribution with N degrees of freedom
$\tilde{\chi}^2_N$	none-central chi-squared distribution with N degrees of freedom
$\mathrm{E}\{\cdot\}$	Expected value
$\sim$	denotes *is distributed according to*
$\mathcal{CN}(0,\sigma^2)$	Complex Gaussian random variable with zero mean and variance of σ^2
$\mathcal{N}(0,\sigma^2)$	Gaussian random variable with zero mean and variance of σ^2
$f_X(\cdot)$	PDF of random variable X
$F_X(\cdot)$	CDF of random variable X
P_{fa}	probability of false alarm
P_d	probability of detection
P_{Nak}	probability of detection under Nakagami fading channel
$P_{d_{Ray}}$	Probability of detection under Rayleigh fading channel
P_m	probability of misdetection
N_0	receiver noise
h	channel fading cooefficient
$x[n]$	the nth sample of the received signal
$s[n]$	the nth sample of a primary user signal
$w[n]$	the nth sample of the AWGN.
$I_r(.)$	rth-modified Bessel function of the first kind
Q_{χ^2}	the right-tail probability of the central chi-squared density function
$Q_{\tilde{\chi}^2_{(.)}}$	the right-tail of the noncentral chi-squared probability density function

$Q(.)$	the complementary cumulative distribution function
$Q_m(.,.)$	the mth generalized Marcum Q-function
$\gamma^*(.,.)$	the lower incomplete gamma function
$\bar{M}(.)$	the bit complexity of multiplication
$\bar{\gamma}$	the average signal-to-noise ratio
$J(.)$	total error (sum of misdetection and false alarm)
$O(.)$	computational complexity
B	the time bandwidth product
λ_p	arrival rate of PUs
λ_s	arrival rate of SUs
$1/\mu_p$	mean service time for PUs
$1/\mu_s$	mean service time for SUs
C	number of channels in the system
$P(i,j)$	the steady-state probability of state i,j
$\mathbf{Q}$	the infinitesimal generator matrix
$\mathbf{p}$	the steady-state probability vector
T	indicates the transpose operation
N_{oc}	the total occupied channels
N_{av}	the total available channels
$\binom{n}{m}$	$\frac{n!}{m!(n-m)!}$
$\Pr(.)$	denotes *probability of(.)*
ρ	traffic load $\rho = \lambda_s/\mu_s$
Π_1 and Π_2	non-standard access PU policies 1 and 2
$\lvert \cdot \rvert$	Absolute value

List of Acronyms

CR	Cognitive Radio
SDR	Software Defined Radio
DSP	Digital Signal Processor
GPM	General-Purpose Microprocessors
CRN	Cognitive Radio Network
GoS	Grade of Service
DSA	Dynamic Spectrum Access
OSA	Opportunistic Spectrum Access
PU	Primary User
SU	Secondary User
PN	Primary Network
QoS	Quality of Service
ISM	Industrial, Scientific, and Medical
FCC	Federal Communication Commission
MAC	Medium Access Control
CTMC	Continuous Time Markov Chain
AWGN	Additive White Gaussian Noise
SH	Spectrum Hole
SNR	Signal-to-Noise Ratio
ROC	Receiver Operation Characteristics
LNA	low noise amplifier
A/D	Analogue-to-Digital
CPU	central processing unit
CTS	Clear-to-Send

MRC	Maximum Ratio Combiner
PDF	Probability Density Function
PSK	Phase Shift Keying
TDMA	Time Division Multiple Access

Chapter 1

Introduction

1.1 Overview

Cognitive radio (CR) is a term coined by Mitloa [1] in 1991 to represent a paradigm in communication systems in which communication improvements can, in many aspects, be achieved via cognition. CR is a broad and versatile term as it neither determines a specific network architecture nor determines the level at which a system would be classified as a full cognitive radio system. Therefore, the word "cognition" has been viewed and interpreted differently by various researchers when classifying radio systems. Software-defined radio (SDR), however, a multiband radio that has the ability to reconfigure itself through software which runs on a digital signal processor (DSP) or a general-purpose microprocessor (GPM), can be seen as the core of a CR.

The term "CR" is defined as

> *"an intelligent wireless communication system that is aware of its surrounding environment (i.e., outside world), and uses the methodology of understanding-by-building to learn from the environment and adapt its internal states to statistical variations in the incoming RF stimuli by making corresponding changes in certain operating parameters (e.g. transmit-power, carrier-frequency, and modulation strategy) in real-time."*

[2]

Why has CR emerged? What is the main goal that CR is to achieve? The answer to these questions can be found in the many research papers that investigate the development of and strive to improve the main functions of cognitive radio networks (CRNs). The question most seek to answer is how we can efficiently elevate spectrum utilization. Or how can white spaces be found and used to reduce spectrum scarcity and enhance spectrum utilization? The static allocation of frequency bands and their under-utilization motivates regulatory authorities, business sectors, and researchers to look for a dynamic approach to reduce spectrum scarcity. Hence, this dissertation is researching practical solutions to an existing problem. In a CRN environment, different users can be categorized as primary users (PUs) or so-called license holders (often called spectrum owners), representing users having higher priority, and secondary users (SUs) or so-called unlicensed users (often called rental users), representing those users who are wishing to opportunistically access the spectrum by sensing the channels already in use for transmissions. CR thus brings invaluable benefits for both spectrum owners and rental users. For example, spectrum owners can increase their sources of revenue by selling the unused portion of their owned spectrum while rental users now have the chance to access a new range of the spectrum that they have not hitherto been allowed to use, which results in increasing their grade-of-service (GoS) to their own users.

Although some communities have different names for CR as well as for its applications, for example spectrum pooling, dynamic spectrum access (DSA) and opportunistic spectrum access (OSA), the idea behind it does not change. That is, different spectral ranges owned by different owners are merged into a common pool. The classification of this technology and other related naming issues, then, are not of concern in this dissertation but interested readers may refer to [3–5] for further clarification.

DSA is, however, considered to be an application of a CR system. This means a secondary radio network (SN) coexists on the same band as a primary network (PN), in which the former does not necessarily utilize only the PN's band as it may also have its own band of operation. In addition, to increase the quality of service (QoS) to its own users it may also utilize other PNs' bands.

It should be noted that in DSA, the access mechanism can be classified in a hierarchal

way, as in Fig. 1.1. When the SUs opportunistically access the spectrum, this access mechanism is called spectrum overlay access or opportunistic spectrum access (OSA). The core function of this access method to sense the PU channel so as to find opportunities for an SU transmission. This access method does not impose severe restrictions on the transmission power of the SUs. However, when SUs access the spectrum simultaneously with the PUs, this is called underlay spectrum access. In this access method the SUs can transmit simultaneously with the PU if they allow their transmission power to be severely constrained. Further, while using this access method, SUs do not rely on the detection and exploitation of spectrum white spaces. To add more flexibility and improve system cognition, combined access utilizing both methods can also be considered which may be called hybrid dynamic spectrum access. However, although this last method adds more flexibility, it considerably increases system complexity as more complex protocols need to be implemented to protect the PUs.

It should also be emphasized that the taxonomy of this technology is not of concern in this dissertation. Therefore, throughout this dissertation the spectrum overlay or OSA system as the basic concept behind CR technology will be concentrated on. In addition, for the purpose of this dissertation, whenever the term 'DSA' is used, it means the spectrum overlay access mechanism or OSA.

It is also worth mentioning that throughout this dissertation, the main concerns are the technical issues and/or the obstacles and challenges that arise when implementing such technology. Therefore, although allowing this concept to be implemented in real systems will result in a multitude of judicial issues and economic consequences, they are not of concern in this dissertation.

To inform readers more about the reasons behind the emergence of CR, the following sections provide more detailed answers to the above questions.

1.1.1 Spectrum Occupancy Measurements

As more and more technological alternatives, such as smart phones and video streaming, are becoming available and the demand for spectrum from both the public and private sectors is increasing very rapidly, the need to ensure access to the radio spectrum is at

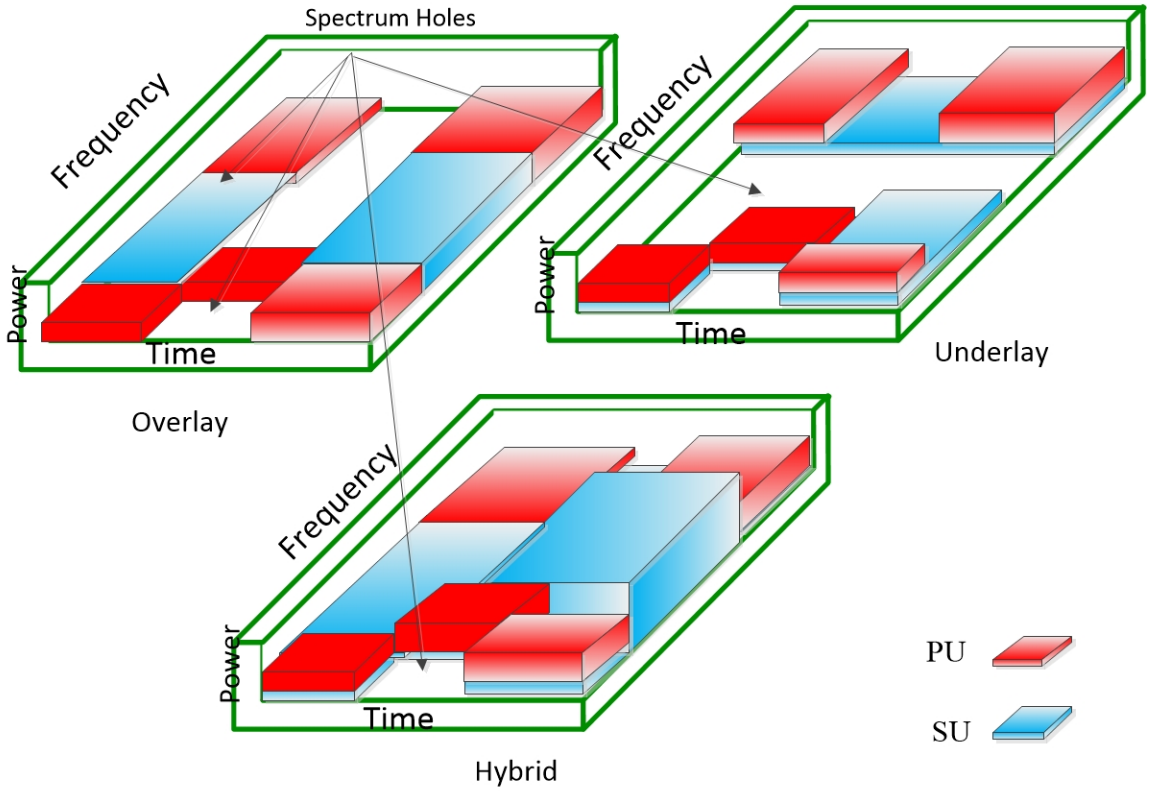

Figure 1.1: Illustration of spectrum holes utilization by SUs in cognitive radio system.

a crossroads. Fortunately, recent studies have revealed that most existing allocations are under-utilized. For example, it has been reported by the Federal Communication Commission (FCC) that although some frequency bands (e.g. unlicensed bands at 2.4 Ghz and 5 Ghz) are overcrowded, others (e.g. the UHF band) are inefficiently used. Another spectrum measurement performed in Lichenau, Germany, in 2001 showed that some of the frequency bands are only sporadically occupied. Other spectrum occupancy measurements performed by the Shared Spectrum Company in conjunction with the Wireless Interference Lab of the Illinois Institute of Technology in Chicago also showed that various frequency bands have different levels of occupancy and that some of them are under-utilized. Increasingly, there is a recognition that most of the spectrum is actually under-utilized and that the real root of the problem is that the present system of spectral regulation is grossly inefficient, (see Fig. 1.2) [6]).

The discontinuous use of the spectrum means that a large portion of spectrum is currently wasted. The shortage of the spectrum in some frequency bands, however, could easily be solved by efficiently utilizing the wasted resources in other bands of the spectrum. The dramatic variation of spectrum usage over time and geographic location has motivated the FCC to improve overall utilization by facilitating new wireless applications and has also motivated the emergence of the CR system.

To summarize, the main objective of CR systems is the efficient utilization of the spectrum. Therefore, an accurate design for a CRN working under a licensed PN needs to be considered. While the CRN may have its own frequency band of operation, it can also utilize the spectrum holes (SHs) or so called white spaces in frequency bands of the PN to increase its performance and to provide a higher QoS to its users. It is then considered to be a secondary network relative to the primary network.

1.1.2 Cognitive Radio Network architecture

CRN architecture is not different from other network architectures. For example, in a centralized architecture (with infrastructure), users, base stations, and other nodes in the hierarchy must exist to form a CR network. Even for other types of architectures, the role of a controller or a base station must exist. For example, in a fully distributed ad hoc network (without infrastructure), an intelligent protocol acts as the controller while in a

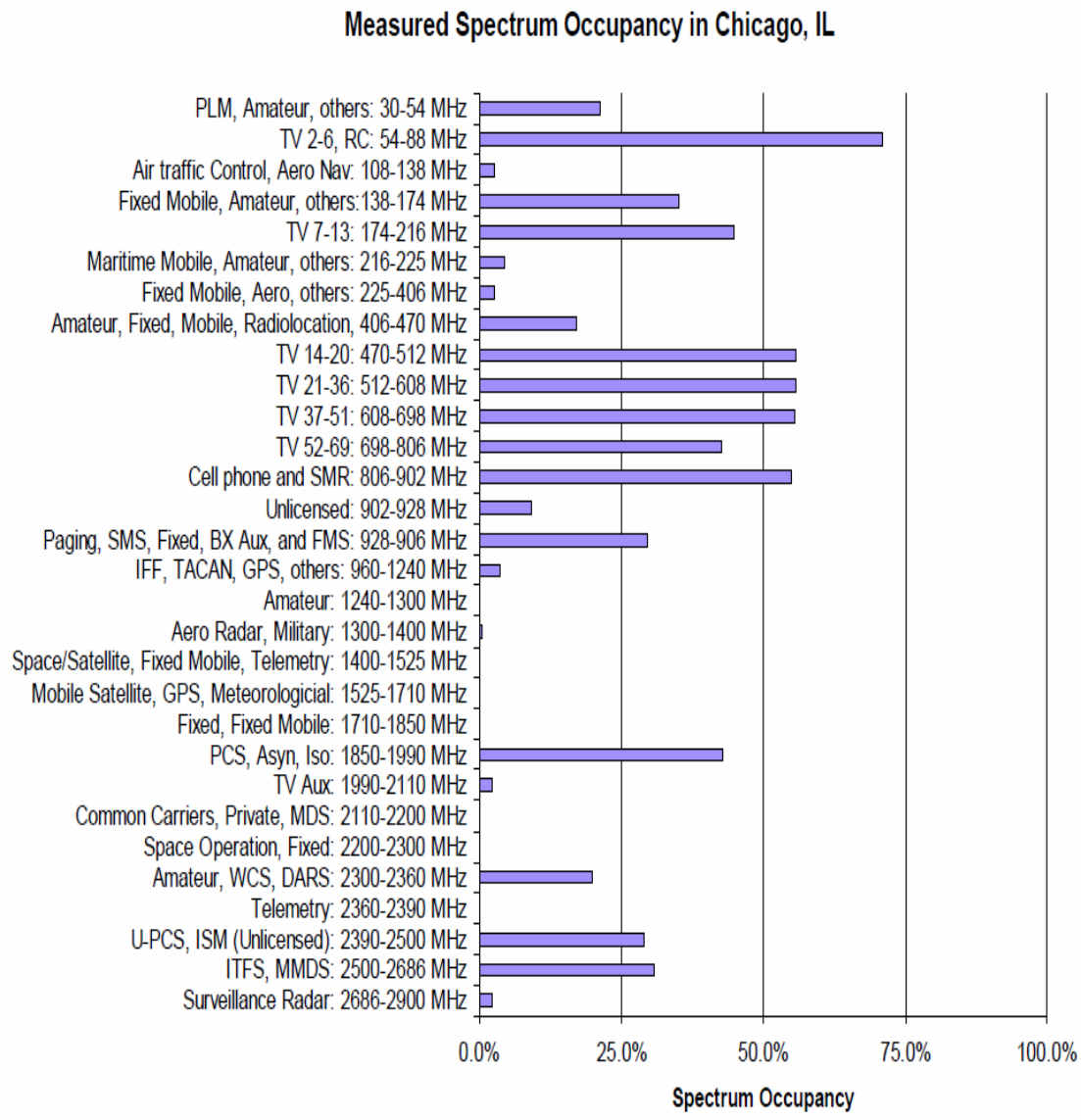

Figure 1.2: Spectrum occupancy of each band measured in Chicago [6].

semicentralized network or so-called mesh network (a combination of the two architectures, i.e. a centralized one and a distributed one), more than one user in a geographic area plays the role of controller and other users play the role of relays to improve signal reception, mitigate against any type of fading, and improve the overall performance of the network.

A visible CR architecture may consist of two networks. One is the legacy network or primary radio network (for example TV channels or some cellular provider networks), wherein the users are free to transmit and receive their data anywhere and/or anytime within the defined band they are legally assigned. The other is the CRN (for example, another cellular provider), wherein the users utilize their own band in addition to accessing the SHs in other PNs. Therefore, fundamentally a CRN is not different in its architecture from any other network system. There are thus three main architectures in this network system, namely: centralized, ad hoc or decentralized and mesh network, (see Fig. 1.3. [7]).

1.2 Cognitive Radio challenges

A number of issues must be resolved before starting the design of a CR system to achieve the goals of spectrum utilization. One is that the CRN must have the ability to sense more than one frequency band to guarantee a QoS threshold. Another issue is that the CRN must ensure that it does not impose any interference on the PN. These issues mean that the CRN must have periodic sensing and fast processing abilities to efficiently use the primary networks' SHs. The fast processing requirement is due to the fact that the primary network may use its resources at any time without informing the CRN; as a result, the CRN must be prepared to vacate the channels it is using and still guarantee an uninterrupted transmission to its users by handing them over to other SHs. This also means that a highly-reliable sensing function must be implemented in the CRN's terminals. In other words, the receiver sensitivity of the CR terminal must be as high as possible to detect the presence or absence of a PU signal.

Therefore, one of the challenges arising from DSA is spectrum sensing, which is the core of such a system as it determines the validity of a transmission opportunity. There is a

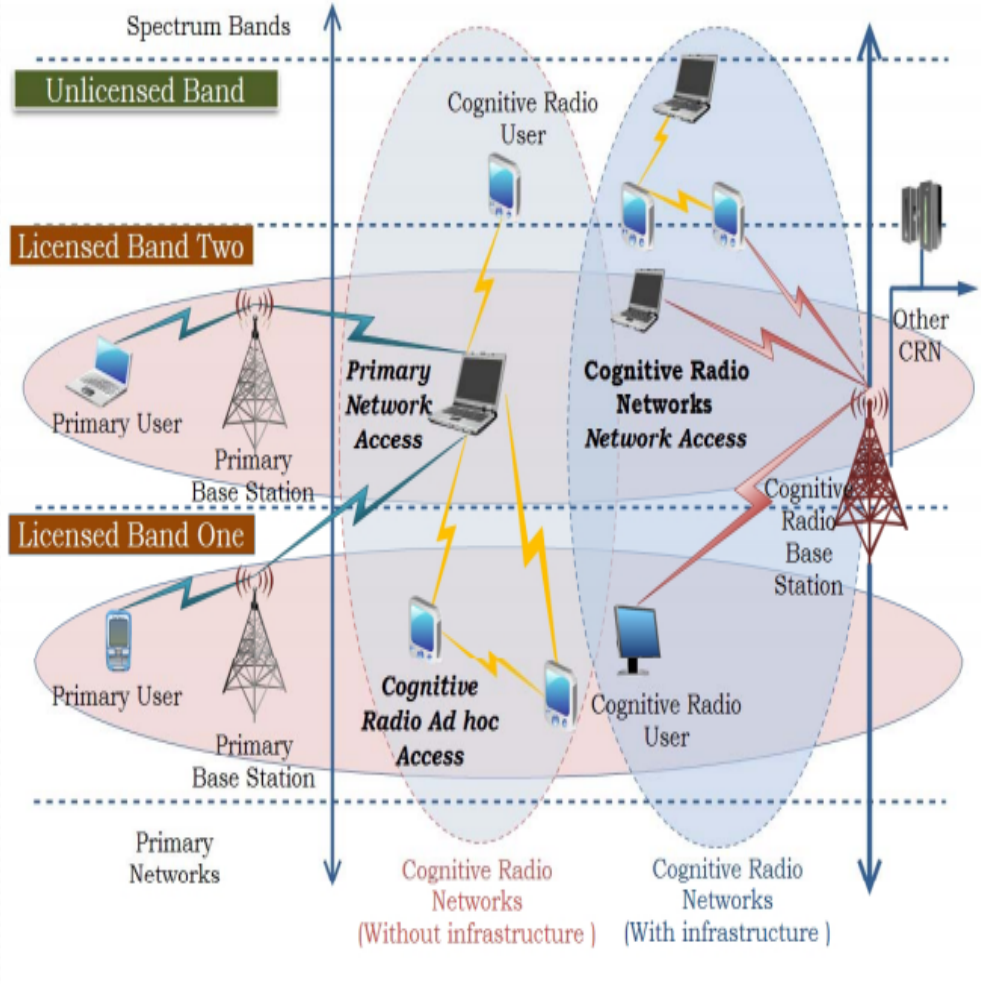

Figure 1.3: CRN architecture [7].

trade-off, however, between reliability and efficiency. The more robust the sensing algorithm, the more reliable the CRN and the lower the amount of interference it may cause to the PN. However, robustness and reliability require a long sensing period whereas the shorter the sensing time, the more efficient the utilization of a spectrum hole will be.

However, even once a reliable sensing function is in place, that will not guarantee an efficient use of SHs. Hence, another issue arises, that is, how the SHs can be efficiently utilized. This requires a careful design of the medium access control (MAC) protocol. In this dissertation, these issues will be visited in order and a tractable solution to the problems that, so far, have not been investigated, will be explored in more detail. The following section outlines what has been accomplished works and the development of this dissertation.

1.3 Thesis Outline and Main Contributions

The following are the main issues that will be analyzed and investigated throughout the dissertation.

Chapter 2 of the thesis deals with local spectrum sensing. In particular, a single CR that senses the available spectrum is investigated. The following is a summary of the main contributions that will be presented in chapter 2.

- A highly accurate recursive algorithm to compute the probability of detection for odd degrees of freedom is presented. It should be noted that the mathematical derivations show the steps of the algorithm when evaluating the detection probability in the case of odd degrees of freedom, i.e. it is an algorithm rather than a mathematical derivation. An example of the algorithm's importance is that the Marcum function in Matlab accepts only integer values in its third argument. Therefore, when the number of degrees of freedom is odd, the third argument is no longer accepted and the Marcum function can not be used to evaluate the detection probability. However, the presented algorithm solves this problem;

- a closed-form expression over a Nakagami-m fading channel is derived. Closed-form is used in the sense that no summation and no integration are required. The accuracy of the closed-form is very close to the previously reported expressions in which summation

and integration are used to get highly accurate results. Our new expressions show how the ratio of the Nakagami parameter m and the average signal-to-noise ratio (SNR) affect the receiver operating characteristics (ROC) curves;

- a comparison between the derived expressions and the reported expressions in [8] and [9], in which summation and integration are used, is performed. The derived expressions are also compared to other recently reported expressions, e.g., [10] and [11], and it is shown that the new derived expressions can be used with no limitations. Moreover, the derived expressions are more accurate than the recently reported ones with less or almost the same computational complexity.

In chapter 3, a cooperative scenario is investigated, i.e. a scenario where a number of CRs are involved in the sensing process and their decisions are forwarded to a central node over a feedback channel. In particular, the optimal number of CRs required to minimize the total error (the sum of the misdetection and false alarm probabilities) of the sensing process when the reporting channel is perfect/imperfect will be analyzed. The following is a summary of the main contributions in chapter 3:

- The total error is shown to have a global minimum. However, such an error will never approach zero, no matter how many CRs participate in the cooperative sensing process;
- a general expression for the optimal number of CRs under a perfect or an imperfect feedback channel is derived;
- the upper and lower boundary expressions for the probability of false alarms are derived;
- it is shown that the optimal number of cognitive radios can easily overcome a high error probability in the feedback channel and can therefore improve the detection probability. Feedback channel errors are also shown to be able to improve the detection probability under low SNR regimes.

Chapter 4 deals with the mathematical modeling of an OSA using a continuous time Markov chain (CTMC). Specifically, the CTMC will be used to model the combined networks of the

PUs or so called license holders, and the secondary users, i.e., those who opportunistically access the unused portion of the spectrum. A standard access policy will be used for the PUs and the effect of imperfect sensing on the performance of the system will be investigated. A number of performance metrics will be analyzed and the secondary system spectrum utilization under perfect/imperfect sensing will be studied.

Is it possible to improve spectrum utilization using different access policies? In other words, can the spectrum utilization of the combined system (primary and secondary systems) be increased without increasing the detection probability? Additional access policies are proposed and their performances are analyzed under an unreliable sensing scenario. Investigating this issue will be the main objective of chapter 5. The analysis will be in terms of the SUs blocked probability, which is defined as the ratio of SUs blocked to the total arrival rate of the secondary system, as well as the SUs dropped probability, which is defined as the ratio of the dropped SUs to the total arrival rate of the secondary system, and the total utilization of the secondary system. The analysis of such policies will also show the upper boundary of spectrum utilization that can be obtained. Furthermore, the utilization of the secondary system when both standard policy and non-standard policies are employed is compared. The contributions in this chapter are summarized by the following:

- Two non-standard policies are modeled and analyzed using a CTMC where imperfect sensing is accounted for. The standard policy is determined to be a special case of one of them.
- The access probability for an SU sensing all channels is accounted for.
- It is shown that adopting different policies results in different system utilizations. Therefore, a dynamic policy may help to improve the spectrum utilization of detected SHs over the standard policy, and increase the accepted range of SU arrival rates that will still satisfy GoS constraints.
- With a focus on a general system architecture where PUs and SUs access available channels using different policies, the performance of the proposed policies is justified in terms of GoS metrics (blocked and dropped probabilities). Another performance metric, i.e. system utilization, which captures the effects of the other two, is introduced and analyzed.

In brief, the rest of my thesis is organized as follows. In chapter 2, local spectrum sensing using energy detector is investigated. In chapter 3, we discuss the cooperative scenario and the effect of the feedback channel error on the detection probability. In chapter 4, we propose a continuous time Markov model to study the effect of sensing errors on the system utilization. The possibility of mitigating the sensing errors by non standard policies is discussed and analyzed in Chapter 5. In Chapter 6, some of the challenges and issues that still need to be investigated and carefully considered before a complete implementation of this technology can be contemplated is discussed.

1.4 Scholarly publications

The research efforts during my Ph.D. program have resulted in the following scholarly publications. The materials in this thesis present only a portion of the works that have been done during this period.

1.4.1 Journal

1. O. Altrad and S. Muhaidat , "A New Mathematical Analysis of the Probability of Detection in Cognitive Radio over Fading Channels", *EURASIP Journal on Wireless Communications and Networking*, vol. 2013 (159), no. 159, June, 2013.

2. O. Altrad, S. Muhaidat and Paul D. Yoo "A Doppler Frequency Estimation-Based Handover Algorithm for LTE Networks", *IET Networks*, vol. 11, no. 1, pp. 199 - 209, Jan. 2013.

3. O. Altrad and S. Muhaidat,"Load Balancing Based on Clustering Methods for LTE Networks ", *Journal of Selected Areas in Telecommunications*, vol. 2, no. 2, pp. 1 - 6, February 2013.

4. O. Altrad and S. Muhaidat, "Opportunistic Spectrum Access in Cognitive Radio Networks with Imperfect Spectrum Sensing", *IEEE Transactions on Vehicular Technology, 2013*,

1.4.2 Submitted research papers

5. O. Altrad, S. Muhaidat, "Analysis of Dynamic Spectrum Access with A None standard Primary System Policies and Imperfect Sensing", *IEEE Transactions on Wireless Communication.*.

6. O. Altrad, S. Muhaidat "Cooperative Sensing: False Alarm Boundaries and the Optimal number of Cognitive Radio with Imperfect Feedback Channels", *EURASIP Journal on Wireless Communications and Networking.*

7. O. Altrad, S. Muhaidat "An Improved Handover Algorithm for Cellular Networks", *IET Networks.*

1.4.3 Conference

1. O. Altrad and S. Muhaidat, "Intra-Frequency Handover Algorithm Design in LTE Networks Using Doppler Frequency Estimation," in *Proc. IEEE Global Commun. , GlOBECOM'12,* Anaheim, California, USA, Dec. 2012.

2. O. Altrad and S. Muhaidat , "A Novel Handover Algorithm Design in WiMAX Networks," in *International Wireless Communications and Mobile Computing Conference(IWCMC)* Greek, April 2012.

3. O. Altrad and S. Muhaidat , "On the Performance of Amplify-and-Forward and Zero-Forcing Relaying in Cooperative Networks" in *Mosharaka International Conference on Wireless Communications and Mobile Computing (MIC-WCMC2011)*, Istanbul, Turkey, 2011.

4. N. Al-Rousan, O. Altrad, and Lj. Trajkovic , "Dual-trigger handover algorithm for WiMAX technology" in *OPNETWORK 2011*, Washington, DC, Aug. 2011.

Chapter 2

Local Spectrum Sensing

This chapter is organized as follows. Introduction and recent works are presented in section 2.1. The energy detector, system model, and the derivation of the recursive algorithm are introduced in section 2.2. A closed-form expressions for Nakagami channels are derived in section 2.3. Simulation and numerical results are introduced in section 2.4 and a summary of the important points discussed will be provided in section 2.5.

2.1 Introduction

Three detection techniques are commonly used for spectrum sensing in CRs; namely, energy detection, e.g. [12], matched filters, e.g. [13,14], and cyclostationary detection e.g. [15,16]. Energy detector is the most widely and acceptable candidate for spectrum sensing. This arises from its simplicity of implementation and incoherent requirements.

In spectrum sensing, however, there are always errors. Two errors which inevitably occur and which are of particular interest here are misdetection and false alarm, which quantify the amount of interference to the PU and the overlooked SHs in the system, respectively. It should be noted that there exists a fundamental tradeoff between these errors, since they are inversely related.

Our study is limited to the energy sensing method [12]. In particular, for a local spectrum sensing scenario, i.e. the sensing is accomplished by a single cognitive radio. This detection method can be applied to any signal type with fewer computational requirements and a simpler implementation. Although several research papers have investigated the detection process using energy detector over a variety of fading channels (cf. [17–19]), the expressions derived for the probability of detection and the probability of false alarm were mainely evaluated for even degrees of freedom (e.g. [8, Eq.

10]). Therefore, we provide an algorithm to **compute** the detection probability in the case of odd degrees of freedom based on the suboptimal energy detector. Moreover, as spectrum sensing must detect a very low signal-to-noise ratio (SNR), which in turn requires a high degree of precision, the previously derived expressions mainly depend on the number of terms in the summation to get highly accurate results. In addition, they are numerically difficult and depend on other functions while their implementation is also susceptible to truncation errors. Therefore, a closed-form expressions for the detection probability are derived. Also, the derived expressions are compared to the reported expressions in [8] and [9] in which summation and integration are used. I also compare the derived expressions to other recently reported expressions, e.g., [10] and [11], and I show the new derived expressions can be used with no limitations. Moreover, the derived expressions are more accurate than the recently reported ones with less or almost the same computational complexity. Finally, I compare our simulation results with the analytical evaluation of the derived expressions.

2.2 Energy Sensing Model

The sensing process consists of two stages and is controlled by signals from the upper layers to sense a specific bandwidth B, as shown in Fig. 2.1. In the first stage, the received signal $x(t)$ is filtered to the bandwidth of interest B, to reject band noise and adjacent signals. It is then amplified using a low noise amplifier (LNA) and is down converted to an intermediate frequency. In the second stage, the received signal is sampled and quantized using an analogue-to-digital (A/D) converter. Next, a square-law device and an integrator with sensing interval T measures the received signal energy. Finally, the output of the integrator, represented by the test statistic Y, is compared to a predetermined threshold λ to determine the existence (H_1) or absence (H_0) of a PU.

The existence or absence of a PU signal can be modeled as a binary hypotheses problem as originally proposed by [12]. This model differentiates between two hypotheses defined as

$$x[n] = \begin{cases} w[n], & H_0 \\ hs[n] + w[n], & H_1 \end{cases} \quad , n = 1, 2, \cdots N \tag{2.1}$$

where $s[n]$ is the primary user signal component which is assumed to be an unknown deterministic signal, and $w[n]$ is the noise component, which is assumed to be additive, white and Gaussian (AWGN) with zero mean and variance σ^2. h is the channel coefficient which is assumed to be constant during the period of observation, i.e., for N samples, H_0 is the hypothesis test when noise only is present and H_1 is the hypothesis test when both noise and signal are present. We also assume that the noise samples are independent and identically distributed, and they are independent of the signal samples.

The suboptimal energy detector is defined as

$$Y = \sum_{N} |x[n]|^2 \tag{2.2}$$

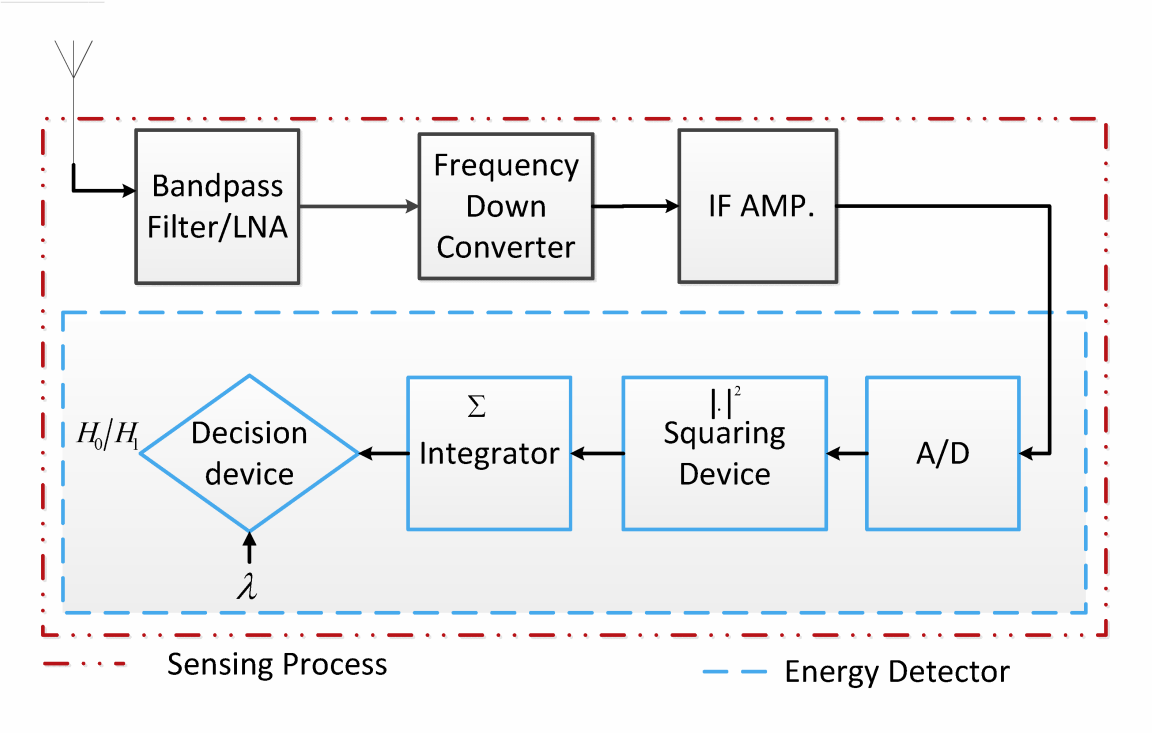

Figure 2.1: Schematic of Sensing Abstraction including Energy Detector

Then, the distribution of the decision variable Y will be central chi-square χ^2_N under H_0 and non-central chi-square $\tilde{\chi}^2_N$ with N degrees of freedom under H_1. Notice that to reduce the overuse of notations, we distinguish between central and noncentral chi-square by the symbol ($\sim$). Thus, using this notation, the distribution can be expressed as [20]

$$Y \sim \begin{cases} \chi^2_N, H_0 \\ \tilde{\chi}^2_N, H_1 \end{cases}$$

and its probability density function can be written as

$$f_Y(y) = \begin{cases} \frac{1}{\sigma^N 2^{\frac{N}{2}} \Gamma\left(\frac{N}{2}\right)} y^{\left(\frac{N}{2}\right)-1} \exp\left(\frac{-y}{2\sigma^2}\right), H_0 \\ \frac{1}{2\sigma^2}\left(\frac{y}{\zeta}\right)^{(N-2)/4} \exp\left[\frac{-1}{2\sigma^2}(y+\zeta)\right] \times I_{\frac{N}{2}-1}\left(\frac{\sqrt{\zeta y}}{\sigma^2}\right), H_1 \end{cases} \tag{2.3}$$

where the noncentrality parameter $\zeta = \sum_{i=1}^{N} \mu_i^2$, and μ_i is the mean of the ith Gaussian random variable of test Y. $I_r(.)$ is the rth-modified Bessel function of the first kind, which has a series representation [21]

$$I_r(u) = \sum_{k=0}^{\infty} \frac{\left(\frac{1}{2}u\right)^{2k+r}}{k!\Gamma(r+k+1)} \tag{2.4}$$

Evaluating test Y by the decision device, which is shown in Fig. 2.1, may result in two types of errors. We define the notation $P(H_i|H_j)$ to distinguish between these errors. When the decision device decides H_1 but H_0 is true, denoted as $P(H_1|H_0)$, this is called the probability of a false alarm (P_{fa}). When the device decides $P(H_0|H_1)$, this represents the probability of misdetection (P_{md}). The complementary to P_{md} is the probability of detection ($P_d = 1 - P_{md} = P(H_1|H_1)$). The performance of the energy detector can be characterized by the probability of detection in a low SNR regime. An alternative performance metric is the ROC curves which are generated by plotting P_{md} versus P_{fa}. Following the shorthand notation mentioned previously, the probability of detection and probability of a false alarm can be computed as:

$$\begin{aligned} P_d = &\quad P(H_1; H_1) = P(y > \lambda; H_1) \\ = &\quad \int_\lambda^\infty f_Y(y)dy, \qquad H_1 \end{aligned} \tag{2.5}$$

$$\begin{aligned} P_{fa} &= P(H_1; H_0) = P(y > \lambda; H_0) \\ &= \int_\lambda^\infty f_Y(y)dy, \qquad H_0 \end{aligned} \tag{2.6}$$

2.2.1 Probability of detection and false alarm under AWGN channels

To derive the probability of false alarm using the right-tail probability of the central chi-squared density function $Q_{\chi^2_N}$, we define γ as $\gamma = \frac{h^2\zeta}{\sigma^2}$. [1] Substituting $t = y/\sigma^2$ and further integrating the probability density function in (2.3) under H_0 results in

$$\begin{aligned} P_{fa} &= \int_{\lambda/\sigma^2}^{\infty} \frac{1}{2^{\frac{N}{2}}\Gamma\left(\frac{N}{2}\right)} t^{\left(\frac{N}{2}\right)-1} \exp\left(\frac{-t}{2}\right) dt \quad \lambda/\sigma^2 \geq 0. \\ &= Q_{\chi^2_N}\left(\lambda/\sigma^2\right) \end{aligned} \tag{2.7}$$

where $Q_{\chi^2_N}$ can be written as [22, eq 26.4.4, eq 26.4.5]

$$Q_{\chi^2_N}(\lambda/\sigma^2) = \begin{cases} 2Q\left(\sqrt{\lambda/\sigma^2}\right) & N{=}\,1 \\ 2Q\left(\sqrt{\lambda/\sigma^2}\right) + \frac{exp\left(-\frac{\lambda}{2\sigma^2}\right)}{\sqrt{\pi}} \sum_{k=1}^{\frac{N-1}{2}} \frac{(k-1)!\left(2\lambda/\sigma^2\right)^{k-\frac{1}{2}}}{(2k-1)!} & N odd \\ exp\left(-\frac{\lambda}{2\sigma^2}\right) \sum_{k=0}^{\left(\frac{N}{2}\right)-1} \frac{\left(\frac{\lambda}{2\sigma^2}\right)^k}{k!} & N even \end{cases} \tag{2.8}$$

where $Q(.)$ is the complementary cumulative distribution function defined as
$Q(x) = \int_x^{\infty} \frac{1}{\sqrt{2\pi}} \exp\left(-\frac{1}{2}t^2\right)$.

The same approach can be used to derive the probability of detection using the right-tail of the noncentral chi-squared probability density function under H_1. By letting $t = y/\sigma^2$, the probability of detection is given by

$$P_d = Q_{\tilde{\chi}^2_{N(\gamma)}}\left(\lambda/\sigma^2\right) = \int_{\lambda/\sigma^2}^{\infty} \left[\frac{1}{2}\left(\frac{t}{\gamma}\right)^{\frac{N-2}{4}} \exp\left[\frac{1}{2}(t+\gamma)\right] \times I_{\frac{N}{2}-1}\left(\sqrt{\gamma t}\right) dt \right] \tag{2.9}$$

We can rewrite (2.9) using [23, eq 2.45] **for an even number of degrees of freedom** as

$$P_d = Q_{N/2}\left(\sqrt{\gamma}, \sqrt{\lambda'}\right) \tag{2.10}$$

where $\lambda' = \lambda/\sigma^2$, and $Q_m(.,.)$ is the mth generalized Marcum Q-function which is given by

$$Q_m(\alpha, \beta) = \frac{1}{\alpha^{m-1}} \int_{\beta}^{\infty} x^m e^{-\left(\frac{x^2+\alpha^2}{2}\right)} I_{m-1}(\alpha x) dx \tag{2.11}$$

which is the same result as in [24].

For **an odd number of degrees of freedom** (2.10) can not be directly evaluated. Therefore,

[1] In AWGN channels, there is no fading, i.e., $h^2 = 1$.

we introduce an algorithm to solve this problem. To do so, we use the series expansion of the modified Bessel function defined in (2.4) and rewrite (2.9) as

$$\begin{aligned} Q_{\tilde{\chi}^2_{N(\gamma)}}\left(\lambda/\sigma^2\right) &= \sum_{k=0}^{\infty} \frac{\exp(-\gamma/2)(\gamma/2)^k}{k!} \int_{\lambda'}^{\infty} \left(\frac{t^{\frac{N}{2}+k-1}\exp\left(-\frac{t}{2}\right)}{2^{\frac{N}{2}+k}\Gamma\left(\frac{N}{2}+k\right)} \right) dt \\ &= \sum_{k=0}^{\infty} \frac{\exp(-\gamma/2)(\gamma/2)^k}{k!} \underbrace{Q_{\chi^2_{N+2k}}(\lambda')}_{second \quad term} \end{aligned} \tag{2.12}$$

The second term of (2.12) represents the right-tail probability of a central chi-square with $l = N+2k$ degrees of freedom. As a result, for N odd, $l = N + 2k$ is also odd. Thus, (2.12) can be rewritten using (2.8) for the odd case which results in (2.13), where $G_{\chi^2_{l-2}}(\lambda')$ is given by

$$\begin{aligned} Q_{\tilde{\chi}^2_{N(\gamma)}}(\lambda') &= \sum_{k=0}^{\infty} \frac{\exp(-\gamma/2)(\gamma/2)^k}{k!} \left[2Q\left(\sqrt{\lambda'}\right) + \frac{exp\left(-\frac{1}{2}\lambda'\right)}{\sqrt{\pi}} \sum_{k=1}^{\frac{N-1}{2}} \frac{(k-1)!\left(2\lambda'\right)^{k-\frac{1}{2}}}{(2k-1)!} \right] \\ &= 2Q\left(\sqrt{\lambda'}\right) + \sum_{k=0}^{\infty} \frac{\exp(-\gamma/2)(\gamma/2)^k}{k!} \\ &\times \left[\frac{exp\left(-\frac{1}{2}\lambda'\right)}{\sqrt{\pi}} \sum_{j=1}^{\frac{l-2-1}{2}} \frac{(j-1)!\left(2\lambda'\right)^{j-\frac{1}{2}}}{(2j-1)!} + \frac{exp\left(-\frac{1}{2}\lambda'\right)}{\sqrt{\pi}} \left(\frac{\left(\frac{l-1}{2}-1\right)!}{2\left(\frac{l-1}{2}-1\right)!} (2\lambda')^{\frac{l-1}{2}-\frac{1}{2}} \right) \right] \\ &= 2Q\left(\sqrt{\lambda'}\right) + \sum_{k=0}^{\infty} \frac{\exp(-\gamma/2)(\gamma/2)^k}{k!} \left[G_{\chi^2_{l-2}}(\lambda') + g(\lambda', l) \right] \end{aligned} \tag{2.13}$$

$$G_{\chi^2_{l-2}}(\lambda') = \frac{exp\left(-\frac{1}{2}\lambda'\right)}{\sqrt{\pi}} \sum_{j=1}^{\frac{l-3}{2}} \frac{(j-1)!(2\lambda')^{j-\frac{1}{2}}}{(2j-1)!} \tag{2.14}$$

and $g(\lambda', l)$ can be rewritten as

$$\begin{aligned} g(\lambda', l) &= \frac{exp\left(-\frac{1}{2}\lambda'\right)}{\sqrt{\pi}} \left(\frac{\left(\frac{l-1}{2}-1\right)!}{2\left(\frac{l-1}{2}-1\right)!} (2\lambda')^{\frac{l-1}{2}-\frac{1}{2}} \right) \\ &= \frac{exp(\lambda'/2)}{\sqrt{\pi}} \left(\frac{((l-5)/2)!}{(l-4)!} (2\lambda')^{(l-4)/2} \right) 2\lambda' \frac{((l-3)/2)}{(l-2)(l-3)} \end{aligned} \tag{2.15}$$

(2.15) can also be reduced to

$$g(\lambda', l) = g(\lambda', l-2)\frac{\lambda'}{l-2} \tag{2.16}$$

where the initialization starts with $G_{\chi^2_{l-2}}(\lambda') = g(\lambda', 3) = \sqrt{\frac{2\lambda'}{\pi}} \exp(-\lambda'/2)$.

2.3 Probability of Detection and False Alarms Under Nakagami Fading Channels

To capture all different types of fading, the parameters of the Nakagami distribution can be adjusted to fit a variety of fading processes. If we define $\bar{\gamma} = E[h^2]\zeta/\sigma^2$ as the average signal-to-noise ratio,

where $E(.)$ denotes the expectation operator, then the probability distribution of γ will be given as

$$P_{Nak}(\gamma) = \left(\frac{m}{\bar{\gamma}}\right)^m \frac{\gamma^{m-1}}{\Gamma(m)} \exp\left[-\frac{m\gamma}{\bar{\gamma}}\right] \tag{2.17}$$

To compute the probability of detection, this must be averaged over the probability density function of the instantaneous value of γ, i.e., it can be written as

$$P_{d_{NAK}} = \int_0^\infty Q_{N/2}\left(\sqrt{\gamma}, \sqrt{\lambda'}\right) f(\gamma)\, d\gamma \tag{2.18}$$

Then, substituting (2.17) into (2.18) results in

$$\begin{aligned} P_{d_{NAK}} &= \int_0^\infty \left(\tfrac{m}{\bar{\gamma}}\right)^m \tfrac{\gamma^{m-1}}{\Gamma(m)} \exp\left(-\tfrac{m\gamma}{\bar{\gamma}}\right) Q_{N/2}\left(\sqrt{\gamma}, \sqrt{\lambda'}\right) d\gamma \\ &= \tfrac{2}{\Gamma(m)}\left(\tfrac{m}{\bar{\gamma}}\right)^m \int_0^\infty x^{2m-1} \exp\left(-\tfrac{\eta^2 x^2}{2}\right) Q_{N/2}\left(x, \sqrt{\lambda'}\right) dx \\ &= \alpha \int_0^\infty x^{2m-1} \exp\left(-\tfrac{\eta^2 x^2}{2}\right) Q_{N/2}\left(x, \sqrt{\lambda'}\right) dx \end{aligned} \tag{2.19}$$

where in the second step we substitute $x = \sqrt{\gamma}$ and $\eta^2 = \frac{2m}{\bar{\gamma}}$, and in the last step we substitute $\frac{2}{\Gamma(m)}\left(\frac{m}{\bar{\gamma}}\right)^m$ with α. Different combinations of m and $N/2$ lead to different results for the integration defined in the last step. In the following, the probability of detection is evaluated over both Rayleigh and Nakagami fading channels.

2.3.1 Special case: Rayleigh Fading

In the case of Raleigh fading we set $m = 1$ and use [23, eq B.53]. Then the probability of detection can be written as

$$P_{d_{Ray}} = \exp\left(-\tfrac{\lambda'}{2}\right)\left[\ \left[1+\eta^2\right]^{u-1}\left\{\exp\left(\tfrac{\lambda'}{2+2\eta^2}\right) - \sum_{k=0}^{u-2} \tfrac{1}{k!}\left(\tfrac{\lambda'}{2+2\eta^2}\right)^k\right\} + \sum_{k=0}^{u-2} \tfrac{1}{k!}\left(\tfrac{\lambda'}{2}\right)^k\ \right] \tag{2.20}$$

where $u = N/2$.

2.3.2 Nakagami Fading

In the case of Nakagami fading, we further simplify the expression in (2.19) by using the series representation of the Marcum Q-function [25], which is given by

$$Q_u\left(\sqrt{\gamma}, \sqrt{\lambda'}\right) = 1 - \sum_{n\geq 0}\left[\ (-1)^n \exp\left(\tfrac{\gamma}{2}\right) \tfrac{L_n^{u-1}\left(\frac{\gamma}{2}\right)}{\Gamma(u+n+1)}\left(\tfrac{\lambda'}{2}\right)^{n+u}\ \right] \tag{2.21}$$

where L_j^k is the generalized Laguerre polynomial of degree j and order k. The absolute convergence of the series in (2.21) has been shown to be absolutely bounded by

$$\sum_{n\geq 0}\left[\ (-1)^n \exp\left(\tfrac{\gamma}{2}\right) \tfrac{L_n^{u-1}\left(\frac{\gamma}{2}\right)}{\Gamma(u+n+1)}\left(\tfrac{\lambda'}{2}\right)^{n+u}\ \right] \leq \exp\left(-\gamma/4\right) \tfrac{1}{\Gamma(u)}\left(\tfrac{\lambda'}{2}\right)^{u-1}\left(\exp\left(\tfrac{\lambda'}{2}\right) - 1\right) \tag{2.22}$$

Then, substituting (2.22) into (2.19) results in (2.23).

$$P_{d_{NAK}} = \alpha \int_0^\infty \left\{ x^{2m-1} \exp\left(-\eta^2 x^2/2\right) \left[1 - \exp\left(-x^2/4\right) \frac{1}{\Gamma(u)} (\lambda'/2)^{u-1} \left(\exp\left(\lambda'/2\right) - 1\right)\right]\right\} dx$$

$$= \left[\begin{array}{l} \underbrace{\alpha \int_0^\infty x^{2m-1} \exp\left(-\eta^2 x^2/2\right) dx}_{first \quad term} \\ \underbrace{-\frac{\alpha}{\Gamma(u)} (\lambda'/2)^{u-1} \exp\left(\lambda'/2\right) \int_0^\infty x^{2m-1} \exp\left(-\eta^2 x^2/2\right) \exp\left(-x^2/4\right) dx}_{second \quad term} \\ \underbrace{+\frac{\alpha}{\Gamma(u)} (\lambda'/2)^{u-1} \int_0^\infty x^{2m-1} \exp\left(-\eta^2 x^2/2\right) \exp\left(-x^2/4\right) dx}_{Third \quad term} \end{array} \right] \tag{2.23}$$

Next, by changing the variable $M = 2m - 1$, and further integrating, the first term of (2.23) can be reduced to

$$\begin{aligned} &\alpha \int_0^\infty x^{2m-1} \exp\left(-\eta^2 x^2/2\right) dx \\ &= \alpha \frac{\Gamma\left((M+1)/2\right)}{2\left(\frac{\eta^2}{2}\right)^{(M+1)/2}} = 1 \end{aligned} \tag{2.24}$$

The second term of (2.23) can be further reduced to

$$\begin{aligned} &\frac{\alpha}{\Gamma(u)} (\lambda'/2)^{u-1} \exp\left(\lambda'/2\right) \int_0^\infty x^M \exp\left(-((\eta^2/2) + 1/4)x^2\right) dx \\ &= \frac{\exp\left(\lambda'/2\right) (\lambda'/2)^{u-1}}{\Gamma\left(u\right)} \frac{\left(\frac{m}{\bar{\gamma}}\right)^m}{\left(\frac{m}{\bar{\gamma}} + 1/4\right)^m} \end{aligned} \tag{2.25}$$

while the third term can be reduced as

$$\begin{aligned} &\frac{\alpha}{\Gamma(u)} (\lambda'/2)^{u-1} \int_0^\infty x^M \exp\left(-((\eta^2/2) + 1/4)x^2\right) dx \\ &= \frac{1}{\Gamma(u)} (\lambda'/2)^{u-1} \frac{\left(\frac{m}{\bar{\gamma}}\right)^m}{\left(\frac{m}{\bar{\gamma}} + 1/4\right)^m} \end{aligned} \tag{2.26}$$

Thus, the probability of detection under a Nakagami fading channel is the result of (2.24), (2.25)

and (2.26) which can be written as

$$P_{d_{NAK}} = 1 - \frac{1}{\Gamma(u)}(\lambda'/2)^{u-1} \frac{\left(\frac{m}{\bar{\gamma}}\right)^m}{\left(\frac{m}{\bar{\gamma}} + 1/4\right)^m} \left[\exp\left(\lambda'/2\right) - 1\right] \tag{2.27}$$

It is clear from (2.27) how changing various parameters affects the detection process. The new derived expression reveals the fact that the ratio of parameter m to parameter $\bar{\gamma}$ is an important consideration when evaluating the probability of detection over Nakagami fading channels. For example, at low $\bar{\gamma} < 2$ dB and when the degree of freedom u is fixed, the Nakagami parameter m has only a minor effect on the detection process. That means no matter how much m increases, the probability of detection stays almost the same. However, at high $\bar{\gamma} > 15$ dB, increasing m will greatly improve the probability of detection. This will be discussed further in the simulation section.

Another expression for the probability of detection over Nakagami fading channels can easily be derived by rewriting the right-hand side of (2.21) as

$$Q_u\left(\sqrt{\gamma}, \sqrt{\lambda'}\right) = 1 - \sum_{n\geq 0} \exp\left(-\gamma/2\right)\left(\frac{\gamma}{2}\right)^n \left(\frac{\gamma^*(u+n, \lambda'/2)}{n!\Gamma(u+n)}\right) \tag{2.28}$$

where we use the notation $\gamma^*(.,.)$ to represent the lower incomplete gamma function. Equation (2.28) is the well-known canonical representation of the uth order generalized Marcum Q-function. Then, with the help of (2.18) and using $\sum_{k=0}^{\infty} {(a/2)^k}/{k!} = \exp(a/2)$, and after simple mathematical manipulation as shown in (2.24-2.26), the probability of detection over Nakagami fading channels can be approximated as

$$P_{d_{NAK}} \cong 1 - \beta^m \left(\frac{\gamma^*(\lambda'/2, u)}{\Gamma\left(u\right)}\right) \tag{2.29}$$

where $\beta = [2m/\left(2m + \bar{\gamma}\right)]$.

2.4 Simulation and Numerical Results

A binary phase shift keying signal[2] with sampling frequency $f_s = 10f_c$, where f_c is the carrier frequency, is used to investigate the detection probability for even/odd degrees of freedom. For the even degree of freedom with N arbitrarily chosen to be $(10, 20)$, the simulation results are compared to (2.10). As shown in Fig. 2.2, it can be seen that increasing N or the SNR enhances the probability of detection. Therefore, this result is consistent with most of the reported results in the literature. We also notice that the simulation results coincide with the theoretical ones.

Fig. 2.3 shows the detection probability using the recursive algorithm for odd/even degrees of freedom with $N = 31, 32$ for comparison. As shown, the recursive algorithm perfectly matches

[2]Different modulation schemes could be used in the simulation since the derived expression is independent of the modulation used.

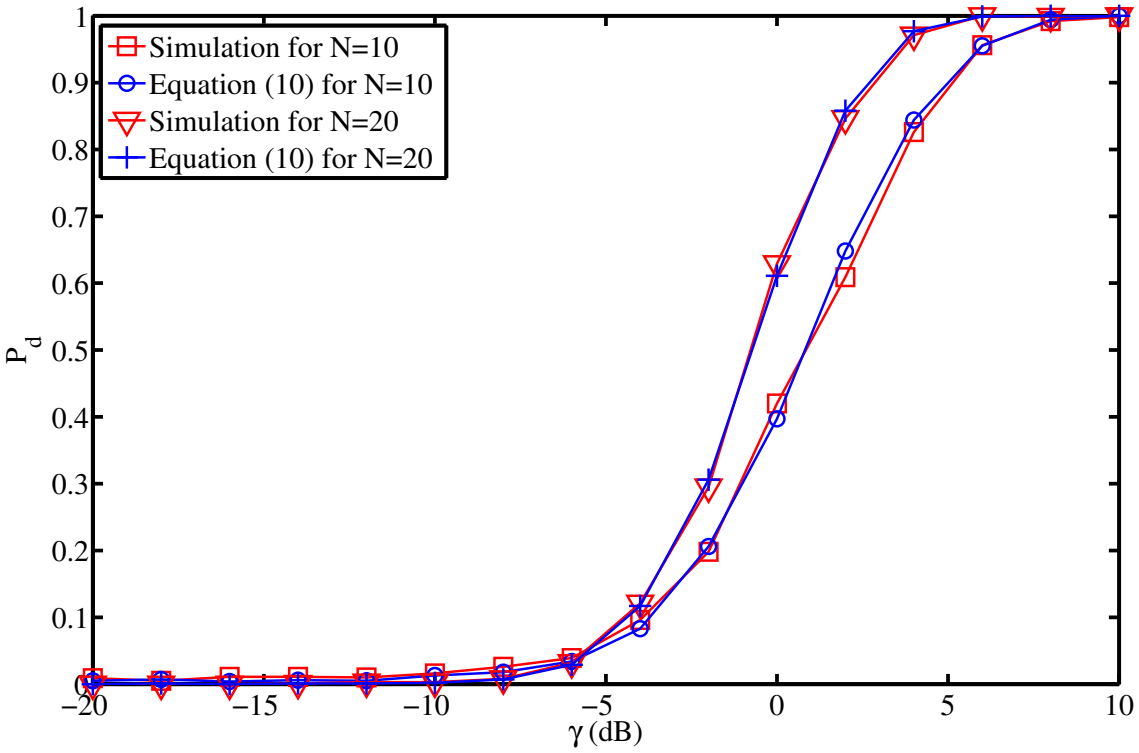

Figure 2.2: Probability of detection vs SNR for BPSK signal with $f_s = 10f_c$, $P_{fa} = 0.01$ and different **even** number of degrees of freedom; the simulation is compared to (2.10) in AWGN channel.

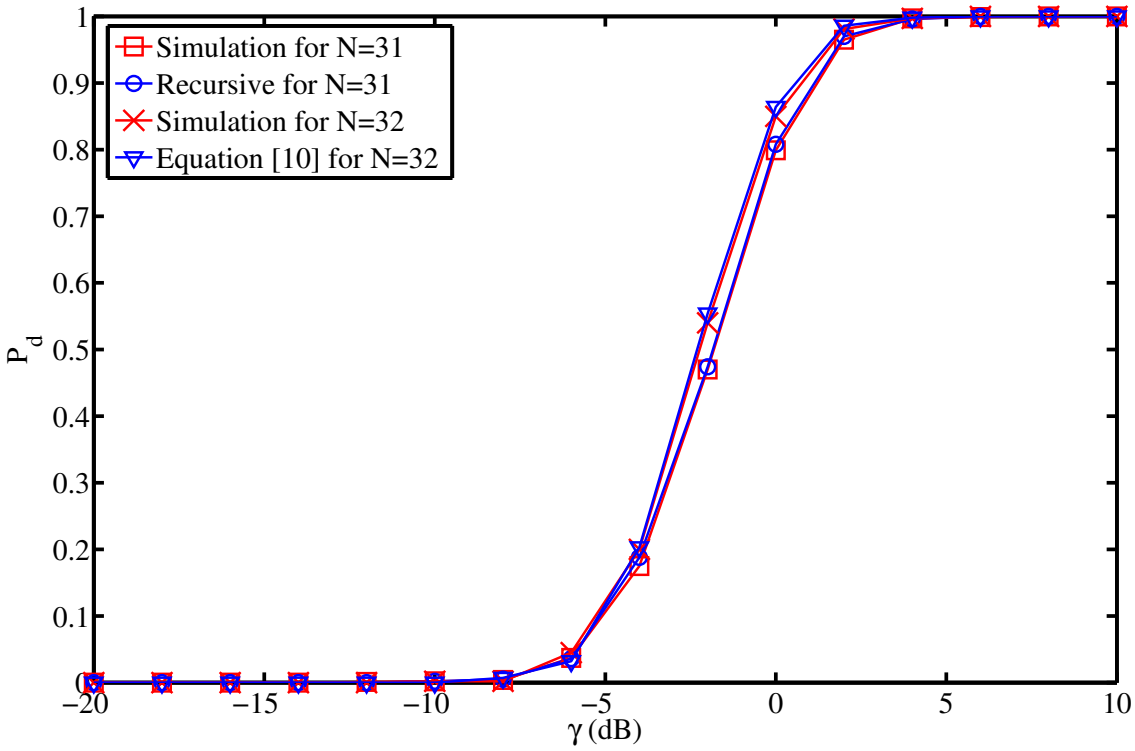

Figure 2.3: Probability of detection Vs SNR for BPSK signal with $f_s = 10f_c$, $P_{fa} = 0.01$ and different **odd with** $N = 31$**, even with** $N = 32$ number of degrees of freedom. In the odd case, the simulation is compared to the recursive formula (2.13-2.16) in AWGC, and in the even case the simulation is compared to (2.10) in AWGC.

the simulation results. Moreover, the accuracy of the recursive algorithm goes up to 15 decimal places, which is the maximum number of digits that Matlab can support. Although there is a small effect on the detection probability when we compare the even/odd cases, in practice and since most current functions deals only with even degree of freedom, this algorithm becomes more beneficial. For example, when evaluating the detection probability using the Marcum function in Matlab with $N = 31$ (odd), the third argument of the Marcum function will be 15.5, hence, the implemented Marcum function in Matlab can't be used to evaluate the detection probability in this case as it accepts only integer numbers. However, our algorithm does.

To evaluate the closed-form expressions derived for Nakagami channels, an extensive simulation has been performed using the ROC. The derived expressions are evaluated and compared with the numerical integration of (2.18) and with the expressions reported by [8], [9], [10] and [11].[3]

[3]For comparison purposes, we have used a value of $n = 1$ in the expression of [11, Eq. 13], where n represents the number of nodes cooperating in the sensing process according to [11] notations.

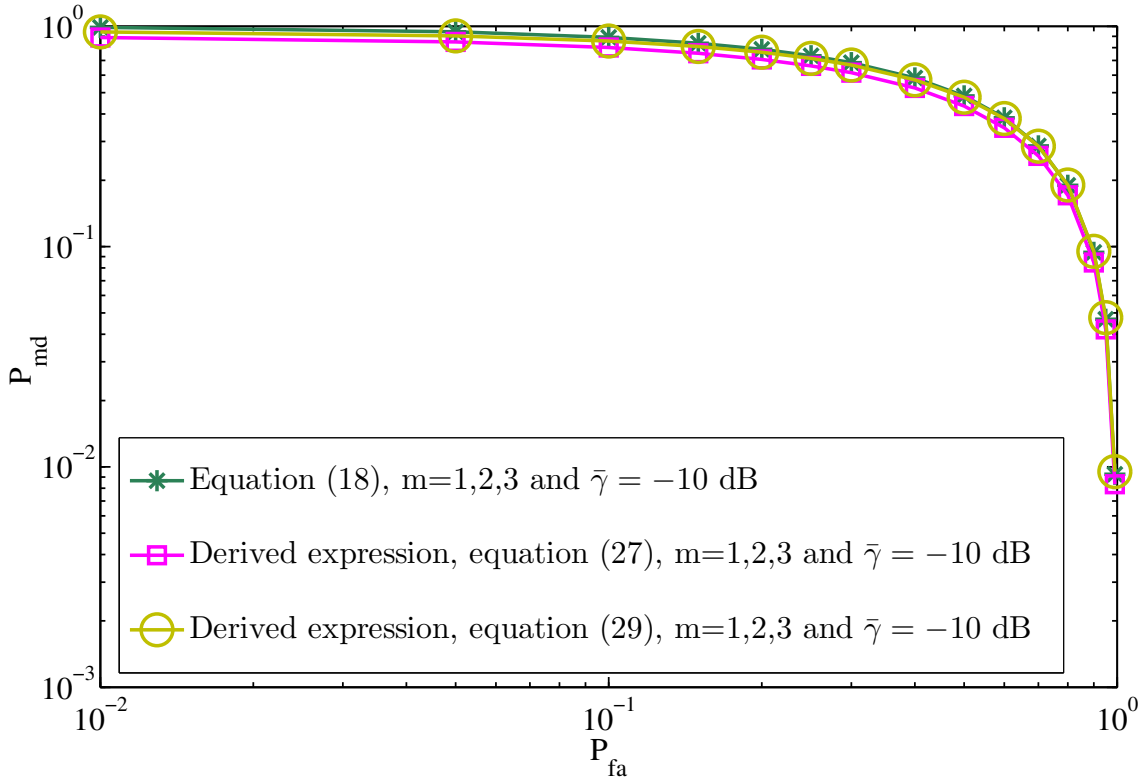

Figure 2.4: Comparison between the derived expressions in (2.27) and (2.29) and the numerical integration of (2.18) for $\bar{\gamma} = -10$ dB and different values of m.

2.4.1 Comparison of the derived expressions with equation (2.18)

In Fig. 2.4 and Fig. 2.5 we compare the derived expressions in (2.27) and (2.29) with the numerical integration of (2.18) for different values of $\bar{\gamma}$ and m. Fig. **??** also shows the effect of varying the Nakagami parameter m on the misdetection probability at low and high values of $\bar{\gamma}$ which will be discussed in the following subsections.

Low value of $\bar{\gamma}$

At a low value of $\bar{\gamma}$, i.e., $\bar{\gamma} = -10$ dB, (see Fig. 2.4), it can be seen that increasing the value of m, $(m = 1, 2, 3)$, does not improve the misdetection probability for both derived expressions which concurs with the numerical integration of (2.18). We also note that (2.29) exactly matches (2.18); on the other hand, there is a minor discrepancy between (2.27) and (2.18).

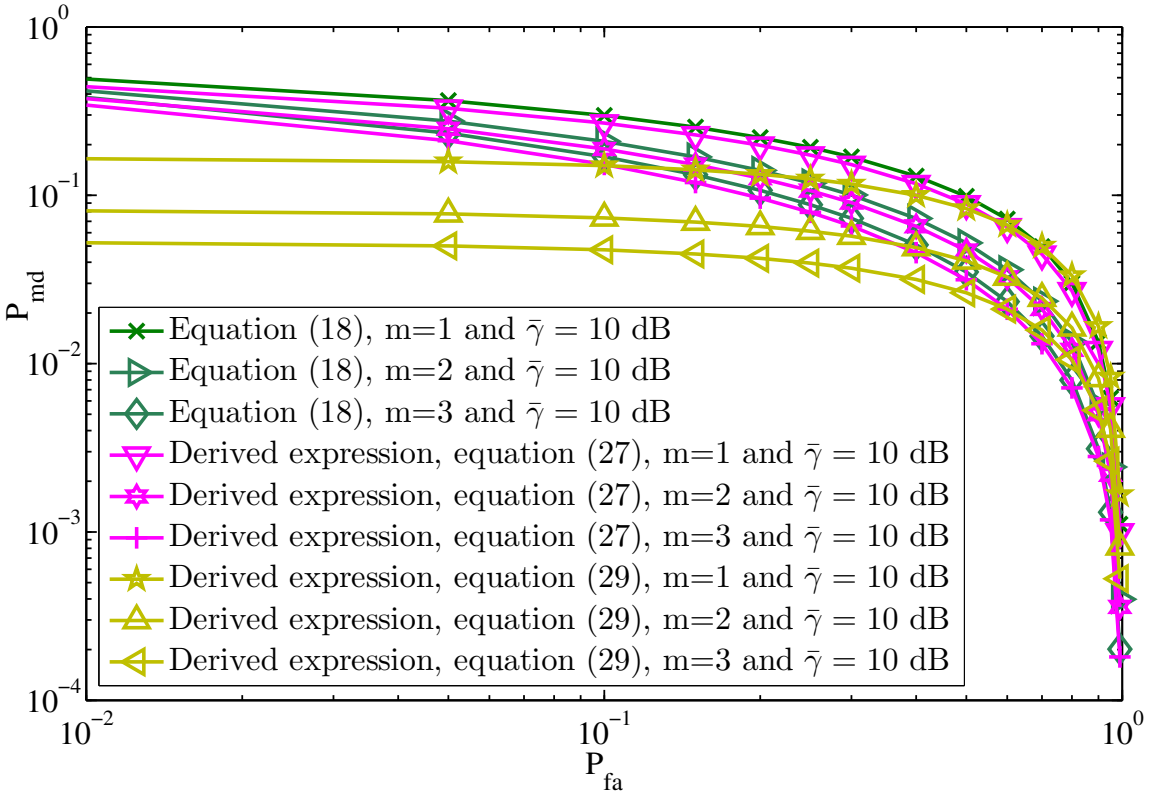

Figure 2.5: Comparison between the derived expressions in (2.27) and (2.29) and the numerical integration of (2.18) for $\bar{\gamma} = 10$ dB and different values of m.

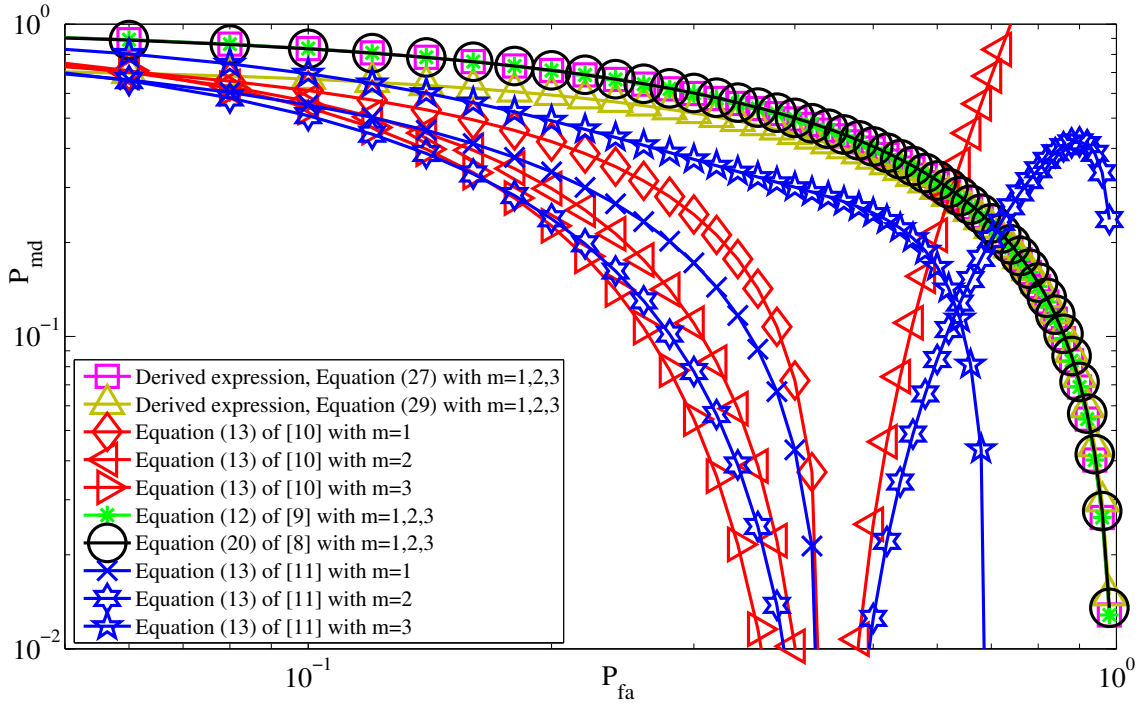

Figure 2.6: Comparison of the new derived expressions, (2.27) and (2.29), with the work of [8, Eq. 20], [9, Eq. 12], [10, Eq. 13] and [11, Eq. 13] with $\bar{\gamma}$= -2 dB, u = 5, and m = 2, 3.

High value of $\bar{\gamma}$

At a high value of $\bar{\gamma}$, i.e., $\bar{\gamma} = 10$ dB, (see Fig. 2.5), increasing m will greatly improve the misdetection probability for both derived expressions (2.27 and 2.29), which also concurs with the numerical integration of (2.18) as can be seen in Fig. 2.5. Further, we notice that at a very low false alarm probability, (2.29) is less accurate compared to (2.27). However, as the false alarm probability increases, the results for both expressions match that of the numerical integration of (2.18).

2.4.2 Comparison of the derived expressions with related works

In this subsection, we compare the new derived expressions with the previously reported expressions for high and low values of $\bar{\gamma}$ and $m = 1, 2, 3$.

Low value of $\bar{\gamma}$

In Fig. 2.6, the new derived expressions are compared with the expressions of [8, Eq. 20], [9, Eq. 12], [10, Eq. 13] and [11, Eq. 13]. It can be seen that at a very low false alarm probability, the results of the new derived expressions in (2.27), (2.29) and all expressions in the previously mentioned

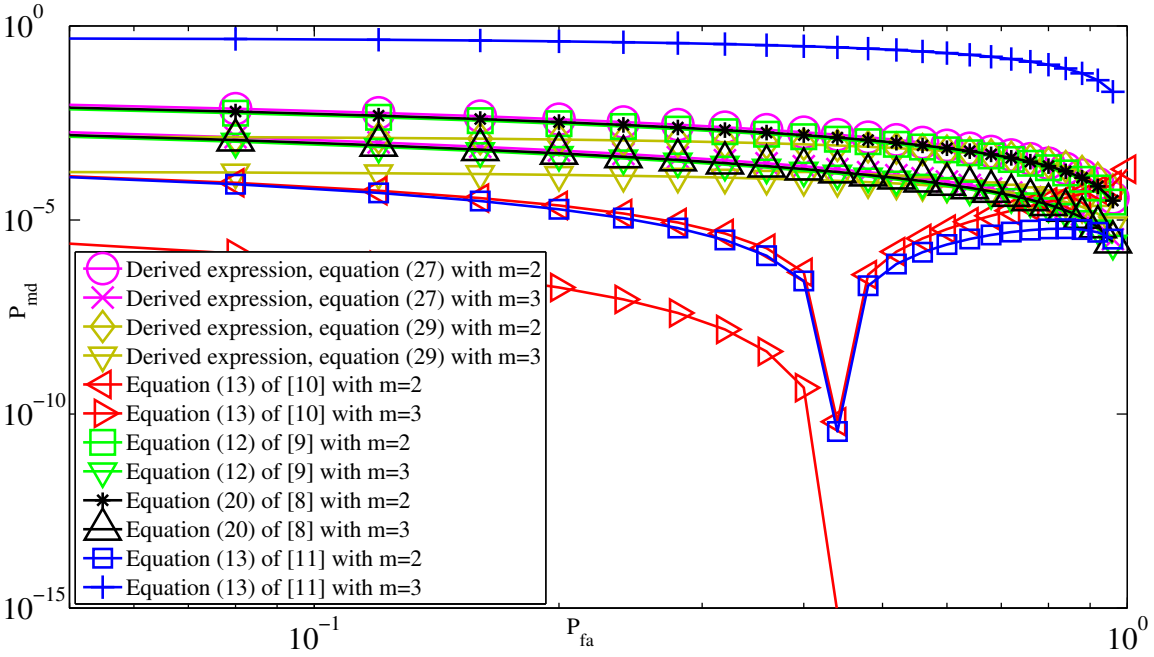

Figure 2.7: Comparison of the new derived expressions, (2.27) and (2.29), with the work of [8, Eq. 20], [9, Eq. 12], [10, Eq. 13] and [11, Eq. 13] with $\bar{\gamma}$= 20 dB, u = 5, and m = 2, 3.

references are a good match. As the probability of false alarm increases, however, a discrepancy arises between [10, Eq. 13] and [11, Eq. 13] when compared to the new expressions and/or the work of [8] and [9]. Moreover, as shown in Fig. 2.6, at low $\bar{\gamma}$ increasing m did not enhance the probability of misdetection. This behavior can be seen from (2.27) and (2.29) which also concurs with the work of [8, Eq. 20] and [9, Eq. 12]. However, the result of [10, Eq. 13] has some discrepancies when the false alarm probability or the value of m increases. Moreover, the result of [11, Eq. 13] is not consistent with increasing m. For example, the result at the value of $m = 3$ is worse than the result at the value of $m = 1, 2$ as can be seen in Fig. 2.6. We note also that the probability of misdetection approaches zero at the point of $(1 - P_{fa})$ for the expressions reported by [10] and [11].

High value of $\bar{\gamma}$

Fig. 2.7 shows the simulation results for all expressions when evaluated at a high value of $\bar{\gamma}$. The result of (2.27) is very close to that of [8, Eq. 20] and of [9, Eq. 12] for the values of $m = 2, 3$. Moreover, although there are some discrepancies when evaluating (2.29) as compared to [8, Eq. 20], [9, Eq. 12], at a high value of a false alarm probability, the expression (2.29) is a perfect match. To this end, we conclude that (2.29) works well at high values of $\bar{\gamma}$ and when $P_{fa} > 0.2$. Moreover,

(2.27) is accurate at low $\bar{\gamma}$ for all values of false alarm probability. On the other hand, the expressions [10, Eq. 13] and [11, Eq. 13] are less accurate for all evaluated points of false alarm probability and the unpredictable behavior of these expressions still exists as discussed in the low value of $\bar{\gamma}$ case. Moreover, results from the expression [11, Eq. 13] are also inconsistent as the value of m is increased. [4]

2.4.3 Computational Complexity

In the previous subsections we discussed the accuracy of the derived expressions and compared them to the expressions in [8, Eq. 20], [9, Eq. 12] that require summation and integration terms to get the needed accuracy. The derived expressions were also compared to the expressions of [10, Eq. 13] and [11, Eq. 13] that depend on evaluating the gamma function as does the derived expression in (2.29). To complete the picture, we need another performance metric that distinguishes between these expressions. To do so, a simple Matlab code was written to measure the computation time required of a central processing unit (CPU) to evaluate a point in the ROC domain. We ran the code on a computer equipped with a CPU with a speed of 3.07 Ghz on which we cleared all background application processes that might run on the system.[5] We used 21 points of false alarm probability; i.e., $(P_{fa} = 0 : 0.05 : 1)$ with a step of 0.05. At each point, the code iterated 1000 times and averaged afterward. The measured computation time of the CPU for all points used and for each expression is plotted in Fig. 2.8. It can be seen that more computation time is required to get highly accurate results. This is evident from the evaluated points of the expressions [8, Eq. 20], and [9, Eq. 12] as they have the highest computation time.[6] On the other hand, the derived expression in (2.27) and the reported expression in [11, Eq. 13] have almost the same computation time. Moreover, the expression of [10, Eq. 13] has the lowest computation time while the expression of [8, Eq. 20] has the highest.

The derived expressions can also be compared in terms of the number of multiplications. For example, the derived expression in [8, Eq. 20] is based on the summation of confluent hypergeometric functions and such functions have a computational complexity of order $O\left[\log^2(n)\,\bar{M}(n)\right]$ for n-digit precision, [26], where n means computing n digits and $\bar{M}(n)$ is the bit complexity of multiplication. However, the reported expression of [9, Eq. 12] is based on an infinite series of gamma

[4] Equation (2.29) comes from another way of calculating the probability of detection over Nakagami fading channels in order to compare with results from the state of the art, which seemed rather optimistic for low false alarm probability, and that for high SNR cases.

[5] The conducted simulations show that the computed time will only be scaled by a constant factor, and that the calculated computation time will not be affected if we do or do not clear the processor cache of any background application processes.

[6] The number of terms used to calculate the summation of [9, Eq. 12] was 20.

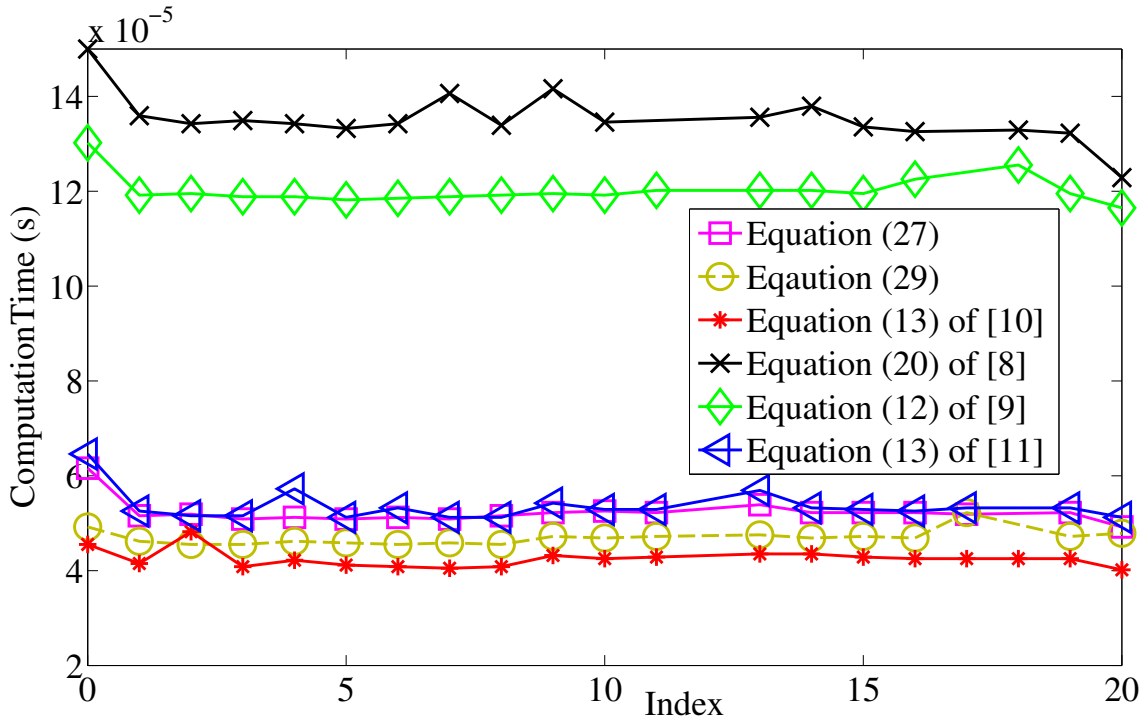

Figure 2.8: Comparison of the computation time, all expressions computed for $\bar{\gamma} = 20$ dB and u = 5.

functions and such functions have a computational complexity of $O\left[\sqrt{n}\bar{M}\left(n\right)\right]$. Using this notation, the derived expressions of (2.27) and (2.29) have a computational complexity of $O(\bar{M}(n))$. Since $O\left[\log^2\left(n\right)\bar{M}\left(n\right)\right] > O\left[\sqrt{n}\bar{M}\left(n\right)\right] > O(\bar{M}(n))$, which is also consistent with the simulation results of Fig. 2.8, therefore, the derived expressions have a lower complexity than [8, Eq. 20], [9, Eq. 12] and have the same computational complexity as [10, Eq. 13] and [11, Eq.13].

2.5 Summary and conclusion

Spectrum sensing using energy detectors under different fading channels was investigated. We derived a tight closed-form expressions for the probability of detection in Nakagami channels. The closed-form expressions can easily be used for Rayleigh fading channels by setting $m = 1$. The results of the closed-form formula as compared with other expressions based on summation and integration terms are very close. Furthermore, the derived expression of (2.27) can be used for all $\bar{\gamma}$; however, there is a minor limitation of using (2.29) specifically at high values of $\bar{\gamma}$. Moreover, the derived expressions have a lower computational complexity compared to other expressions with only a very small loss of accuracy. In addition, we introduced an accurate recursive algorithm to compute the probability of detection for an odd number of degrees of freedom under AWGN channels. Our simulation shows that the detection process for a binary phase shift keying signal using the recursive formula perfectly coincides with the recursive algorithm.

Chapter 3

Cooperative Spectrum Sensing: The Optimal Number of Cognitive Radios under Imperfect Feedback Channels

In the previous chapter, the local spectrum sensing is studied, i.e. the spectrum sensing using energy detector is performed by one CR. However, the performance of local sensing significantly degrades because of fading and shadowing of the PU-SU link. Therefore, cooperative spectrum sensing (multiple SUs sense the PU signal) has been proposed to enhance the detection probability of the PU. In this chapter, centralized cooperative sensing is considered in which a number of CRs are involved in the sensing process and forward their decision to a central node over a feedback channel.

This chapter is organized as follows. The main objective is stated in section 3.1. In Section 3.2, the state of the arts on cooperative sensing is discussed. System model is presented in section 3.3. The total error, the optimal number of CRs under perfect/imperfect feedback channels are presented in sections 3.4, 3.5 and 3.6, respectively. A summary of this chapter is given in section 3.7.

3.1 Objective

The main objective of this chapter is to study and analyze the detection probability at the fusion center (FC) of the centralized cooperative spectrum sensing under the effect of feedback channel errors. The total error is a new criterion that has been adopted to study the effect of the feedback

channel errors on the detection probability. The optimal number of CRs required to minimize the total error of the sensing process when the reporting channel is perfect/imperfect will be analyzed. As the main focus of this chapter is to investigate the sensing functionality, analyzing its performance when employing cooperative spectrum sensing in terms of the total error concept and where imperfect feedback reporting channels are found, we limit our research to a centralized architecture where all CRs report their final decision to a fusion center. Doing so will not affect applying the same methodology to other system architectures. We might also consider the centralized architecture as the baseline for the performance of other architectures, e.g., ad hoc networks.

3.2 Introduction

The optimal sensing method for stationary Gaussian noise is a matched filter [14]. However, the coherency requirement and the need for knowledge of the PU's signal structure prevent the use of this method in DSA systems. Spectrum sensing in which the primary user signal has unknown distribution was studied in [27]. Other sensing methods include cyclostationary feature detection [15, 16] and energy detection [12, 28, 29]. In the former, the high computational requirements and the knowledge needed of cyclic frequencies of the primary signal, which may not be available, also prevent this method from being usable by DSA. Compared to matched filtering and cyclostationary techniques, the energy-sensing technique is more desirable. The preference for this technique is due to its simplicity of implementation, lack of computational requirements, and there being no need for knowledge of the channel and/or PU signal. One drawback of this technique is the noise uncertainty [30]; however, several means have recently been proposed to solve this problem [31]. A further drawback to the energy-sensing method is its degradation in shadowing/fading environments. To overcome this degradation and to improve the sensing functionality, cooperative sensing has been introduced.

Cooperative sensing in wireless communication is being developed to achieve diversity gain and to reduce outage probability [32–44]. As cognitive radios emerge, and the need to enhance sensing functionality arises, researchers have begun to investigate cooperative spectrum sensing using an energy detector [45–50]. Cooperative sensing using beamforming techniques was studied in [51–53]. The sensing throughput tradeoff based on energy sensing was investigated in [54]. Optimal linear cooperation for spectrum sensing based on the linear combination of local statistics from individual CRs was analyzed in [55]. Sensing performance based on multiple antennas was studied in [56–59]. The optimization of cooperative spectrum sensing with perfect feedback channels was studied in [60].

In most cooperative sensing schemes (soft or hard combining), the feedback channels which are used to forward the CRs decisions to a FC are assumed to be perfect. However, in practical systems, feedback channels are not error free. In [61], a performance analysis of hard decisions versus soft decisions in the presence of reporting channel errors was investigated. In [62, 63], cooperative

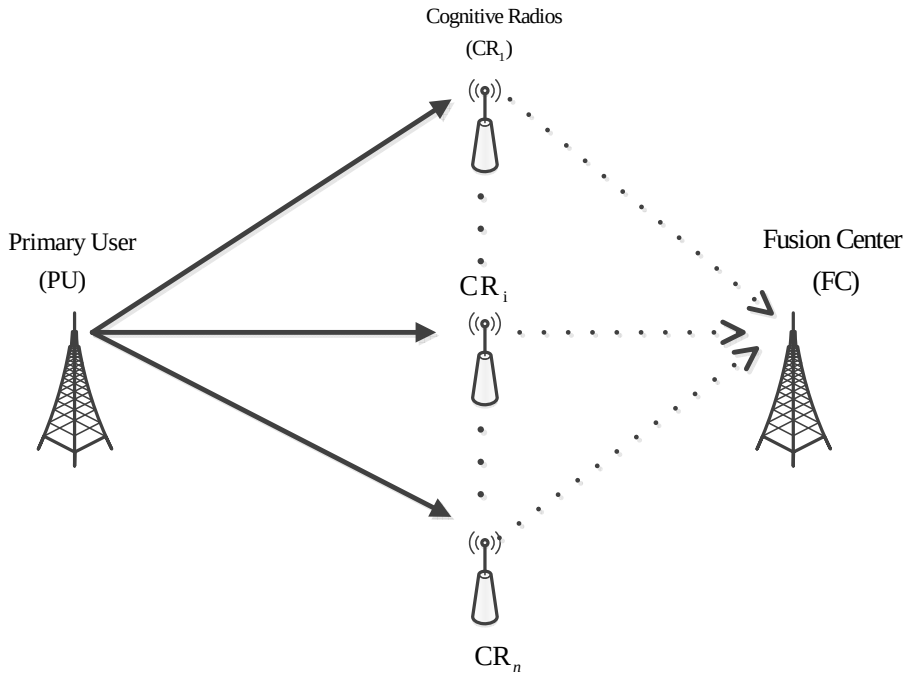

Figure 3.1: System model of cooperative spectrum sensing.

spectrum sensing in the presence of a feedback error using hard decision combining was studied. Recently, in [64], cooperative sensing with imperfect feedback channels and multiple antennas at the CRs was investigated.

3.3 System Model

We consider a network of n CRs, each of which employs a likelihood ratio test based on its own observations and a threshold. Each CR decides on the existence or absence of a PU, then sends its decision to the FC as shown in Fig. 3.1. The existence or absence of a PU signal can be modeled as a binary hypothesis problem. For n CRs, the two hypotheses can be defined as

$$x_i = \begin{cases} w_i, & H_0 \\ h_i s + w_i, & H_1 \end{cases}, i = 1, 2, \cdots n, \tag{3.1}$$

where s is the PU signal vector, and w_i, h_i are the ith CR noise vector and the ith channel gain for $i = 1, ..., n$, respectively. H_0 is the hypothesis test when noise only is present, and H_1 is the hypothesis test when both noise and signal are present. We also assume that the noise samples are independent and identically distributed, and that they are independent of the signal samples. The decision at the ith CR can be written as

$$CR_i = f(x_i) = \begin{cases} 0, & H_0 \\ 1, & H_1 \end{cases}, i = 1, 2, \cdots n \tag{3.2}$$

The observation x_i at the ith CR has the joint probability density function $P(x_i|H_j)$ under hypothesis j, for $j = 1, 2$. The decision at the ith CR may cause two types of errors. When the ith CR decides H_1 but H_0 is true, i.e., $P(CR_i = 1|H_0) = P_{fa_i}$, this represents the probability of false alarm (P_{fa_i}). When the ith CR decides H_0 but H_1 is true, i.e., $P(CR_i = 0|H_1) = P_{m_i}$, this represents the probability of misdetection (P_{m_i}). The complementary to P_{m_i} is the probability of detection $P_{d_i} = 1 - P_{m_i}$. Because the observations of all CRs are independent, it follows that the CRs' decisions are also statistically independent. Thus, the joint probability density function at the FC can be written as

$$P(CR_1, ..., CR_n|H_j) = \prod_{i=1}^{n} P(CR_i|H_j). \tag{3.3}$$

If we assume that all CR users have the same threshold, then the likelihood ratio test at the FC can be written as

$$\Lambda\left(FC_D\right) = \prod_{i=1}^{n} \frac{P(CR_i|H_1)}{P(CR_i|H_0)} \underset{\mathcal{H}_0}{\overset{\mathcal{H}_1}{\gtrless}} \lambda, \tag{3.4}$$

where λ is a threshold determined by a fixed false alarm probability at the FC, and $\mathcal{H}_j$ for $(j = 0, 1)$, is the hypothesis that the FC decides a PU is absent or present, respectively.

At the FC, when all CRs operate at the same probability of false alarm and the same probability of detection, the probability of false alarm Q_f and the probability of detection Q_d using the k-out-of-n fusion rule can be written as [65]

$$Q_f = \sum_{m=k}^{n} \binom{n}{m} P_{fa}^m (1 - P_{fa})^{n-m} \tag{3.5}$$

$$Q_d = \sum_{m=k}^{n} \binom{n}{m} P_d^m (1 - P_d)^{n-m} \tag{3.6}$$

The value of the parameter k determines the logic fusion rule, that is, for $k = 1$ the fusion rule becomes the OR rule and for $k = n$ it becomes the AND rule. Both rules have their own drawbacks. In the OR rule, the detection probability increases when the number of CRs increases. However, this increase is at the expense of increasing the number of false alarms, which is not desirable in cognitive radio systems. If there is an increase in false alarms, the probability of wasting resources arises, which results in an under-utilization of the available SHs in a PN. On the other hand, using

the AND rule will decrease the false alarm probability as the number of CRs increases. Therefore, greater utilization of SHs is guaranteed but at the expense of increasing the misdetection probability, which causes more interference to the PN. To summarize, in the OR rule, although the probability of misdetection is decreased by increasing the number of cooperative users, the probability of false alarm increases as well. The opposite can be seen in the AND rule, where as the probability of misdetection increases, the probability of false alarm decreases.

Based on the previous discussion, a question arises: should we ignore the implementation of these rules (OR rule, AND rule) when designing CR systems? The best approach is to consider a new metric that accounts for both probabilities. We define the concept of total error as the new metric in order to analyze the performance of the system considered. The total error is defined as

$$\begin{aligned} J(m,n,P_d,P_{fa}) &= Q_m + Q_f \\ &= 1-(Q_d - Q_f) \\ &= 1-\phi, \end{aligned} \tag{3.7}$$

where $Q_m = 1 - Q_d$ is the misdetection probability at the FC, and ϕ is defined as $\phi \triangleq Q_d - Q_f$. The total error is plotted in Fig. 3.2. It can be seen that there is a number k that minimizes both probabilities and prevents secondary system behavior from becoming overly aggressive or greedy when using primary system resources. In the next section, we provide further analyses of and insights from our previous discussion.

3.4 Total Error Analysis

The maximum value of $J(.)$ will not exceed one. This can be justified as follows. As $P_{fa} \to 1$, this results in $P_d \to 1$. Then $Q_f \to 1$, and $Q_d \to 1$. This is because the last term of the vector Q_f, Q_d defined in (3.5,3.6) will always be 1 as $m = n$. It follows then that $J(.) \to 1$. Also, As $P_{fa} \to 0$, this results in $P_d \to 0$. Then $Q_f \to 0$, and $Q_d \to 0$. It follows from both cases that the maximum value of $J(.)$ is one.

Lemma 3.4.1. *For a finite n, given that $n - k = L$, where $L < \infty$, J will not reach zero.*

Proof. As J has a maximum value of 1, and as J is given in (3.7) by $J = 1 - \phi = Q_m + Q_f$, then it is sufficient to prove that Q_m will not approach zero in the finite case. Therefore, we rewrite (3.6) as follows

$$Q_d = P_d^n + \sum_{m=1}^{L} \binom{n}{m} {P_d}^{n-m}(1-P_d)^m. \tag{3.8}$$

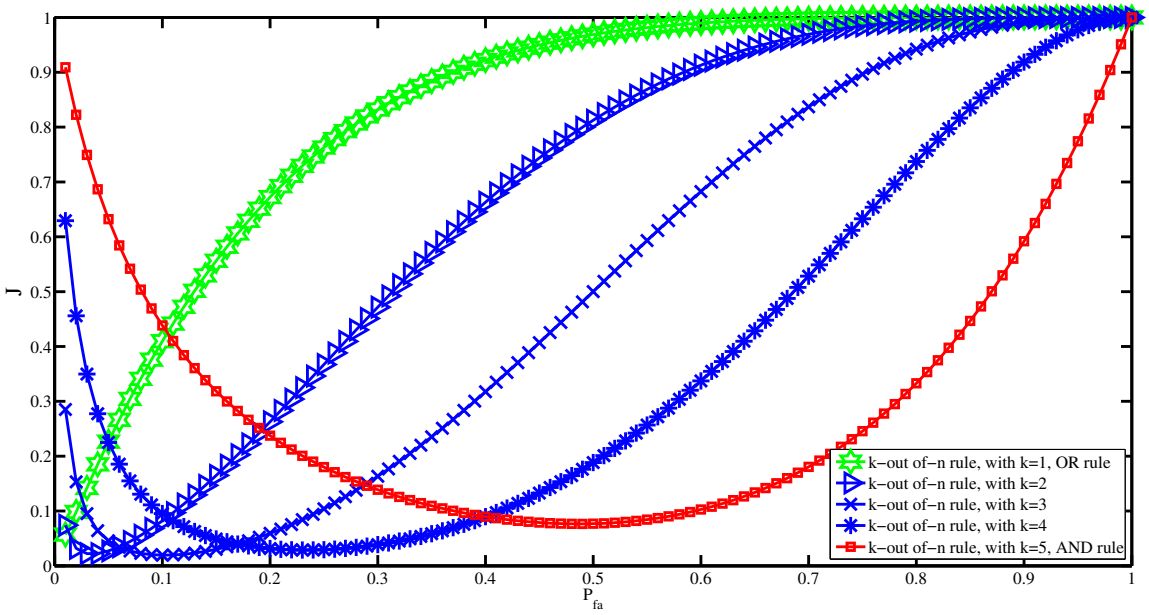

Figure 3.2: Total error with n=5, and k=1:5.

Let $P_d^n = \theta_0$ and R_j denote the ratio of the jth term to the $(j-1)$ term inside the summation of (3.8). Hence, we can rewrite (3.8) as

$$Q_d = \theta_0 + R_1\theta_0 + R_2R_1\theta_0 + ... + R_LR_{L-1}...R_1\theta_0. \tag{3.9}$$

Therefore (3.9) in terms of θ_0 can be written as

$$Q_d = e^{-a} + e^{-a}\sum_{j=1}^{L}\frac{a^j}{j!}, \quad \text{where} \quad a = -ln(\theta_0). \tag{3.10}$$

As the right-hand side of (3.10) is a monotone decreasing function of a, then Q_d can reach a value of 1 only when $a = 0$, which requires $-nln(P_d) = 0$. □

3.5 Optimal Number of CRs under Perfect Feedback Channels

In this section, we consider the feedback channel between the CRs and the FC to be perfect. Therefore, based on the previous results, we are looking for the minimum number of cognitive radio users, k, that are required to successfully detect the presence of a PU given a fixed false alarm probability. In other words, in cooperative spectrum sensing it is not necessary for all the users to detect the existence of a PU to minimize the error produced. There exists a number k that minimizes the error

that occurs. To find such a number, we have to revisit (3.5,3.6). Since Q_d and Q_f are the cumulative of a binomial distribution function, then from *Lemma 1*, it is known that (3.7) is a decreasing function of $\phi(n, m, P_d, P_{fa}) = (Q_d - Q_f)$. Obviously, $J \to 0$ as $\phi \to 1$. It follows then, from the cognitive radio system perspective, as a necessary and sufficient condition for $\phi \to 1$, we must have $Q_d \to 1$ and $Q_f \to 0$. That means we need to maximize Q_d and minimize Q_f, but both of them share the same two parameters m, n that affect the behavior of the binomial function. We conclude our finding by the following *Theorem*.

Theorem 3.5.1. *The optimal number of cognitive radios required to minimize the error $J(.)$ is*

$$k_{op} = \frac{\sigma_{Q_d}\mu_{Q_f} + \sigma_{Q_f}\mu_{Q_d}}{\sigma_{Q_d} + \sigma_{Q_f}}, \tag{3.11}$$

where $\mu_{Q_d} = nP_d$, $\mu_{Q_f} = nP_{fa}$, and $\sigma_{Q_d} = \sqrt{nP_d(1-P_d)}$, $\sigma_{Q_f} = \sqrt{nP_{fa}(1-P_{fa})}$.

Proof. Using the Demoivre-Laplace theorem [66], Q_d and Q_f are approximated as the cumulative distribution of a normal random variable when $n \to \infty$, i.e., J can be written as

$$J = 1 - (P_X(X \leq k) - P_Y(Y \leq k),$$

where X, Y are random variables representing Q_d and Q_f, respectively, and where $P_X(X < k)$, $P_Y(Y < k)$ represent the cumulative probability density function of the random variables X and Y, respectively. Then, deriving J with respect to k results in

$$\frac{\partial J}{\partial k} = -\frac{\partial X}{\partial k} + \frac{\partial Y}{\partial k} = 0$$

$$P_X(X = k) = P_Y(Y = k)$$

$$-\frac{k - nP_d}{\sqrt{nP_d(1-P_d)}} = \frac{nP_{fa} - k}{\sqrt{nP_{fa}(1-P_{fa})}},$$

which is the same point of the domain as the two random variables that reflect the minimum value k. Hence, J has a unique global minimum at the value of k. It follows then

$$k_{op} = \frac{\sigma_{Q_d}\mu_{Q_f} + \sigma_{Q_f}\mu_{Q_d}}{\sigma_{Q_d} + \sigma_{Q_f}}$$

□

3.6 Optimal Number of CRs under Imperfect Feedback Channels

In the previous section, we derived the optimal number of CRs which produced the minimum total error value when the feedback channel was perfect. However, in reality, the system is affected by the

channel between the CR user and the FC. Hence, when this channel is not perfect, the probability of false alarm and the probability of detection at the FC will also be affected by the probability of an error. If we define the probability that the FC receives an erroneous decision from the ith CR as P_{e_i}, written as $P_{e_i} = \Pr(FC_D = 0|PU = H_0, CR_i = H_1) = \Pr(FC_D = 0|CR_i = H_1) = \Pr(FC_D = 1|CR_i = H_0)$, where $\Pr(.)$ means probability, then, assuming that P_{e_i} is the same [1], the probability of false alarm with imperfect feedback channels at the FC can easily be found as [2]

$$\begin{aligned} Q_f^* &= \sum_{m=k}^{n} \binom{n}{m} [\Pr(FC_D = 1|PU = H_0)]^m [\Pr(FC_D = 0|PU = H_0)]^{n-m} \\ &= \sum_{m=k}^{n} \binom{n}{m} [\Pr(FC_D = 1|PU = H_0)]^m [1 - \Pr(FC_D = 1|PU = H_0)]^{n-m}. \end{aligned} \tag{3.12}$$

We denote the probability term $\Pr(FC_D = 1|PU = H_0)$ of (3.6) by α, which can be found as

$$\begin{aligned} \alpha &= \Pr(FC_D = 1|CR = H_1)\Pr(CR = H_1|PU = H_0) \\ &\quad + \Pr(FC_D = 1|CR = H_0)\Pr(CR = H_0|PU = H_0) \\ &= (1 - P_e)P_{fa} + P_e(1 - P_{fa}). \end{aligned} \tag{3.13}$$

Then, using (3.6) and (3.13), Q_f^* can be written as

$$\begin{aligned} Q_f^* &= \sum_{m=k}^{n} \binom{n}{m} [(1 - P_e)P_{fa} + P_e(1 - P_{fa})]^m [(1 - P_e)(1 - P_{fa}) + P_e P_{fa}]^{n-m} \\ &= \sum_{m=k}^{n} \binom{n}{m} \alpha^m (1 - \alpha)^{n-m}. \end{aligned} \tag{3.14}$$

Likewise, the probability of detection with an imperfect feedback channel at the FC can be found as

$$\begin{aligned} Q_d^* &= \sum_{m=k}^{n} \binom{n}{m} [\Pr(FC_D = 1|PU = H_1)]^m [\Pr(FC_D = 0|PU = H_1)]^{n-m} \\ &= \sum_{m=k}^{n} \binom{n}{m} [\Pr(FC_D = 1|PU = H_1)]^m [1 - \Pr(FC_D = 1|PU = H_1)]^{n-m} \end{aligned} \tag{3.15}$$

---

[1] This assumption have been adopted to ease the analysis and will not harm the idea presented. In other words, the purpose of using this assumption is mainly to provide a tractable performance expression but again, this assumption will not harm the key idea, i.e., deriving the optimal value of cognitive radios and the bounds of false alarm under imperfect sensing. Our key idea is still workable even if we relax this assumption, but the expression of the analysis will be too complicated and may prevent the readers from understanding the key idea. Also the CRs may be considered in a cluster of small size and in this case the feedback channel between them and the FC has the same effect on their decisions.

[2] The probability of a final decision at the FC is independent of which hypothesis is true, a property of a Markov chain.
To reduce the extensive use of notations, we distinguish the various parameters of an imperfect feedback channel by "*".

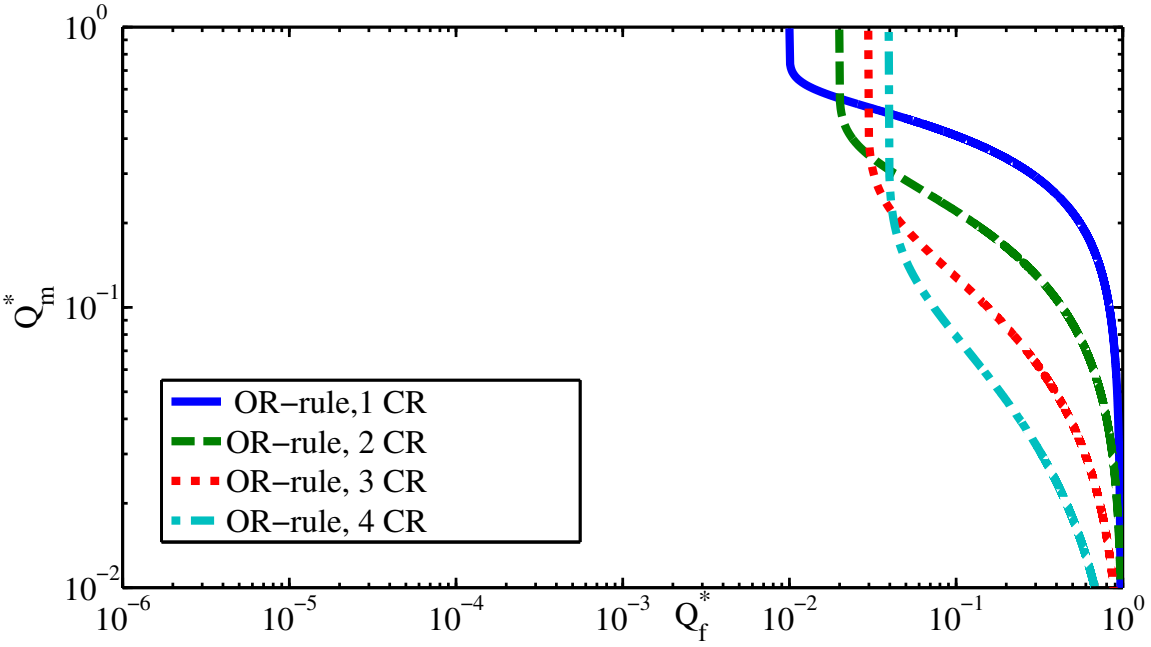

Figure 3.3: Performance results of the OR rule with $P_e = 0.01$ and SNR=10 dB.

We denote the probability term $\Pr(FC_D = 1|PU = H_1)$ of (3.15) by β, which can be found as

$$\begin{aligned}\beta &= \Pr(FC_D = 1|CR = H_1)\Pr(CR = H_1|PU = H_1) \\ &\quad + \Pr(FC_D = 1|CR = H_0)\Pr(CR = H_0|PU = H_1) \\ &= (1 - P_e)P_d + P_e(1 - P_d). \end{aligned} \tag{3.16}$$

Then, using (3.15) and (3.16), Q_d^* can be written as

$$\begin{aligned} Q_d^* &= \sum_{m=k}^{n} \binom{n}{m} [(1 - P_e)P_d + P_e(1 - P_d)]^m [(1 - P_e)(1 - P_d) + P_e P_d]^{n-m} \\ &= \sum_{m=k}^{n} \binom{n}{m} \beta^m (1 - \beta)^{n-m} \end{aligned} \tag{3.17}$$

Special cases of Q_f^*, Q_d^* when employing the OR rule, i.e., $k = 1$, and when employing the AND rule, i.e., $k = n$, can be easily obtained from (3.14) and (3.17), respectively.

To find the optimal value of k that minimizes the cost function $J(.)$ when the feedback channel is in error, we use (3.14) and (3.17). Note that Q_f^* and Q_d^* can also be approximated as the cumulative distribution of a normal random variable as $n \to \infty$. Hence, by applying *Theorem 1*, the optimal value of k, denoted as k_{op}^*, is given as

$$k_{op}^* = \frac{\sigma_{Q_d^*}\mu_{Q_f^*} + \sigma_{Q_f^*}\mu_{Q_d^*}}{\sigma_{Q_d^*} + \sigma_{Q_f^*}}, \tag{3.18}$$

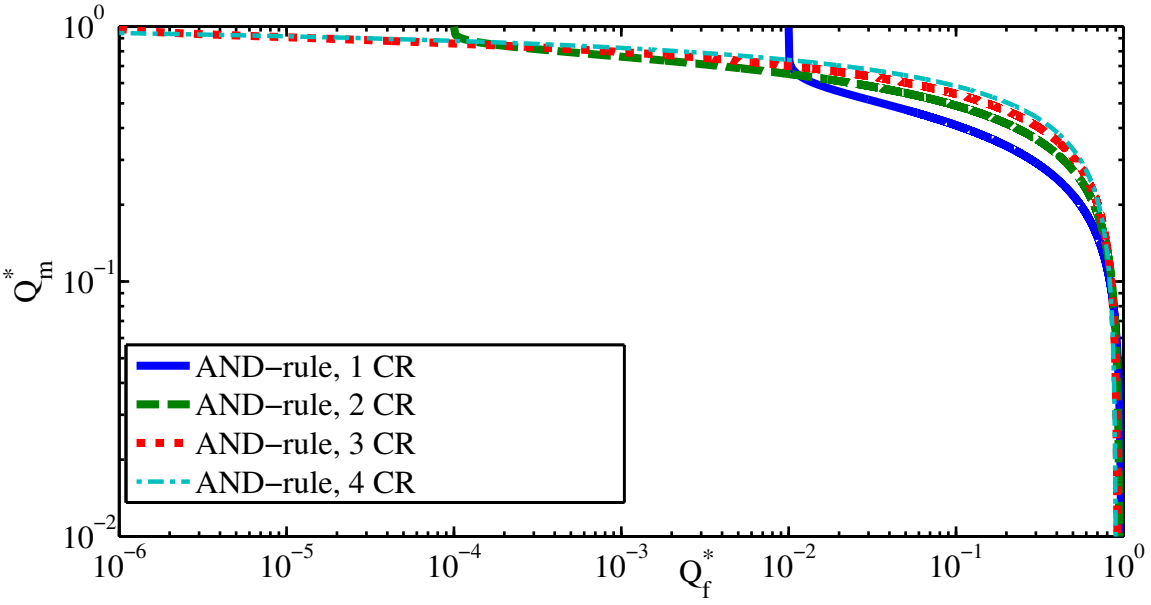

Figure 3.4: Performance results of the AND rule with $P_e = 0.01$ and SNR=10 dB.

where $\mu_{Q_f^*} = n\alpha$, $\mu_{Q_d^*} = n\beta$, and $\sigma_{Q_f^*} = \sqrt{n\alpha(1-\alpha)}$, $\sigma_{Q_d^*} = \sqrt{n\beta(1-\beta)}$.

3.6.1 Boundary of Q_f^* and the effect of the value k_{op}^*

Based on (3.14), Q_f^* will be bounded by the error in the feedback channel and this boundary affects the utilization of the SHs. To verify this statement mathematically, we take the limit of (3.14) as $P_f \to 0$. Then

$$\begin{aligned} lim_{P_{fa}\to 0} Q_f^* &= \sum_{m=k}^{n} \binom{n}{m} [(1-P_e)P_{fa} + P_e(1-P_{fa})]^m [(1-P_e)(1-P_{fa}) + P_e P_{fa}]^{n-m} \\ &= \sum_{m=k}^{n} \binom{n}{m} P_e^m (1-P_e)^{n-m}. \end{aligned} \tag{3.19}$$

The result indicates that the value of k will also affect this boundary, e.g., using the OR rule as a special case, the boundary will be

$$\bar{Q_f^*} = 1 - (1-P_e)^n \approx nP_e \tag{3.20}$$

Fig. 3.3 shows the performance results of cooperative spectrum sensing using the OR rule in which we plot the probability of misdetection $Q_m^* = 1 - Q_d^*$ versus the probability of false alarm at the FC with an imperfect feedback channel. It is obvious that increasing the number of CRs will increase this boundary, which is undesirable from a cognitive radio perspective. For example, the boundary

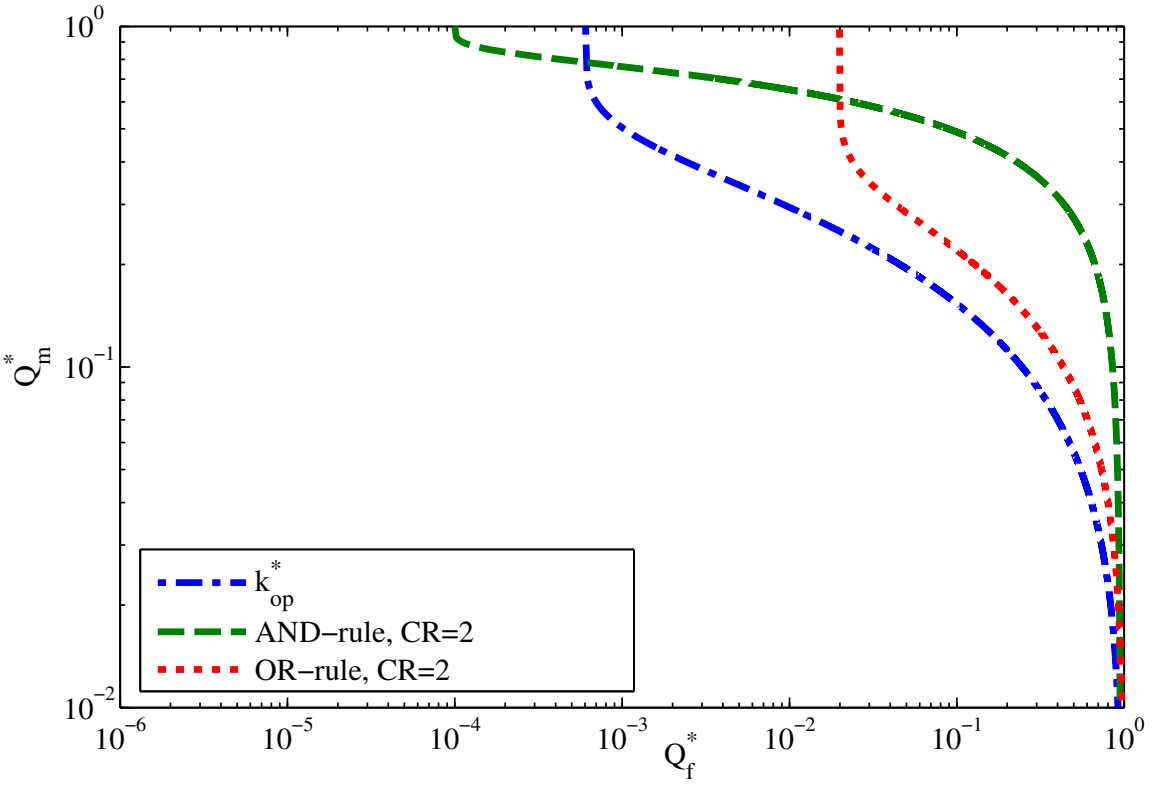

Figure 3.5: Performance results of AND rule, OR rule and k_{op}^*, with $P_e = 0.01$ and SNR=10 dB.

has a value of 0.01 for $CR = 1$ and 0.04 for $CR = 4$. This result is also consistent with (3.20). Therefore, in that sense, using one CR is better than using more CRs.

When using the AND rule, the boundary can be easily found by substituting $k = n$ into (3.19), which results in $\bar{Q}_f^* = P_e^n$. The result is plotted in Fig. 3.4. Obviously, the boundary decreases as we increase the number of CRs or when the feedback channel is in perfect condition. To have a clear picture of this boundary, in Fig. 3.5 we plotted the performance results for the AND rule, OR rule and k_{op}^*. It is now clear that increasing k will decrease such a boundary, and we conclude that the boundary has an upper limit when $k = 1$ and a lower limit when $k = n$. However, in case of k_{op}^* the value of this boundary lies in between these two extreme cases. Therefore, we conclude that $\bar{Q}_f^*$ is bounded as

$$P_e^n \leq \bar{Q}_f^* \leq nP_e \tag{3.21}$$

. However, although we are looking for an optimum point to choose as our constraint at the FC and despite the results obtained by the previously discussed cases, this boundary is far from being sharp as can be seen from (3.21). Therefore, the decision on how to optimize the design of CR systems is dependent not only on this boundary, but also on verification that this boundary value will guarantee a low misdetection probability. By looking carefully at the performance of the (OR rule, AND rule), we see that the more this boundary decreases, the worse the probability of misdetection is and vice versa. Therefore, these results assure us that the criterion represented by J is the optimal criterion to use in designing a CR system as it is the one that minimizes both probabilities in this application. The fact that the crux of cognitive radios is to protect the PU and at the same time maximize the utilization of SHs requires us to trade off between these two probabilities at the FC.

In Fig. 3.6, we compare the optimal value of k with a perfect/imperfect feedback channel, i.e., k_{op}, k_{op}^*. It can be seen that for a low value of λ, k_{op} tends to the AND rule implementation. On the contrary, for a high value of λ, k_{op} tends to the OR rule implementation. Also, in the imperfect feedback channel case, i.e., k_{op}^*, it can be seen that for a probability of error $P_e = 0.01$ in the feedback channel and a fixed λ, increasing the average SNR of the PU-SU link would result in k_{op}^* tending to the AND rule implementation.

Fig. 3.7 shows that we can easily compensate for a very high probability of error in the feedback channel. In other words, no matter what our threshold is and no matter how imperfect the feedback channel is, the choice of k_{op}^* will maximize utilization and minimize interference to the primary network.

Another point to consider given the result presented in (3.18) is the bandwidth of the feedback channel. This is considered to be one of the drawbacks of cooperative sensing as the CRs' decisions must be forwarded to a FC. This can be achieved by sending the local decisions through separate time slots within a frame or concurrently. However, such a method greatly affects the utilization of the SHs since the sensing time becomes longer or the system complexity increases. Another approach is to send the local decisions through orthogonal channels. However, a considerable bandwidth is

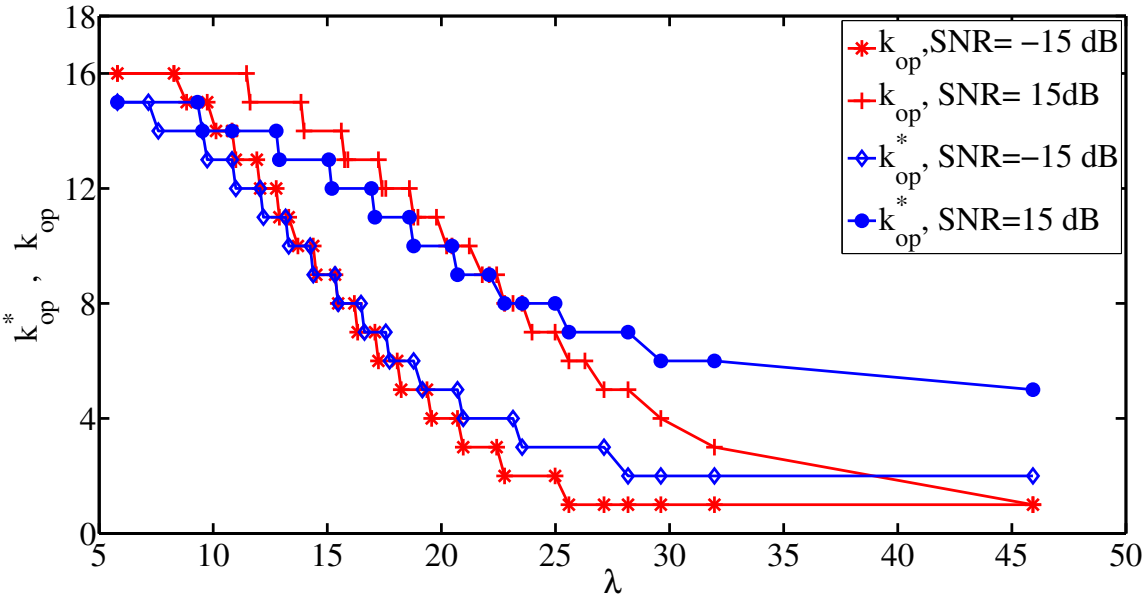

Figure 3.6: k_{op}, k^*_{op} comparison between a perfect and an imperfect feedback channel with $n = 16$, $P_e = 0.01$ and different values of SNR.

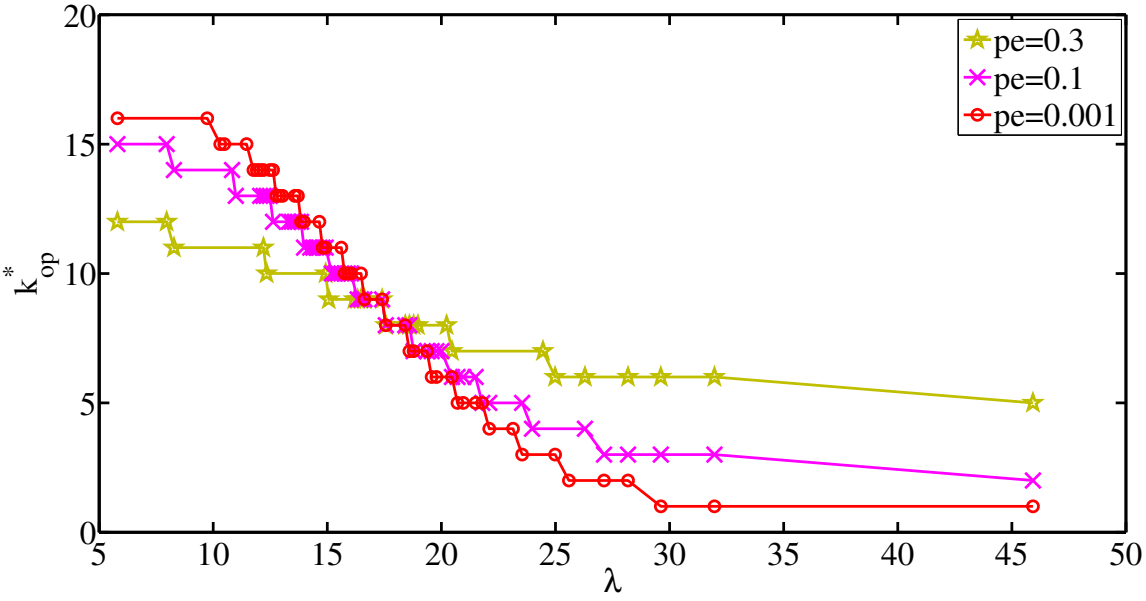

Figure 3.7: k^*_{op} with an imperfect feedback channel, $n = 16$, SNR=5dB, and different values of P_e.

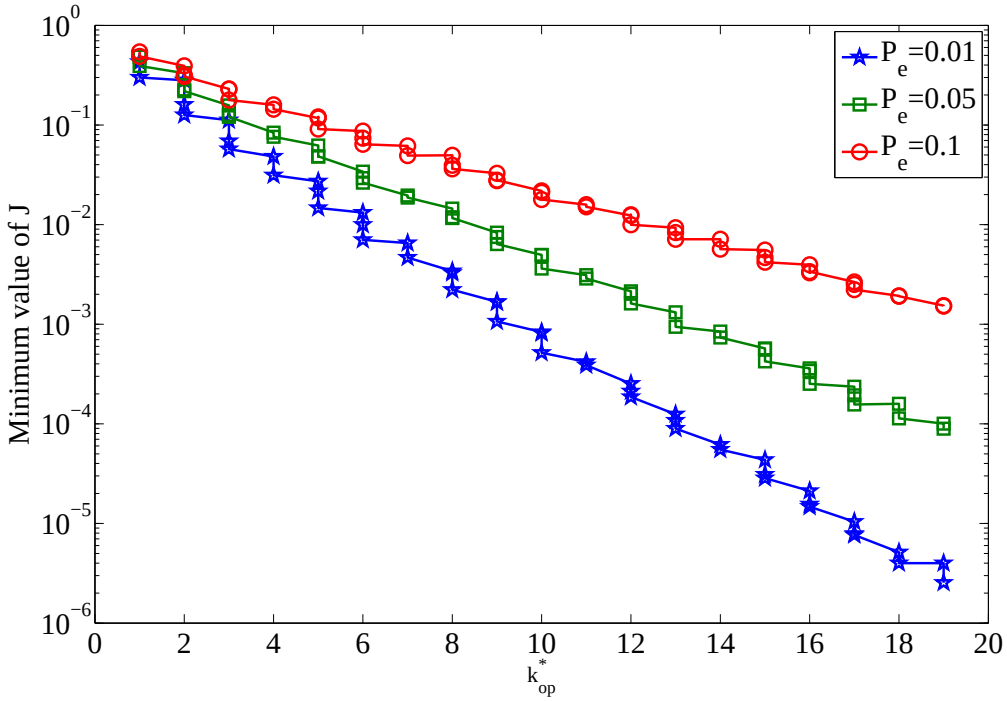

Figure 3.8: Minimum value of J vs. k^*_{op}, for $n = 1 : 50$, SNR=10 dB, $\lambda = 20$, and different values of P_e.

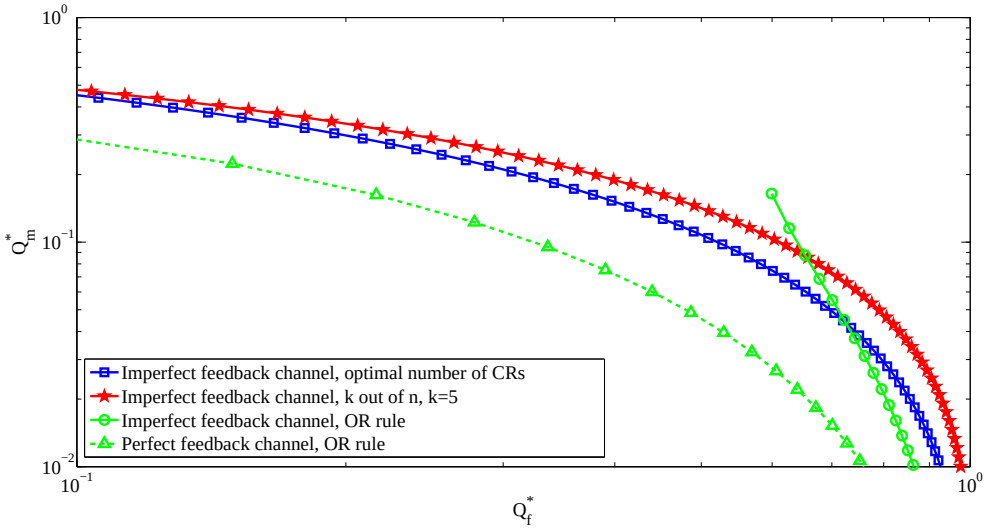

Figure 3.9: Probability of misdetection vs. probability of false alarm when applying the optimal number of CRs under a Rayleigh fading channel for SNR=5 dB, $n = 8$ and feedback channel error of $P_e = 0.1$.

needed. Therefore, the result presented in (3.18) is an efficient rule for the designers of CR systems enabling them to reduce the feedback channel bandwidth by choosing the optimal number of CRs to satisfy a target minimum error J. For example, as shown in Fig. 3.8, to achieve a total error J less than 0.01 with a feedback channel error of $P_e = 0.01, 0.05, 0.1$, the optimal numbers of CRs, according to (3.18), are 6, 8, and 12 respectively. Therefore, using no more than the optimal number of CRs considerably reduces the required bandwidth of the feedback channel while maintaining the minimum error value of J. Fig. 3.9 shows the complementary of the receiver operating characteristic (ROC) curves using the optimal number of CRs which is derived in (3.18). We also plot the OR rule with perfect/imperfect feedback channels and the k-out-of-n rule as references. It can be seen that the OR rule has a high rate of false alarms in the case of imperfect feedback channels. However, it can be seen that when the PU-CRs link is Rayleigh faded with SNR=5 dB and feedback channel error probability of $P_e = 0.1$, the optimal number of CRs outperforms the k-out-of-n rule for all false alarm values.

Fig. 3.10 shows a comparison between the optimal number of CRs, the OR rule and the k-out-of-n rule in terms of detection at the FC. As mentioned previously, the OR rule has a high false alarm probability. At $Q_f^* \leq 0.1$, it can be seen that the optimal number of CRs based on (3.18) performs better than the k-out-of-n rule for all values of p_e and SNRs.

Interestingly, with a high probability of error in the feedback channel, the detection probability at the FC is improved when the link between the PU and the CRs has a very low SNR value, i.e. at

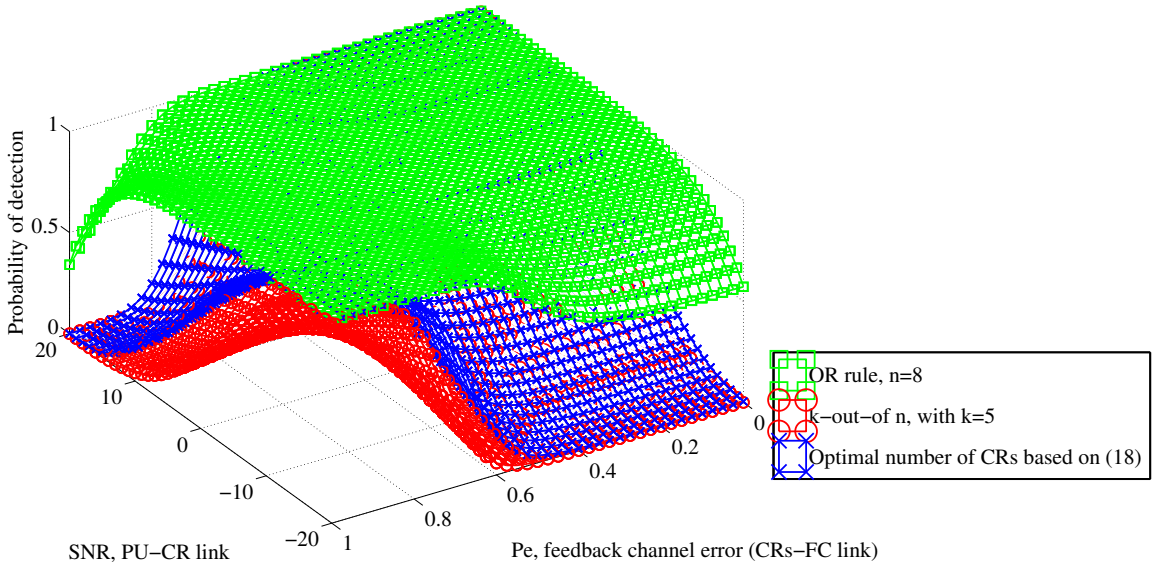

Figure 3.10: Performance of the detection probability Q_d^*, vs. P_e and the SNR of the PU-CRs link in a Rayleigh fading channel for $Q_f^* \leq 0.1$ and $n = 8$

a very low detection probability for individual CRs. This property can be easily proven from (3.17). As $P_e \to 1$, (3.17) can be written as

$$Q_d^* = \sum_{m=k}^{n} \binom{n}{m} [(1 - P_d)]^m [P_d]^{n-m}.$$

As a special case, when k=1, i.e. the OR rule, (3.22) can be written as

$$Q_d^* = 1 - (P_d)^n. \tag{3.22}$$

However, in this case (a high probability of error in the feedback channel), (3.22) also states that the high detection probability of individual CRs decreases the detection probability at the FC. However, the purpose of introducing cooperative sensing is to improve detection when fading and shadowing occur. Therefore, a low detection performance by CRs is always dominant in case of fading, and hence feedback channel errors can improve the detection probability at the FC if properly used. This can be seen from Fig. 3.10, where the three-dimensional plot shows the detection probability at the FC vs the feedback channel error probability P_e and the SNR of the PU-CRs link. In this case, that of a high rate of feedback channel error, as the individual detection probability of CRs decreases, the probability of detection at the FC increases. On the other hand, the detection probability at the FC worsens when the PU-CRs link is improved. This also confirms the fact that it is useless to use cooperative sensing when a single CR can do the job perfectly. The question to be asked here is: How we can utilize such errors to improve detection at the FC?

3.7 Conclusion

In this chapter, cooperative spectrum sensing under perfect/imperfect feedback channels is investigated. In particular, the optimal number of CRs required to minimize the total error of the sensing process when the reporting channel is perfect/imperfect is derived. Minimizing the total error reduces the number of orthogonal channels or the number of time slots needed to transmit the CRs' decisions in the feedback stage; hence, bandwidth expansion is avoided. In addition, we show that no matter how many cognitive radios cooperate in the sensing process, the total error will never reach zero. We also derive a general formula to calculate the boundaries of a false alarm probability, recognizing that reducing the value of this boundary *alone* will not result in improved system performance. However, the boundary resulting from the false alarm probability can easily be compensated for when the optimal value of k is chosen.

Further, we find that errors in the reporting feedback channel can easily be compensated for when the optimal number of CRs participating in the sensing process is used; therefore, the overall detection probability is improved. Interestingly, we find that errors in the feedback channel can improve the detection probability at a low SNR link between the PU and the CRs. But, how we can utilize the sensing errors in the feedback channel to improve the detection probability at the FC is still need more studies. Finally, as an indirect result of this study, we showed that having a dynamic threshold at the FC improves the overall performance of the two networks (PN and CRN).

Chapter 4

Opportunistic Spectrum Access Under Imperfect Sensing

In the previous chapters, local and cooperative spectrum sensing when using energy detector are researched. It has been shown that there are always inevitable errors (misdetection and false alarm) that occur during the sensing stage. These errors affect the performance of upper layers. Therefore, extensive research has been conducted in order to enhance the physical layer of DSA systems. There also an on-going research that investigates and proposes new protocols and algorithms to exploit the SHs that are detected by the sensing function. However, only minor research has been undertaken to develop a cross-design mechanism able to maximize DSA performance under imperfect sensing. To fully understand system behavior, a proper model is developed and its performance is investigated under different scenarios. We will illustrate this in the subsequent sections. In the following, we briefly discuss some previous works and elaborate on some of the reported results.

4.1 Objective

The main objective of CR is to utilize the SHs; then, it is a crucial to have an insightful view of the effect of the sensing errors on the system utilization. In this chapter a CTMC is used to model the considered system , and then evaluate it in terms of a number of GoS metrics. The analysis will be in terms of the SUs blocked probability which is defined as the ratio of SUs blocked to the total arrival rate of the secondary system, as well as the SUs dropped probability, which is defined as the ratio of the dropped SUs to the total arrival rate of the secondary system, and the total utilization of the secondary system.

4.2 Introduction

Recently, there has been considerable research on spectrum access in cognitive radio networks, e.g. [67–69]. These papers have addressed spectrum access and evaluated the system in terms of the aforementioned metrics. However, in these cases, the performance of the system was studied and the system analyzed under idle channel sensing, i.e. perfect sensing.

Recently, Tang et al. [29] studied the OSA system under unreliable sensing. In this work, the SUs were assumed to sense only one channel at a time to determine the access probability. However, a fundamental requirement for an SU is to sense a wide band of the spectrum [**?**]. This is because of the lower priority of SUs compared to PUs, meaning an SU must sense a wide band of the spectrum to enable it to determine which channels are spare channels which can be used for its transmission. Such a sensing ability will enhance the SU's reliability and enable it to continue its transmission when a PU requests, with no warning, a channel already occupied by an SU. The problem of switching channels or spectrum handoff under unreliable sensing and prioritized traffic was studied in [70]. In [71, 72], the modeling of opportunistic spectrum access under unreliable sensing was studied. However, the authors again consider that an SU can only sense one channel at a time. In addition, only cases where SU calls are blocked are considered. We will discuss this further later.

In this work, we consider that the SUs have the ability to sense all channels in the system. The result reported by [29] suggests that spectrum efficiency can be improved even under unreliable sensing; however, our mathematical and simulation models confirm that the SUs must be equipped with a reliable sensing function to fully exploit spectrum opportunities. Cooperative sensing does improve the detection of an SH; however, sensing errors still cannot be avoided as they can occur at any time. In this work, we do not consider a cooperative sensing scenario; however, the analysis can be easily extended to our case. Since sensing errors may occur at random, our objective in this chapter is to analyze and evaluate OSA in terms of a number of performance metrics when imperfect sensing by SUs is considered; specifically, we derive the probability of blocked calls and the probability of dropped calls for the primary system and the secondary system under imperfect sensing. Moreover, we evaluate secondary system utilization when sensing errors occur. Finally, a closed-form expressions for all of the mentioned metrics under perfect and imperfect sensing are derived.

4.3 Spectrum Sensing Model

Spectrum sensing is a binary hypothesis problem [12], which distinguishes between two hypotheses defined as

$$\begin{aligned} H_0: &\quad x(t) = w(t) \\ H_1: &\quad x(t) = s(t) + w(t) \end{aligned} \tag{4.1}$$

where H_0 is the hypothesis test when noise only is present, H_1 is the hypothesis test when both noise and signal are present, $w(t)$ is the noise component, and s(t) is the primary user signal component. Evaluating test Y, which is defined as $Y = \frac{1}{N_o}\int_0^T x(t)^2 dt$ [12], where N_o represents the one-sided noise spectral density, may cause two types of errors. When an SU detects H_1 while the actual state is H_0, this event is called a false alarm which occurs with a probability denoted by $P_{fa} = P(H_1|H_0) = Q\left(\frac{\lambda-2B}{\sqrt{4B}}\right)$, [1] where $Q(.)$ is the tail probability of the standard normal distribution, B is the time bandwidth product, λ is the detection threshold and γ is the SNR. When an SU detects H_0 while the actual state is H_1, this event is called misdetection which occurs with a probability denoted by $P_m = P(H_0|H_1) = 1 - Q\left(\frac{\lambda-2B-\gamma}{\sqrt{4(B+\gamma)}}\right)$ [12]. The complementary to P_m is the probability of detection $P_d = 1 - P_m = P(H_1|H_1)$.

4.4 Markov Chain Modeling

Consider a system of C channels, where all channels are available to the PUs. Access is controlled by the primary controller, and the system is opportunistically available to secondary users when PUs are absent. From a practical point of view, the PUs, also known as licensed users, are unaware of the activity of the SUs, also known as unlicensed users; therefore, a PU may use a channel already occupied by an SU, causing the SU transmission to drop. The drop occurs because of a lack of communication between the two systems or an unwillingness to modify the infrastructure of the PU system due to cost. The SUs, however, maintain an awareness of the PUs activity by employing a sensing function and transmitting whenever a channel is available.

We assume the arrival rate of PUs and SUs follows a Poisson process with arrival rates of λ_p and λ_s respectively. The service time is exponentially distributed with mean service times $1/\mu_p$ and $1/\mu_s$ respectively. These assumptions are valid considering that the number of users is much greater than the number of available channels [29, 73]. Consider the general state (i, j), where i represents the number of PUs and j represents the number of SUs. Fig. 4.1 summarizes the transition states, under

[1] For large number of samples and using the central limit theorem, the distribution of test Y can be approximated as Gaussian [12].

perfect sensing, of a PU arrival/departure denoted by the solid line, and an SU arrival/departure denoted by the dotted line.

4.4.1 Perfect Sensing

The following cases describe system behavior when a PU arrives:

- Case I: A PU arrives and finds an idle channel not occupied by any other PU. The probability of this event is equal to $\frac{C-i-j}{C-i}$; therefore, the transition rate from state (i,j) to $(i+1,j)$ is given as $\frac{(C-i-j)}{(C-j)}\lambda_P$ [74].
- Case II: A PU chooses a channel occupied by an SU, which causes a collision with the SU transmission; in this case, the transition rate from state (i,j) to state $(i+1,j-1)$ will be $\frac{j}{C-i}\lambda_p$, and the total probability of a dropped SU call can be computed as

$$P_{drop,SU} = \sum_{\substack{i,j \\ i+j \leq C}} \frac{j\lambda_p}{(C-i)\lambda_s}. \tag{4.2}$$

- Case III: A PU arrives and all channels in the system are occupied by other PUs, i.e., $i = C, j = 0$; in this case, the new PU request will be blocked. Hence, the probability of a PU being blocked is given by

$$P_{block,PU} = P(C,0), \tag{4.3}$$

  where $P(i,j)$ is the steady-state probability of state i,j.

Now we will consider an SU arrival, which can be described by the following cases:

- Case I: An SU arrives and a channel is available; therefore, the transition rate from state (i,j) to state $(i,j+1)$ is λ_s, for $i+j<C$.
- Case II: An SU arrives and no channel is available, resulting in a blocked request; therefore, an SU request will be blocked only when $i+j=C$, and the probability of a blocked SU is given by

$$P_{block,SU} = \sum_{\substack{i,j \\ i+j=C}} P(i,j). \tag{4.4}$$

All other cases, i.e. with no PU or SU arrival, are considered to be successfully completed, hence the PU departure rate from state (i,j) to $(i-1,j)$ is $i\mu_p$. Likewise, the SU departure rate from state (i,j) to state $(i,j-1)$ is given as $j\mu_s$.

If we define $s=(i,j)$ as the instantaneous state of the CTMC model presented in Fig. 4.1, then it has the state space:

$$\Omega = \{s : 0 \leq i,j \leq C, i+j \leq C\}.$$

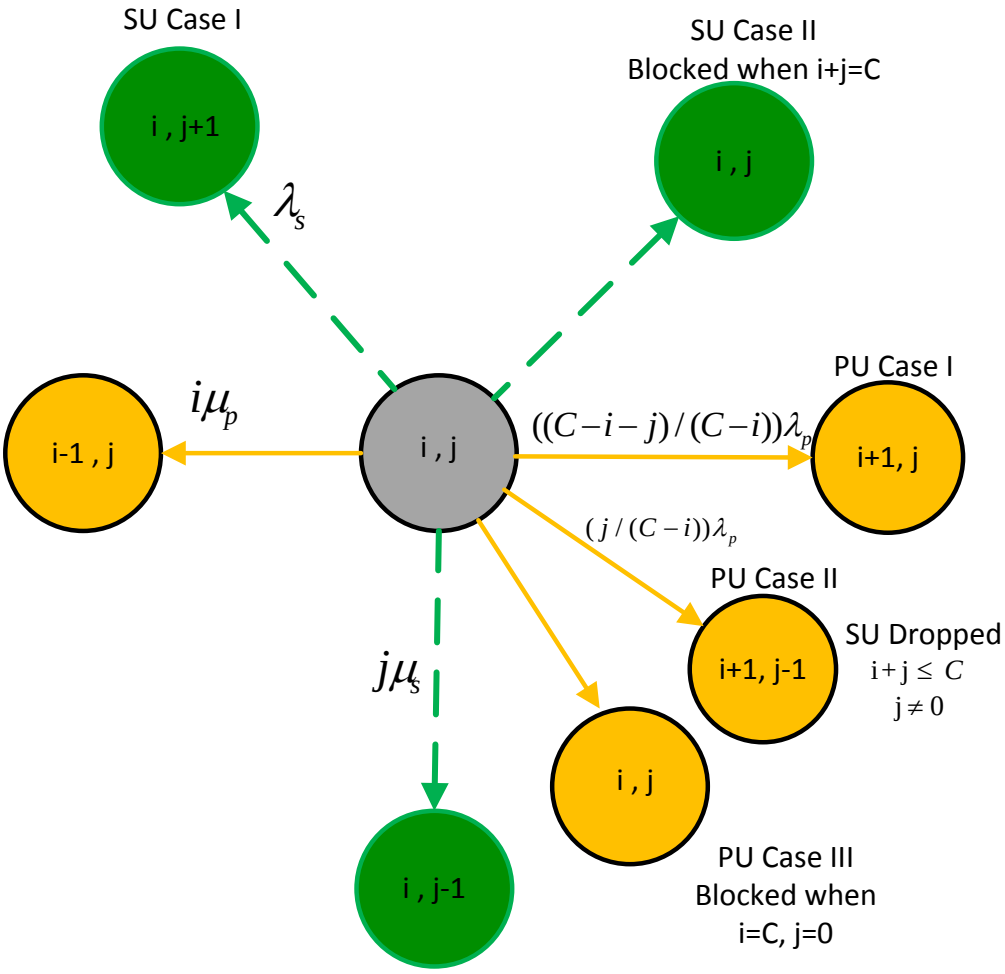

Figure 4.1: Transition diagram under ideal sensing.

The system of linear equations which is formed from the Markov chain model can be written in vector-matrix form as

$$\mathbf{pQ} = \mathbf{0}, \tag{4.5}$$

where $\mathbf{p}$ is the steady-state probability vector, and $\mathbf{Q}$ is the infinitesimal generator matrix which characterizes the transition of the states of the Markov chain [75]. To yield a unique positive solution, (4.5) can be solved with the imposed normalization condition of the steady state probability, which is defined as

$$\sum_i \sum_j P(i,j) = \mathbf{p1} = 1, \quad \forall (i,j) \leq C \tag{4.6}$$

where $\mathbf{1} = [1, 1, 1, ..., 1]^T$, where T indicates the transpose operation. Hence, the steady state probability vector $\mathbf{p}$ can be found by changing the last column of $\mathbf{Q}$ by the vector $\mathbf{1}$, which yields the new invertible matrix $\mathbf{Q'}$, i.e. (4.5) becomes $\mathbf{pQ'} = \mathbf{b}$, where $\mathbf{b}$ is a row vector which was formed by this operation, i.e. $\mathbf{b} = [0, 0, ..., 1]$. Then, $\mathbf{p}$ can be found as

$$\mathbf{p} = \mathbf{bQ'^{-1}} \tag{4.7}$$

The dimension of the matrix $\mathbf{Q}$ in terms of C is given as $[(C+1)(C+2)/2, (C+1)(C+2)/2]$. It follows then, and by using (4.7), Equations (4.2), (4.3) and (4.4) can easily be evaluated in the ideal sensing case. In what follows, we will evaluate the system with imperfect sensing results.

4.4.2 Imperfect Sensing

The probability that an SU detects an idle channel is the probability that it detects H_0 when H_0 is true, denoted as $\beta = P(H_0|H_0) = 1 - P_{fa}$, which is the complement of the false alarm probability. Since the PUs are not aware of the SUs, then the transition diagram shown in Fig. 4.1 will be modified only for cases in which an SU arrives. Before analyzing the proposed system with respect to an SU arrival under imperfect sensing, we should note that at any time the number of available channels in the system will be $N_{av} = C - N_{oc}$, where N_{oc} is the total occupied channels and is given as $N_{oc} = i + j$. Then, the probability of an arriving SU sensing l busy channels of the occupied channels incorrectly is given as[2] $\binom{N_{oc}}{l} P_d^{N_{oc}-l} P_m^l$. Among the available channels, the probability of an SU sensing k idle channels correctly is $\binom{N_{av}}{k} {P_{fa}}^{N_{av}-k} \beta^k$. As we considered earlier that the system is in the general state (i, j), the following summarizes all of the SU arrival cases it may face:

- Case I: An SU arrives and there is no collision with a PU or other SUs. We denote this event as E_1, and the probability of this event can be computed as

$$P_{E_1} = \sum_{k=1}^{N_{av}} \binom{N_{av}}{k} \beta^k P_{fa}^{N_{av}-k} \sum_{l=0}^{N_{oc}} \frac{k}{l+k} \binom{N_{oc}}{l} P_d^{N_{oc}-l} P_m^l. \tag{4.8}$$

[2] the symbol $\binom{n}{m} = \frac{n!}{m!(n-m)!}$

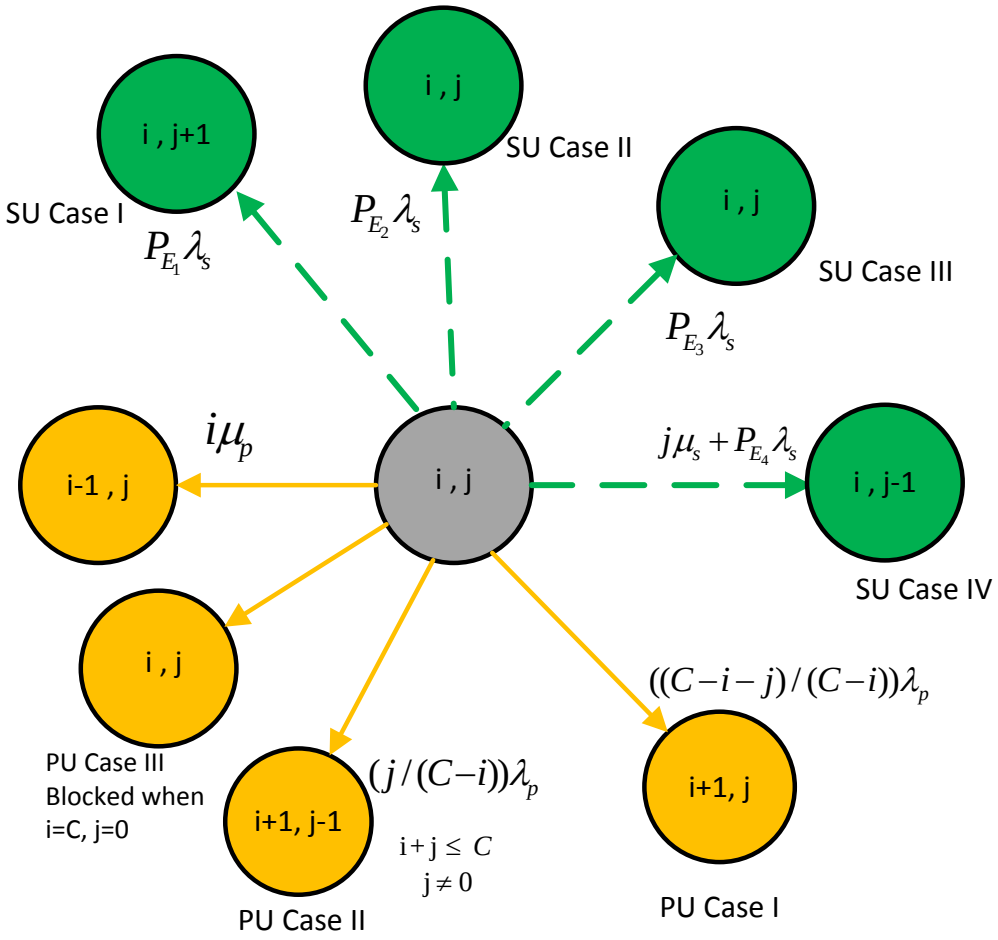

Figure 4.2: Transition diagram under imperfect sensing.

The transition rate from state (i, j) to state $(i, j+1)$ is then $P_{E_1}\lambda_s$.

- Case II: An SU arrives and all channels are busy. We represent this event by E_2 and its probability is given by

$$P_{E_2} = P_d^{N_{oc}}(1-\beta)^{N_{av}}. \tag{4.9}$$

This event represents the probability of a blocked call in the current state; it follows then that the total probability of an SU being blocked with imperfect sensing will be[3]

$$P^*_{block,SU} = \sum_{i,j} P(i,j)P_{E_2}(i,j). \tag{4.10}$$

- Case III: An SU arrival interferes with a PU transmission due to a sensing error in detecting a PU occupied channel; we denote this event by E_3. The probability of this event will be the probability of wrongly detecting a channel already occupied by a PU or an SU and the probability of right-detecting the actual available channels N_{av}, i.e., mathematically we can write the probability of this event as

$$P_{E_3} = \sum_{k=1}^{i} \binom{i}{k} P_d^{(i-k)} P_m^k \sum_{n=0}^{j} \binom{j}{n} P_d^{(j-n)} P_m^n \sum_{l=0}^{N_{av}} \frac{k}{l+n+k} \binom{N_{av}}{l} P_{fa}^{(N_{av}-l)} \beta^l. \tag{4.11}$$

The rationale for (4.11) is that the SU cannot distinguish between an SU transmission and a PU transmission. In this case, the arriving SU will be dropped and the probability of a dropped call due to this event is given as

$$P^*_{drop_{E_3},SU} = \lambda_s P_{E_3}/\lambda_s = P_{E_3} \tag{4.12}$$

Note that the system will stay in its current state and no transition occurs here.

- Case IV: An SU arrives and collides with another SU transmission. We denote this event by E_4. Thus, the probability of this event can be computed as in event E_3, and is given as

$$P_{E_4} = \sum_{k=1}^{j} \binom{j}{k} P_d^{(j-k)} P_m^k \sum_{n=0}^{i} \binom{i}{n} P_d^{(i-n)} P_m^n \sum_{l=0}^{N_{av}} \frac{k}{l+n+k} \binom{N_{av}}{l} P_{fa}^{(N_{av}-l)} \beta^l. \tag{4.13}$$

[3]To reduce the excessive use of notation, we distinguish the probabilities and all related parameters of imperfect sensing by an "*".

The probability of a dropped call due to this event will then be

$$P^*_{drop_{E_4},SU} = \lambda_s P_{E_4}/\lambda_s = P_{E_4}. \tag{4.14}$$

Hence the transition rate from state (i, j) to state $(i, j-1)$ will be $j\mu_s + P_{E_4}\lambda_s$, where the first term indicates an SU successfully completed its transmission and the second term indicates a dropped call caused by a collision between two SUs.

To compute the total probability of a dropped call in the secondary system in the current state (i, j), we add the probability of a dropped call for all events that cause an arriving SU to be dropped. Therefore, the total probability of a dropped call in the current state will be

$$P^*_{drop,SU} = P_{E_3} + 2P_{E_4} + \frac{j\lambda_p}{(C-i)\lambda_s}, \tag{4.15}$$

where the first term represents a collision with a PU, the second term represents a collision between two SUs (the new arrival and the already connected SUs), and the third term represents a dropped call caused by a PU arrival (PU case II). Fig. 4.2 summarizes the potential transitions with imperfect sensing results. Using the previous discussion and the transition diagram of Fig. 4.2, we can reconstruct the infinitesimal generator matrix $\mathbf{Q}$ due to imperfect sensing. Following the same procedure discussed earlier and after modifying the transition matrix $\mathbf{Q}$, we can solve for the steady state probability using (4.7). To account for the total probability of a dropped call in the secondary system, we use (4.15). The total probability of a dropped call can then be computed as

$$P^*_{drop,SU} = \sum_{i,j} P(i,j)[P_{E_3}(i,j) + 2P_{E_4}(i,j) + \frac{j\lambda_p}{(C-i)\lambda_s}]. \tag{4.16}$$

Since dropped and blocked services do not count as successful radio traffic, another performance metric of importance to the considered secondary system is the effective spectrum utilization U, which is defined as

$$U = [1 - P^*_{block,SU} - P^*_{drop,SU}]\rho/C \tag{4.17}$$

where $P^*_{block,SU}$ is total blocked probability as defined in (4.10), $P^*_{drop,SU}$ is the total dropped probability as defined in (4.16) and ρ is defined as $\rho = \lambda_s/\mu_s$. Using this definition we account for only the actual SU traffic served by the considered system.

4.5 Simulation Performance and Results Discussion

An event-based simulation using Matlab was used to evaluate and verify the theoretical results derived from the considered performance metrics. Assuming $C = 10$, $\lambda_p = 2.15$ min^{-1}, $\mu_p = 0.5$

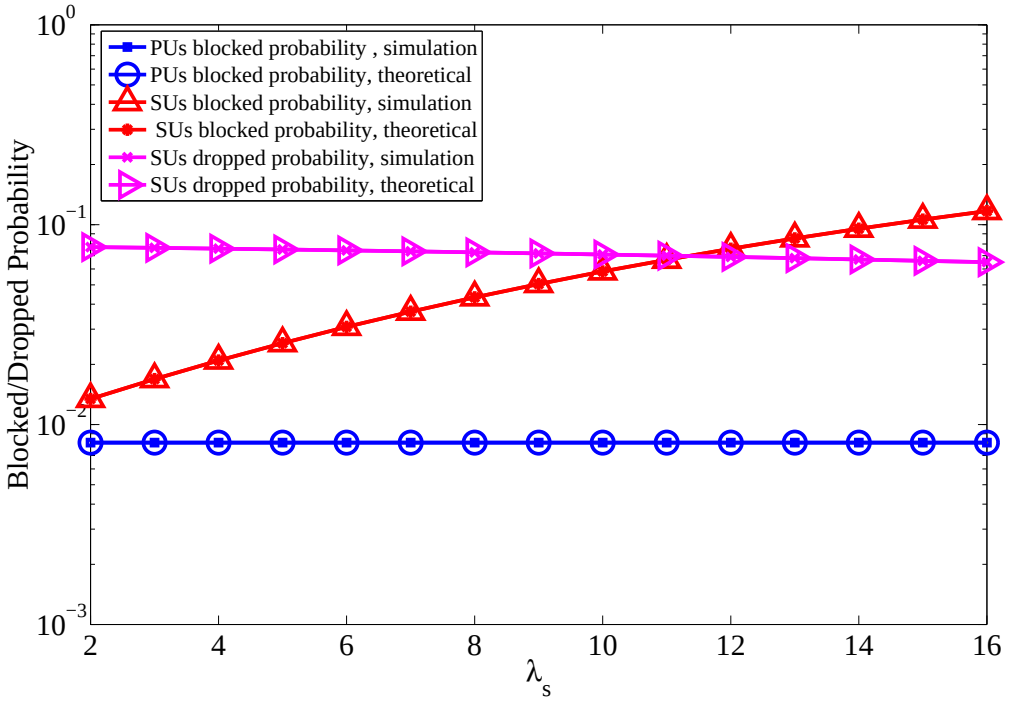

Figure 4.3: Blocked/Dropped probability: Comparison between simulation and theoretical probabilities under perfect sensing.

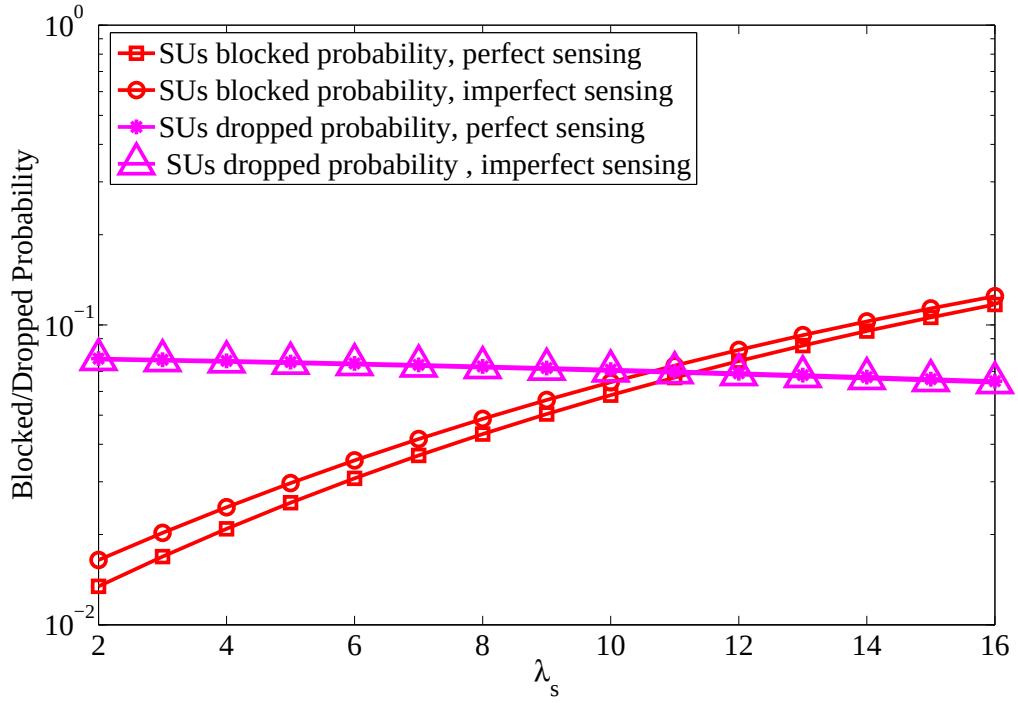

Figure 4.4: Blocked/Dropped probability: Comparison between perfect and imperfect sensing with SNR = -5 dB, $P_{fa} = 0.1$, and $\mu_s = 5$.

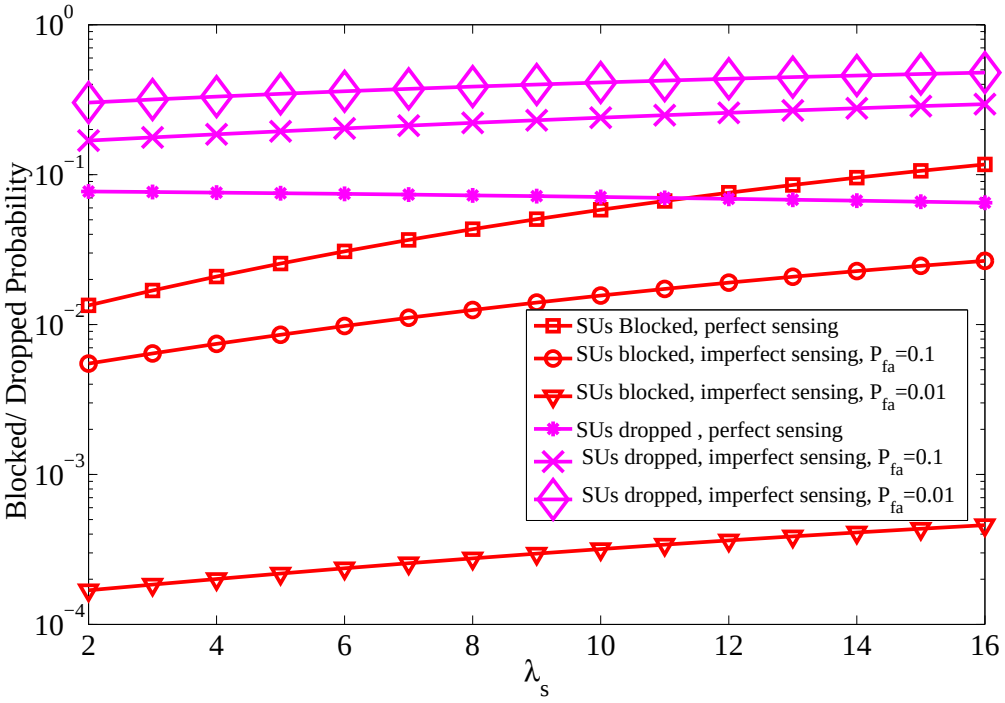

Figure 4.5: Blocked/Dropped probability: Comparison between perfect and imperfect sensing with SNR = -10 dB, and $\mu_s = 5$.

min^{-1} and $\mu_s = 5\ \text{min}^{-1}$, Fig. 4.3 shows a comparison between the theoretical results and the event-based simulation results in the ideal sensing situation. We plot $P_{block,PU}$, $P_{block,SU}$ and $P_{drop,SU}$, which correspond to equations (4.2)-(4.4) respectively, versus λ_s. As a function of λ_s, $P_{block,PU}$ remains constant and coincides with the theoretical finding as the traffic load λ_p/μ_p for the primary system is fixed and the primary system has higher precedence than the secondary system. Having a closer look at $P_{block,SU}$ and $P_{drop,SU}$, the former is an increasing function of λ_s; the greater the arrival rate of SUs, the more likely they will be blocked, as SUs have lower precedence. However, the latter will slightly decrease with an increasing λ_s. We should also note that the probability of a dropped call is initially higher than the probability of a blocked call for the secondary system; however, a point is reached where dropping becomes less severe than blocking. The reason for this is the greater the number of calls being blocked, the less probability there is of having SUs collide with PUs or other SUs in the system, which causes them to be dropped.

To evaluate and analyze the effect of imperfect sensing on the considered system, extensive simulations were conducted by changing various parameters. Fig. 4.4 shows a comparison between perfect and imperfect sensing, with SNR = -5 dB, $P_{fa} = 0.1$, and the number of samples equaling 200. It can be seen that the probability of a dropped call is not affected at all by imperfect sensing, as fewer collisions with PUs and/or SUs occur due to the higher detection probability. On the other hand, the probability of a blocked call is higher than in the ideal sensing case, and this is due to the effect of the probability of false alarms as can be seen from (4.10).

In order to detect the very low level of a PU signal, the SU must have a sensitivity as much as 20-30 dB higher than that of the PU [76]. Therefore, in Fig. 4.5, two cases are studied. In the first case, we have reduced the SNR value to -10 dB and have kept the $P_{fa} = 0.1$ to see the effect of reducing the detection performance of the system. We note that the probability of a dropped call is considerably increased. This is expected, as more collisions with PUs and SUs occur due to events E_3, E_4. The unexpected result is the reduction of the probability of blocked calls and that can be explained as follows. Since the probability of dropped calls increases, more already connected SUs are dropped. This results in the availability of more channels to incoming SUs. The more channels are available, the lower the probability of event E_2 occurring; as a consequence, the probability of a call being blocked is reduced as seen in (4.10). In the second case, we have kept the SNR at -10 dB and have decreased $P_{fa} = 0.01$. It can be seen in Fig. 4.5 that the dropped probability slightly increased as reducing false alarms increases the misdetection probability, which then causes more collisions between PUs and SUs. However, the blocked probability is considerably decreased. The reason for the decrease is that more dropped calls allows more channels to be available to newly arrived SUs, and also reduces false alarms allowing the SUs to be more aggressive. This results in fewer occurrences of event E_2 and therefore the number of blocked calls is reduced.

Finally, we ran the simulation to compare the spectrum utilization of the secondary system in ideal and non-ideal sensing situations according to (4.17). Fig. 4.6 and Fig. 4.7 show the results

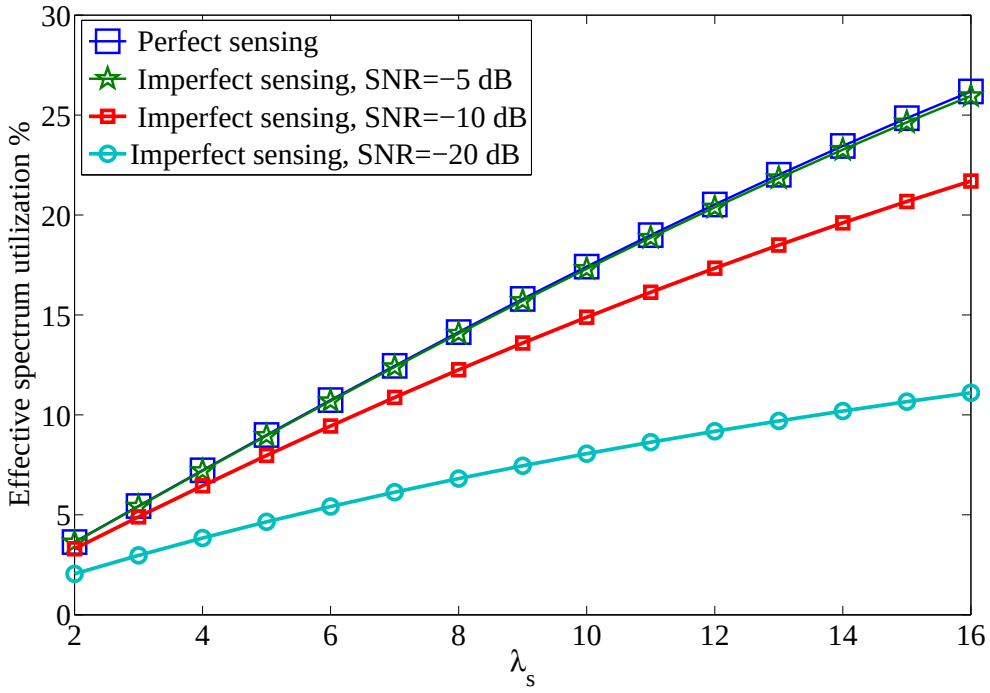

Figure 4.6: Secondary system utilization: Comparison between perfect and imperfect sensing with different values of SNR, $P_{fa} = 0.1$, $\mu_s = 5$.

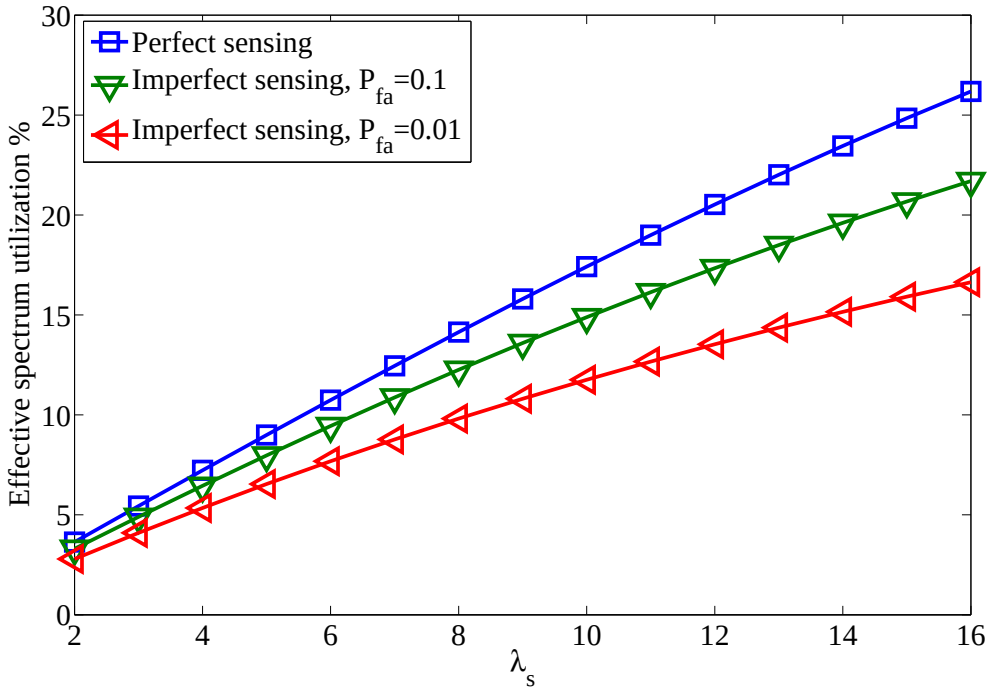

Figure 4.7: Secondary system utilization: Comparison between perfect and imperfect sensing with different values of P_{fa}, $\mu_s = 5$, and SNR = -10 dB.

of this comparison. It can be seen that sensing degradation considerably reduces the utilization of the whole system. For example, in Fig. 4.6 at SNR = (-10, -20) dB, the spectrum utilization of the secondary system is much lower than in the case of perfect sensing. In this case, more SHs are underutilized by the secondary system due to the increase in the dropped probability. However, reducing the misdetection by increasing the SNR value to -5 dB results in only minor differences in secondary system utilization. In Fig. 4.7, it can be seen that reducing the false alarm probability also degrades the spectrum utilization of the secondary system as reducing false alarms increases the misdetection probability which then causes more collisions between PUs and SUs. It should be noted that the utilization shown in Fig. 4.6 and Fig. 4.7 is for the secondary system only.

4.6 Conclusion

In this chapter, we introduce a complete mathematical analysis for an OSA system with imperfect sensing results. We analyze three performance metrics, the probability of blocked calls, the probability of dropped calls and the spectrum utilization of the secondary system, using a continuous Markov chain model. A simulation study is presented to corroborate the analytical results and to demonstrate the performance of OSA under imperfect sensing conditions. An extensive simulation is conducted to evaluate and analyze the effect of sensing errors on the considered system. Our results demonstrate the usefulness of a reliable sensing function for the effective utilization of SHs. Our mathematical modeling may be considered as a basic milestone for further analysis and investigation.

Chapter 5

Opportunistic Spectrum Access Under Imperfect Sensing with Nonstandard Policies

In chapter 4, the effect of imperfect sensing on the performance of OSA is investigated. A continuous-time Markov chain is used to model the interaction between the PUs and SUs on the considered system, and then evaluate it in terms of the probabilities of users being blocked or dropped. Our results demonstrate that the performance of the underlying system degrades significantly when imperfect sensing is considered; thus, there is a pressing need for a reliable spectrum sensing scheme to improve the overall quality of service in practical scenarios. However, there should be other means to improve the spectrum utilization even with sensing errors. This will be discussed and analyzed in the following sections.

This chapter is organized as follows. The main objective, related works and the sensing process are discussed in Section , and . Markov chain-based analysis of all proposed policies are presented in section . The simulation results are discussed in Section , and chapter is concluded in section .

5.1 Objective

The main objective of this chapter is to study and analyze the DSA system when non-standard policies are adopted by the primary system. In this chapter, two non-standard access policies are proposed for a cognitive radio network. For each policy, we develop a CTMC model to describe the DSA system and evaluate its performance in terms of blocking probability, dropping probability and

system utilization. Further, we consider the effect of sensing errors and compare the performance of these access policies with the DSA standard policy.

5.2 Introduction

In [67], Xing et al. investigated CTMC models for DSA in open spectrum cognitive wireless networks. The following assumptions were considered:

- [1]AS1: the sensing of the radio system is perfect, i.e. the detection of spectrum holes is perfect;
- AS2: a standard-access policy, which has been analyzed in chapter 4 and will briefly be clarified later, is adopted by the radio systems sharing the specified bandwidth;
- AS3: the radio systems are unaware of each other and when collisions occur due to erroneous idle channel detection by the radio systems, one radio system at random will pick the channel and the others will be dropped, i.e. under this assumption, collisions are omitted or the effects of collisions are not considered in any of the discussed scenarios;
- AS4: all of the radio systems which are using or could in the future use the shared channels are synchronized;
- AS5: all radio systems operate on a non-licensed band with equal priority.

All of the above were assumed to simplify the model of the system; however, some of these assumptions need to be relaxed so that our model will represent the real system reasonably well. For example, in reference to AS1, sensing is not perfect and sensing errors must be considered so that a system model will be close to the practical one. AS3 is also a critical assumption as collisions occur in practice. The same applies to AS4, since it requires communication between these radio systems. However, if such communication existed, there would be no need for sensing, as the central node or a known non-central node that is equipped with a management protocol could be used to allocate the available spectrum. On the other hand, AS5 is a non-critical assumption; however, this means the priority of any radio system is the same whereas it is well known that in DSA, PUs have priority over SUs.

Recently, in [77], the tradeoff between spectrum efficiency and fairness for DSA using a CTMC approach was investigated. Therein, AS5 was relaxed by giving higher priority to PUs; however, AS1 was considered to hold. AS3 was relaxed by adding another assumption, that is, that the access of SUs is controlled by a secondary management node that tells them if idle-detected SHs are already occupied by PUs or SUs. This enables collisions to be avoided. However, a further simplification to

[1]AS_i means assumption number i

the model is possible if we consider only the central node as the SU instead of modeling the SUs that communicate with this node.

In other work (e.g. [78–81]), the central node assumption was relaxed by considering a common control channel to do the work instead of using a central node; this is considered to be a distributed system. In a recent work [70], prioritized SU traffic with perfect sensing and full awareness of the channel status used by either PU or SU systems was analyzed. Other works (e.g. [82–85]) modeled the DSA system at the frame level or the call level. They also utilized some of the above assumptions while relaxing others, and different performance metrics were evaluated.

While various assumptions have been made in the works previously discussed, all of the above related works share one major assumption: AS1. However, since sensing is not perfect, then sensing errors should also be considered in modeling DSA system.

In [29, 71, 72], the modeling of DSA with unreliable sensing was studied. However, the authors considered only a standard access policy for the PU system and assumed that an SU could only sense one channel at a time. In addition, only the cases where an SU call was blocked were considered. We will discuss this further later.

Modeling and analysis of DSA depend mainly on the primary system policy, the secondary system policy, and the ability of the SU sensing functionality (single channel or multichannel). If we assume that the primary system uses the standard policy (that PUs are unaware of the SUs existence and that they have priority over the SUs), then collisions will occur between the two systems. This type of system and the performance metrics which may be affected by this policy are discussed and analyzed in chapter 4.

Under the standard policy, PUs are unaware of the SUs occupancy; in this case, the SUs dropped probability will be affected even if the system was not fully loaded. To clarify this point, assuming perfect sensing results, the dropped probability will occur in all states except states where there is no PU. Such a policy will entail more degradation to the GoS from the point of view of the secondary system because the dropped probability has a greater effect on system performance than the blocked probability does. Therefore, the total spectrum utilization of the combined system will also be affected even with perfect sensing results and the number of less satisfied secondary users will increase.

Although adopting different policies may sometimes require a change in the infrastructure of the primary system, such policies can often be easily implemented without change, i.e. by a noise signal from the secondary system that indicates that a channel is in use, or by using existing protocols, such as a clear to send/request to send (CTS/RTS) protocol. Hence, there is no need to fully modify

the infrastructure of the primary system and the priority of PUs over SUs is kept. The analysis of such policies will also show the upper boundary of spectrum utilization that can be obtained. Furthermore, we compare the utilization of the secondary system when both standard policy and non-standard policies are employed.

5.3 Sensing Process

The sensing process, no matter how reliable and robust the employed detection function is, will cause two unavoidable errors. When the sensing function decides that a PU exists when it is absent, this is called the probability of false alarm denoted as (P_{fa}). When the sensing function decides that a PU has not occupied a channel when it is in fact transmitting, this represents the probability of misdetection (P_m). The complementary to P_m is the probability of detection ($P_d = 1 - P_m$). These two types of error can be calculated as shown in chapter **??** which were given as

$$P_m = 1 - Q\left(\frac{\lambda - 2B - \gamma}{\sqrt{4(B+\gamma)}}\right) \tag{5.1}$$

and P_f can be computed as

$$P_{fa} = Q\left(\frac{\lambda - 2B}{\sqrt{4B}}\right) \tag{5.2}$$

where γ is the SNR, B is the time bandwidth product, λ is the detection threshold, and $Q(.)$ is the tail probability of the standard normal distribution, which is defined as $Q(t) = \frac{1}{\sqrt{2\pi}} \int_t^\infty \exp\left(-\frac{t^2}{2}\right)$.

5.4 System Model and Markov Chain Analysis with Imperfect Sensing

Consider a system of C channels, where all channels are available to the PUs. Access is controlled by the primary controller, and the system is opportunistically available to SUs when PUs are absent. We assume the arrival rate of PUs and SUs follows a Poisson process with arrival rates of λ_p and λ_s, respectively. The service times are exponentially distributed with means $1/\mu_p$ and $1/\mu_s$, respectively. These assumptions are valid considering that the number of users is much greater than the available channels [29, 73]. In practical, the PUs are unaware of the activity of the SUs; therefore, a PU may use a channel already occupied by an SU which causes SU's transmission to drop. The drop occurs because of a lack of communication between the two systems, or an unwillingness to modify the infrastructure of the primary system due to cost issues. The SUs, however, maintain an awareness of the PUs activity by employing a sensing function, and transmitting whenever a channel is available. The access policy of such a system is called the standard policy. However, in the following we consider this system when two non-standard access policies have been adopted. For easy reference to these policies later in the chapter, we denote them as Π_1 and Π_2.

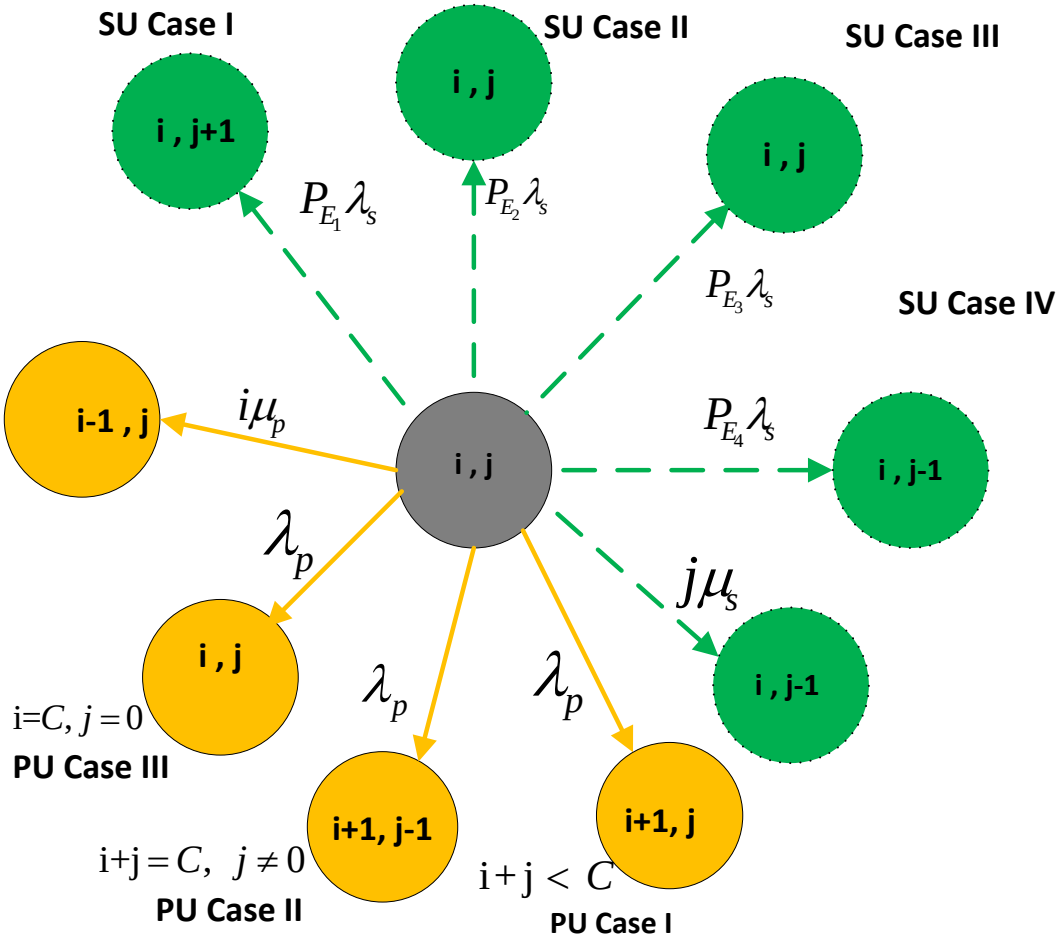

Figure 5.1: Policy Π_1 State transitions diagram.

5.4.1 Primary User Policy Π_1

Under this policy, the PUs act as follows:[2] all PUs are aware of the channels used by other PUs and other SUs. This can be achieved when the PU controller employs the CSMA-CA protocol; therefore, no collisions occur between a PU and an SU as long as the following conditions are simultaneously satisfied:

- there are unoccupied channels in the system;
- the sensing result is perfect.

Such a policy is important for the primary system if, for example, it is willing to tolerate changes. To clarify the importance of this policy, consider a network operator interested in sharing its spectrum with another network operator (a secondary operator/system in our case). This policy will be more attractive to the secondary operator as it is more reliable for its users. The secondary system policy is as follows: all SUs employ a sensing function and are required to sense channels periodically before accessing the system. All SU arrivals are employing the same sensing function and are thus aware of other SUs currently occupying a channel; therefore, no collisions occur between them in the *perfect sensing case*. In the following, we will clarify all the events that may arise because of imperfect sensing.

We assume the system is in the general state $s(i,j)$, where i represents PUs and j represents SUs. The following cases describe the system behavior when a PU arrives:

- Case I: A PU arrives and finds an idle channel with $i+j<C$; therefore, the system state transfers from state (i,j) to $(i+1,j)$ with rate λ_P. Note that in this case there are no collisions with SUs currently occupying a channel as the PU is aware of the current PUs and SUs when employing this strategy.
- Case II: A PU arrives and all channels are occupied by a PU or an SU, i.e. $i+j=C$ and $j\neq 0$. The SU will then be interrupted, as the primary system has priority, and the system state transfers from i,j to $i+1,j-1$ with rate $\delta(s)\lambda_P$, where $\delta(s)$ is an indicative function, $\delta(s)=1$ if $i+j=C$, and $j\neq 0$. Hence, the probability of a dropped SU call in this case can be computed as

$$P_{drop,SU}=\sum_{\substack{i,j\\ i+j=C, j\neq 0}} P(i,j)\frac{\lambda_p}{\lambda_s}, \tag{5.3}$$

  where $P(i,j)$ denotes the steady-state probability of state $s(i,j)$.

[2]For all policies of the considered system the PUs have priority over the SUs.

- Case III: A PU arrives and all channels in the system are occupied by other PUs, i.e. $i = C, j = 0$; in this case, the new PU request will be blocked. Hence, the probability of a PU being blocked is given by

$$P_{block,PU} = P(C, 0). \tag{5.4}$$

Note that case II is the only case that affects the secondary system. All these events can be seen in Fig. 5.1 with solid lines representing the PU cases and dotted lines representing the SU cases.

Based on the sensing model, the probability that an SU will find a channel as idle is the complement of the false alarm probability denoted as $\beta = 1 - P_{fa}$. It should be noted that at any time the number of available channels in the system will be $N_{av} = C - N_{oc}$, where N_{oc} is the total number of occupied channels and is given as $N_{oc} = i + j$. Then, the probability of an arriving SU sensing l wrong-idle channels among the occupied channels is given as $\binom{N_{oc}}{l} P_m^l P_d^{N_{oc}-l}$.[3] Among the available channels, the probability of an SU arrival sensing k right-idle channels is $\binom{N_{av}}{k} \beta^k {P_{fa}}^{N_{av}-k}$. As we considered earlier that the system is in the general state $s(i, j)$, the following summarizes all the arrival cases an SU may face:

- Case I: An SU arrives and there are no collisions with any current PUs or SUs. We denote this event as E_1, and the probability of this event can be computed as

$$P_{E_1} = \sum_{k=1}^{N_{av}} \binom{N_{av}}{k} \beta^k P_{fa}^{N_{av}-k} \sum_{l=0}^{N_{oc}} \frac{k}{l+k} \binom{N_{oc}}{l} P_d^{N_{oc}-l} P_m^l. \tag{5.5}$$

  Then the transition rate from state (i, j) to state $(i, j + 1)$ is $P_{E_1}\lambda_s$.

- Case II: An SU arrives and all channels are busy; therefore, the arriving SU will be blocked. We represent this event by E_2 and its probability is given by $P_{E_2} = P_d^{N_{oc}}(1-\beta)^{N_{av}}$. It follows then that the total probability of an SU being blocked with imperfect sensing will be

$$P_{block,SU} = \sum_{i,j} P(i, j) P_{E_2(i,j)}. \tag{5.6}$$

- Case III: An SU arrives and collides with a PU transmission due to a sensing error in detecting a PU-occupied channel; we denote this event by E_3. The probability of this event will be the probability of wrong-detecting a channel among all channels occupied by PUs or SUs,[4] and the probability of right-detecting the actual available channels N_{av}. Therefore, we can write

[3] The symbol $\binom{n}{m} = \frac{n!}{m!(n-m)!}$.

[4] The rationale for this is that the SU cannot distinguish between an SU transmission and a PU transmission.

the probability of this event as

$$P_{E_3} = \sum_{k=1}^{i} \binom{i}{k} P_d^{(i-k)} P_m^k \sum_{n=0}^{j} \binom{j}{n} P_d^{(j-n)} P_m^n \sum_{l=0}^{N_{av}} \frac{k}{l+n+k} \binom{N_{oc}}{l} P_{fa}^{(N_{av}-l)} \beta^l$$

In this case, the arriving SU will be dropped and the probability of a dropped call due to this event is given as

$$P_{drop_{E_3},SU} = \lambda_s P_{E_3}/\lambda_s = P_{E_3} \tag{5.7}$$

Note that the system will stay in its current state and no transition occurs here.

- Case IV: An SU arrives and collides with another SU transmission. We denote this event by E_4, and the same argument could be used as in case III. Thus, the probability of this event can be computed as in event E_3, and can be written as

$$P_{E_4} = \sum_{k=1}^{j} \binom{j}{k} P_d^{(j-k)} P_m^k \sum_{n=0}^{i} \binom{i}{n} P_d^{(i-n)} P_m^n \sum_{l=0}^{N_{av}} \frac{k}{l+n+k} \binom{N_{oc}}{l} P_{fa}^{(N_{av}-l)} \beta^l$$

The probability of a dropped call due to this event will then be

$$P_{drop_{E_4},SU} = 2\lambda_s P_{E_4}/\lambda_s = 2P_{E_4}. \tag{5.8}$$

Hence the transition rate from state (i, j) to state $(i, j-1)$ will be $j\mu_s + 2P_{E_4}\lambda_s$.

To compute the total probability of a dropped call in the secondary system, we add the probabilities of a dropped call for all events that cause an arriving SU to be dropped. Hence, the total probability of a dropped call can be expressed as

$$P_{drop,SU} = \sum_{i,j} P(i,j)[P_{E_3}(i,j) + 2P_{E_4}(i,j)] + \sum_{\substack{i,j \\ i+j=C, j\neq 0}} P(i,j)\frac{\lambda_p}{\lambda_s}. \tag{5.9}$$

The system of linear equations which is formed from the Markov chain model can be written in vector-matrix form as

$$\mathbf{pQ} = \mathbf{0}, \tag{5.10}$$

where $\mathbf{p}$ is the steady-state probability vector, and $\mathbf{Q}$ is the infinitesimal generator matrix which characterizes the transition of the states of the Markov chain. Since all states of the system are

reachable from all other states, it follows that the CTMC is irreducible. To yield a unique, positive solution, (5.10) can be solved with the imposed normalization condition of the steady state probability, which is defined as

$$\sum_i \sum_j P(i,j) = \mathbf{p1} = 1, \quad \forall (i,j) \leq C \tag{5.11}$$

where $\mathbf{1} = [1, 1, 1, ..., 1]^T$, where T indicates the transpose operation.

5.4.2 Primary User Policy Π_2

To add more flexibility to the considered system, we introduce a new policy denoted by Π_2. In this policy, the SUs are limited to accessing $C - q$, where q, $0 \leq q \leq C$ is an optimization parameter allowing a trade-off between blocked and dropped probabilities. Note that the primary system still has priority over the secondary system. The CTMC model for the case when $0 \leq i \leq q$ is shown in Fig. 5.2. In this case, as long as the number of PUs is less than q, the SUs will be dropped only when imperfect sensing occurs, represented by the discussed events E_3, E_4. However, if a new PU arrives, i.e. $i \geq q$, then the newly arrived PU will be randomly assigned a remaining channel. Therefore, the CTMC in this case will be modified as shown in Fig. 5.3.

Based on the cases of PUs and SUs in the previous discussion, we can compute the dropped and blocked probabilities of the SUs with the help of the transition diagrams shown in Fig. 5.2 and Fig. 5.3. The dropping probability will consist of two parts. The first part is due to sensing errors which are the result of the two events E_3, E_4, and the second part is caused by the arrival of a PU which collides with an SU (Case II of a PU arrival). Hence, the overall dropped probability of the SU system according to this policy can be expressed as

$$\begin{aligned} P_{drop,SU} = & \sum_{\substack{i,j \\ j<C-q}} P(i,j)[P_{E_3}(i,j) + 2P_{E_4}(i,j)] \\ & + \sum_{\substack{i,j \\ i\geq q, j\neq 0}} P(i,j)\frac{j\lambda_p}{(C-i)\lambda_s}. \end{aligned} \tag{5.12}$$

The blocked probability of the secondary system also consists of two parts. The first part is due to a sensing error of an SU arrival that finds all channels busy (represented by event E_2), and the second part is the state where SUs are not allowed access to a channel, i.e. $j \geq C - q$. Hence, we can express the blocked probability of the SUs as

$$P_{block,SU} = \sum_{\substack{i,j \\ j<C-q}} P(i,j)P_{E_2(i,j)} + \sum_{\substack{i,j \\ j\geq C-q}} P(i,j). \tag{5.13}$$

The steady state solution for this policy can easily be computed using (5.10) and the normalization condition defined in (5.11) with $j \leq C - q$.

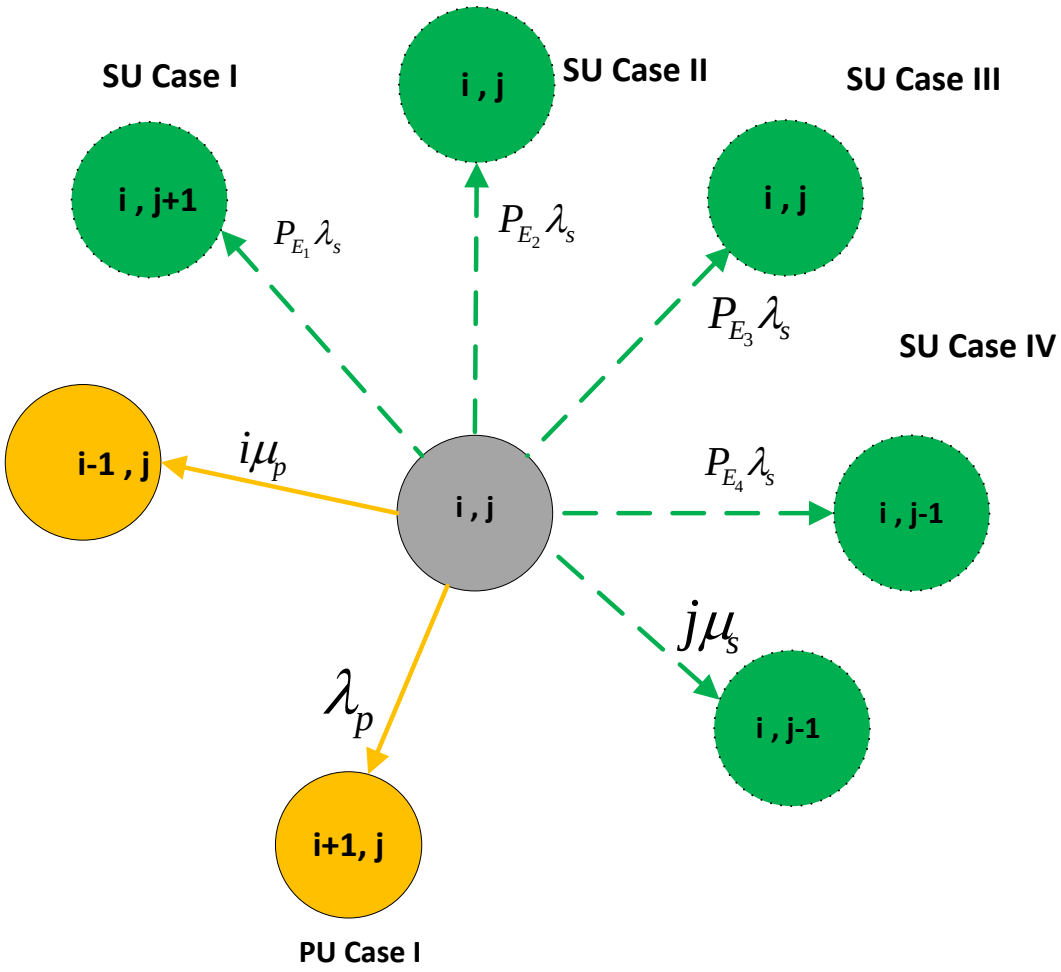

Figure 5.2: Policy Π_2. State transitions diagram when $0 \leq i < q$.

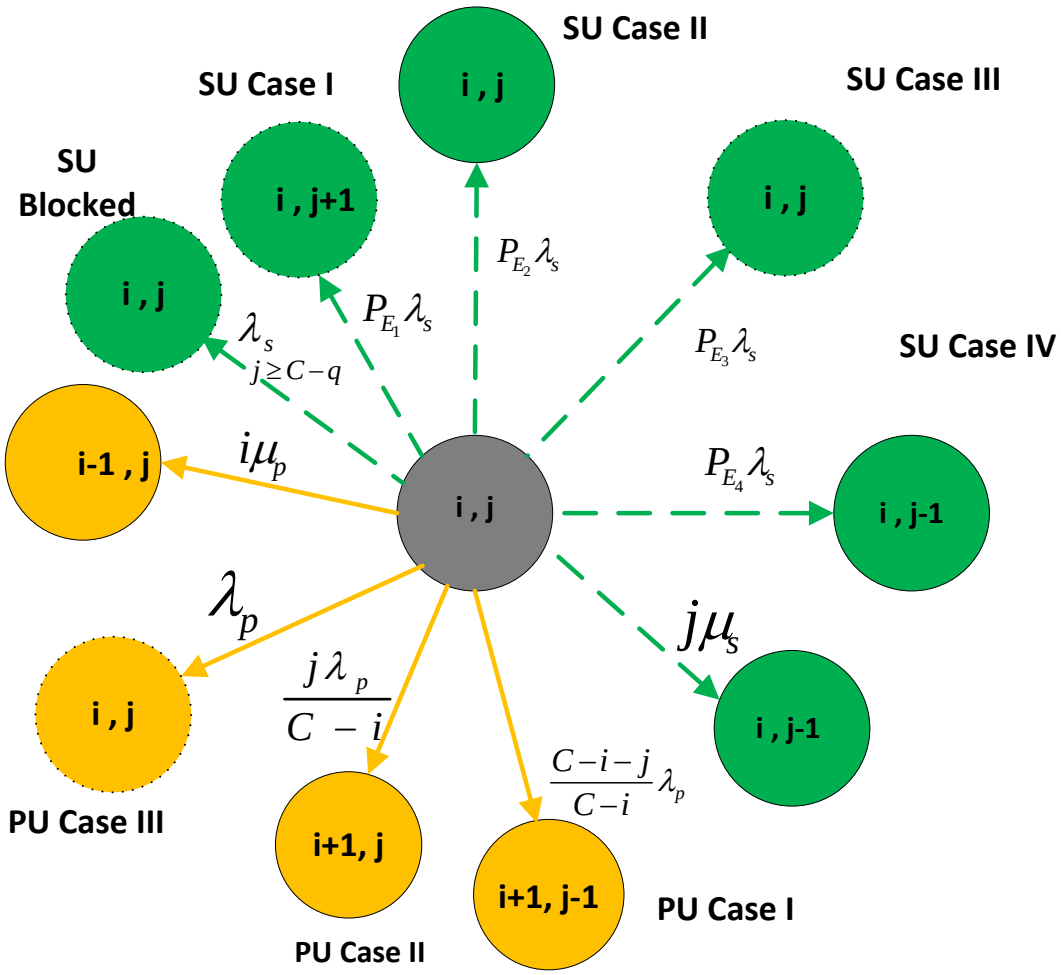

Figure 5.3: Policy Π_2. State transitions diagram when $q \leq i \leq C$.

Note that the considered system will be reduced to the well-known model M/M/C/C, which corresponds to a single primary system, and can be evaluated using the well-known Erlang loss formula [86] if no SU exists, i.e. $j = 0, \lambda_s = 0 and \mu_s = 0$.

The model has been discussed and analyzed for two performance metrics, i.e., blocked and dropped probabilities. However, another significant performance metric that quantifies the effect of the two GoS metrics (blocked and dropped probabilities) is system utilization. This metric captures the successfully served traffic of a communication system. Therefore, we define primary system utilization as

$$U_p = \rho_p(1 - P_{block,PU}) \tag{5.14}$$

where $\rho_P = \lambda_p / C\mu_p$. Secondary system utilization is defined as

$$U_s = \rho_s(1 - P_{block,PU} - P_{drop,SU}) \tag{5.15}$$

where $\rho_s = \lambda_s / C\mu_s$. Then, the total utilization, U, of the combined system is the sum of the utilization of both systems, i.e., $U = U_p + U_s$. With no SUs, the total utilization will only be computed for the PUs; therefore, the utilization of the system becomes $U = U_p$.

5.5 Simulation and Discussion

Before evaluating the previously discussed policies of the considered system with imperfect sensing, we will start with a simple design example to focus on the usefulness of the introduced policies and their mathematical analysis. Let us assume that there are no secondary users, i.e. $j = 0$, $\lambda_s = 0$ and $\mu_s = 0$. The considered system will then consist only of the primary system. Let the system designer restrict the number of channels to $C = 10$ and the blocking probability of the primary system to under 1%. The question is: what is the maximum allowable primary traffic that this system can support given a service time of 0.5 min^{-1}? The answer to this question can easily be found with the help of Fig. 5.4. We plot the primary system blocked probability, i.e., (5.4), and the primary system utilization. Assuming $\lambda_p = 1 : 10$, the blocked probability of the primary system is 0.01 at the value of $\lambda_p = 2.26$, which corresponds to a primary system utilization of 44.7%. This example was introduced to enable us to compare the utilization of the whole system under perfect/imperfect sensing when using standard and non-standard policies. This will be discussed further in the following sections.

Based on the previous parameters, a Matlab code was written to compare our analytical results with the simulation ones. A large number of SU service requests (100 000) were generated for each policy. Then, for each service request the Matlab code checked and admitted requests according to each policy. The blocked and dropped probabilities were recorded and compared to

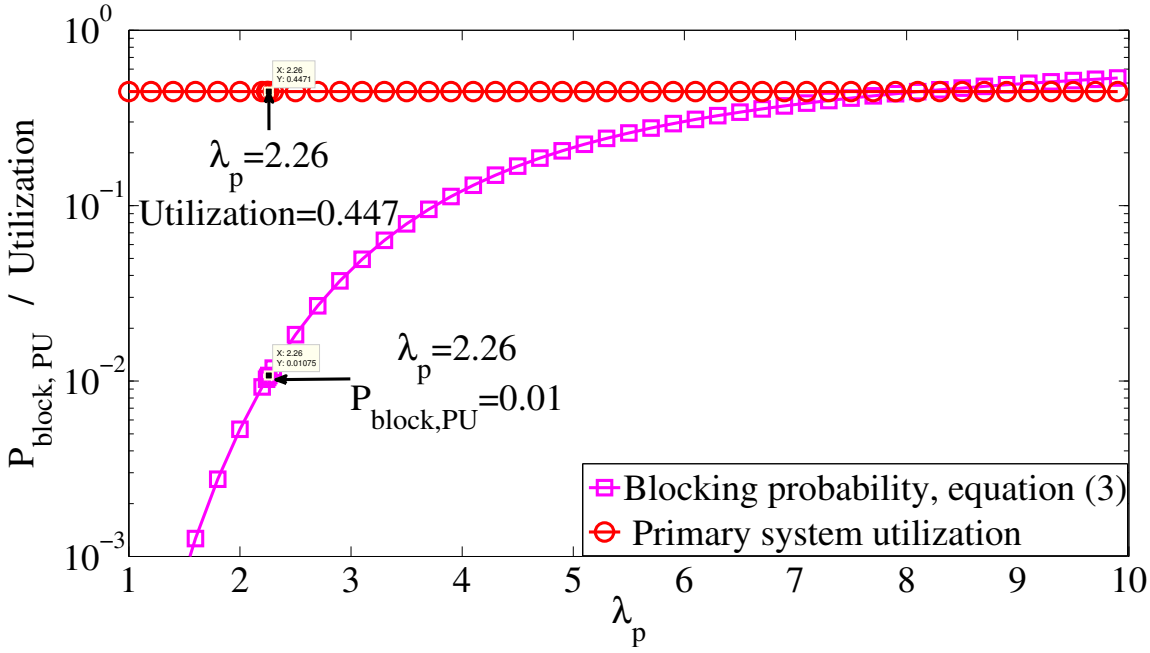

Figure 5.4: Performance evaluation of the primary system in terms of blocked probability and system utilization, with $C = 10$ and $\mu_p = 0.5$

the computed ones. In the following subsection, we compare the performance metrics for all policies under perfect/imperfect sensing results.

5.5.1 Blocked probability: Perfect sensing

In Fig. 5.5, we compare the blocked probability for the two non-standard policies in the perfect sensing case, i.e., $P_{fa} = 0$ and $P_d = 1$. The following observations can be noted from Fig. 5.5.

- There is no change in the primary system blocked probability; it has the same value as shown in Fig. 5.4. This is also consistent with (5.4) since a PU is blocked only when the system is in state (C, 0).
- The blocked probability of SUs is an increasing function of λ_s. This is expected as the more SUs arrive, the more likely they will be blocked.
- Policy Π_1 has a higher blocked probability than Π_2 when $q = 0$. The reason is that in Π_1, the new PUs are aware of SUs occupying a channel. As a consequence, newly arrived PUs start occupying the empty channels and hence the available channels are occupied faster. Therefore, the arriving SUs will be blocked as more channels are occupied by PUs.

- The blocked probability of policy Π_2 when $q = 0$ is less than when $q > 0$. The reason is that when q increases, more channels are reserved for PUs and hence the blocked probability of SUs increases.

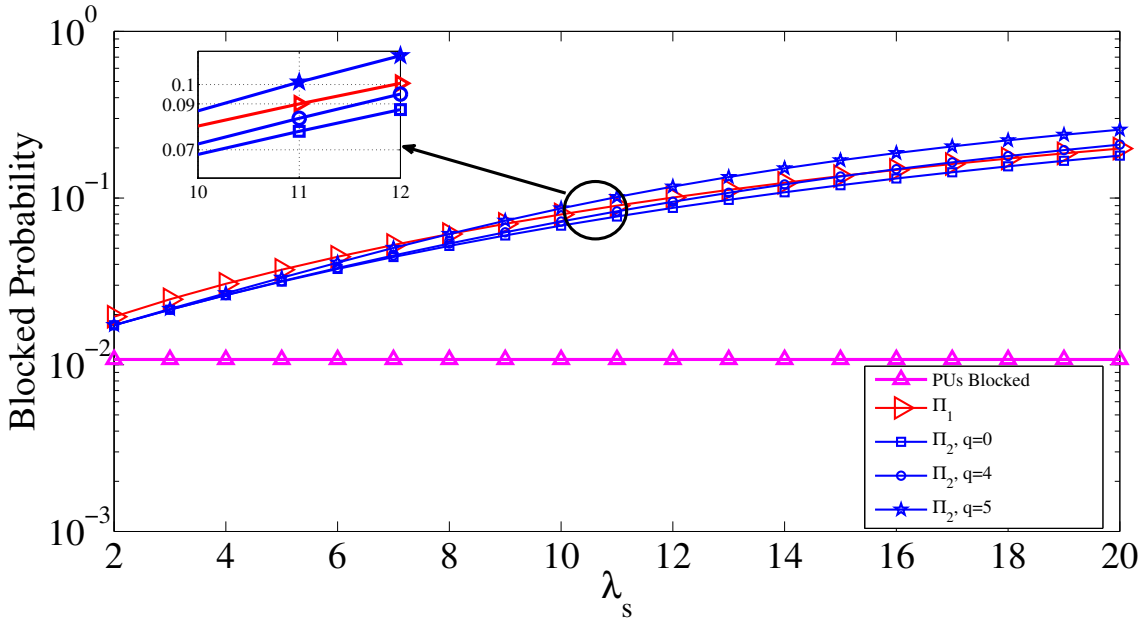

Figure 5.5: Perfect sensing: Evaluation of Π_1 and Π_2 in terms of blocked probability of SUs and PUs, with $C = 10$, $\lambda_p = 2.26$, $\mu_p = 0.5$, $\mu_s = 5$

5.5.2 Blocked probability: Imperfect sensing

In Fig. 5.6, we evaluate the blocked probability of the system under imperfect sensing. The following can be observed:

- As the arrival rate of the PUs is fixed, the blocked probability of the PUs is the same as in the perfect sensing case. This is also consistent with (5.4).
- The behavior of the blocked probability for both non-standard policies is the same as in perfect sensing, i.e. the probability is an increasing function of λ_s, the blocked probability of Π_1 is higher than Π_2 when $q = 0$, and as q increases the blocked probability of Π_2 is increased.
- Compared to the perfect sensing case (Fig. 5.5), the blocked probability for both policies is reduced. The reason for such behavior is that as the SNR is reduced, the PUs detection probability is reduced. This causes more PUs to be misdetected and therefore the newly arrived SUs are allowed access without being blocked.

- The blocked probability of Π_2 increases when q is increased. This can be justified as before, i.e. as q increases, more channels are reserved for the PUs which results in the SUs blocked probability increasing.

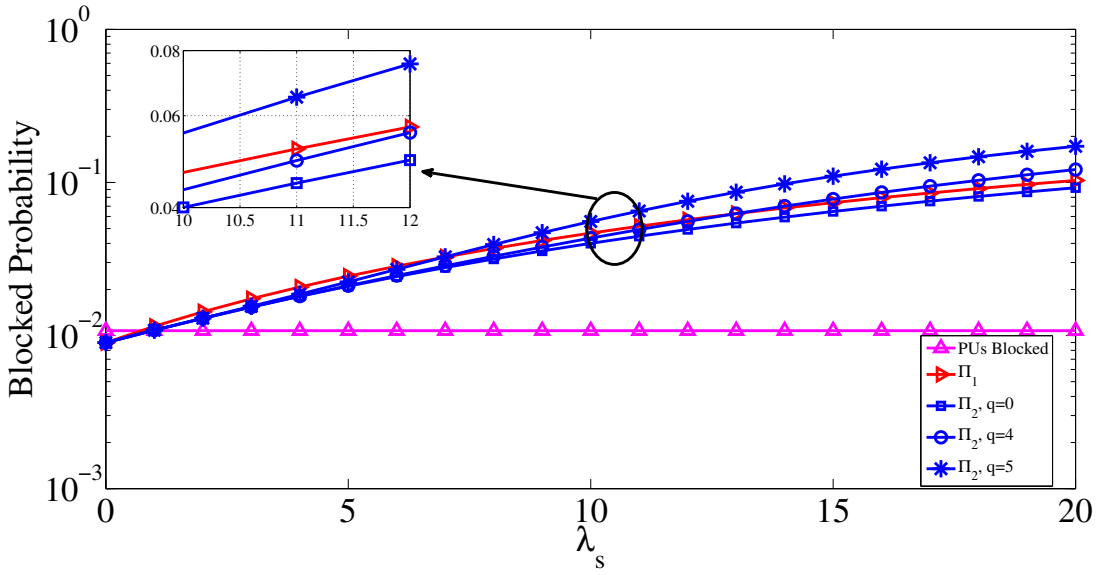

Figure 5.6: Imperfect sensing: Evaluation of Π_1 and Π_2 in terms of blocked probability of SUs and PUs, with $C = 10$, $\lambda_p = 2.26$, $\mu_p = 0.5$, $\mu_s = 5$, $P_{fa} = 0.1$ and SNR= -15 dB

5.5.3 Dropped probability: Perfect sensing

The dropped probability for both policies under perfect sensing can be seen in Fig. 5.7. We summarize our observations as follows:

- The dropped probability of Π_1 is an increasing function of λ_s. This can be justified as follows: in this case (perfect sensing) we consider only the second term of (5.9) and (5.12), i.e., the events E_3 and E_4 are not involved. In this term, the dropped probability is related to states in the system where $i + j = C$, $j \neq 0$. The result is that the more SUs access the system, the more likely they are to be dropped.

- The dropped probability of Π_2 decreases as q is increased. This is because as q increases more SUs are blocked and therefore the SUs become less likely to be dropped. Also, if we compare this figure (Fig. 5.7) with Fig. 5.5, there is, as always, a tradeoff between the dropped and blocked probability which can be seen in policy Π_2, i.e. increasing q will affect both probabilities, and if one increases the other will decrease.

- For a fixed value of q, the dropped probability of Π_2 slightly decreases with λ_s. This can be related to the blocked probability (see Fig. 5.5); as more SUs are denied access to the system, i.e. blocked, this results in fewer SUs in the system, and therefore the dropped probability decreases.

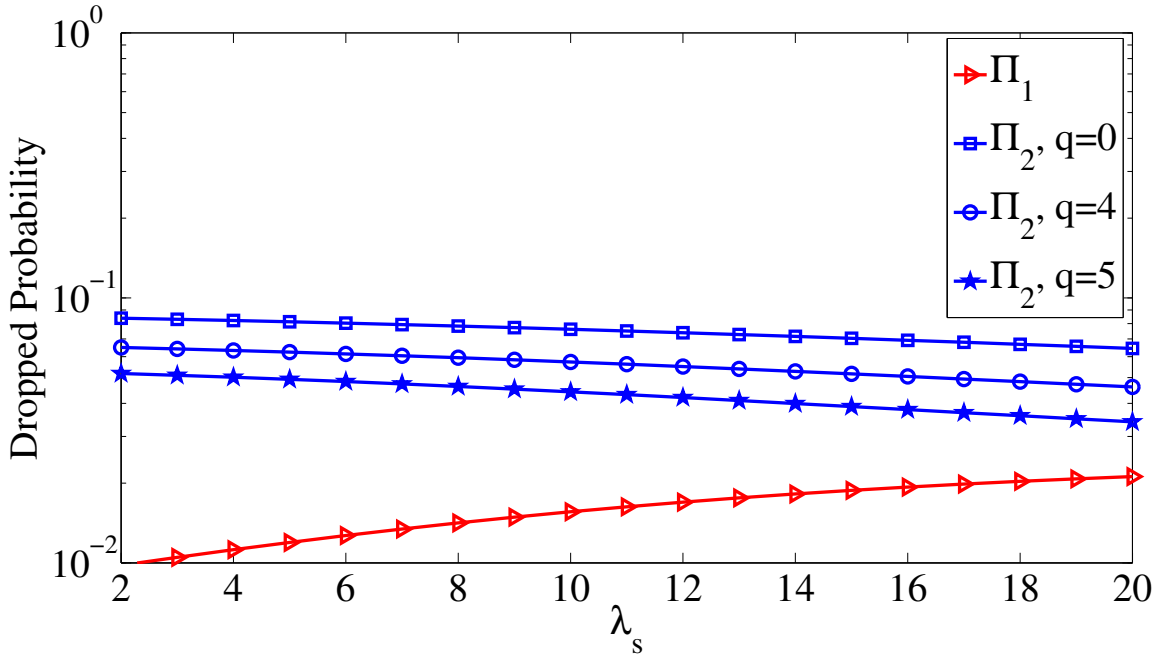

Figure 5.7: Perfect sensing: Evaluation of Π_1 and Π_2 in terms of dropped probability of SUs and PUs, with $C = 10$, $\lambda_p = 2.26$, $\mu_s = 5$ and $\mu_p = 0.5$

5.5.4 Dropped probability: Imperfect sensing

Fig. 5.8 shows the dropped probability of both non-standard policies in the imperfect sensing case. The following can be observed:

- The dropped probability for both policies is an increasing function of λ_s. This is as previously justified; the more SUs that are not blocked, i.e., that are able to access the system, the more likely they are to be dropped. Note that, in this case, the two terms of (5.12) and (5.9) are involved, which causes more dropped SUs compared to the perfect sensing case.
- For a given range of λ_s, the dropped probability of Π_2 is higher than that of Π_1 as the latter is aware of the SUs currently in the system and tries to avoid a collision with them.
- The value of q will affect the dropped probability of Π_2 in such a way that it may be higher or lower than Π_1. This is because, besides the sensing errors represented by the events E_3, E_4,

in Π_1 the states in which the SUs will be dropped are the states when $i+j=C$, $j\neq 0$ as seen in (5.9). In Π_2, however, it also involves the states where $i+j<C$ since a newly arrived PU will randomly select a channel when $q\leq i\leq C$, as seen in (5.12) and the transition diagram of Fig. 5.3. Therefore, when q is decreased, more states are involved in the second term of (5.12) which results in a higher dropped probability compared to Π_1. On the other hand, when q is increased, fewer states are involved in the second term of (5.12) and hence lower numbers of dropped calls will occur.

- The model perfectly catches the false alarms and misdetections of the PUs which are represented by events E_3, E_4. This can be seen if we compare the dropped probability in perfect sensing which is shown in Fig. 5.7 with Fig. 5.8, as the dropped probability increases due to these events.
- For policy Π_1, increasing the value of q causes a reduction in the dropped probability. This can be related to the blocked probability, as when q increases more channels are reserved for the PUs. Hence, fewer SUs access the system which causes fewer SUs to be dropped.

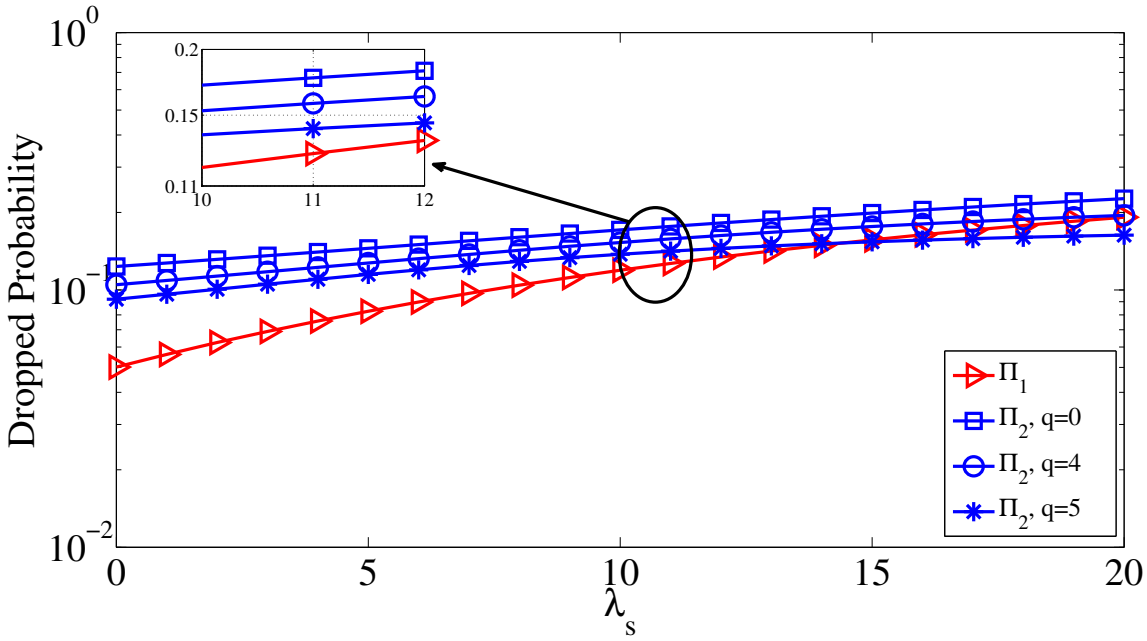

Figure 5.8: Imperfect sensing: Performance evaluation of Π_1 and Π_2 in terms of dropped probability of SUs and PUs, with $C=10$, $\lambda_p=2.26$, $\mu_p=0.5$, $\mu_s=5$,$P_{fa}=0.1$ and SNR= -15 dB

5.5.5 System utilization: Perfect and imperfect sensing

In this section we evaluate system utilization for the considered policies under perfect/imperfect sensing.

Perfect sensing

It can be seen from Fig. 5.9 that the system shows a considerable improvement in total system utilization, i.e. in the absence of the SUs, the system utilization is 44.7% which is consistent with our previous analysis (see Fig. 5.4). As λ_s increases, the system utilization increases in both policies. For example, at $\lambda_s = 9$, the utilization is 61.2%, 60.58% and 60.25% for Π_1, $(\Pi_2, q = 5)$ and $(\Pi_2, q = 0)$. The utilization percentage can then be computed as

$$\left.\frac{U - U_p}{U_p}\right|_{\lambda_s, \lambda_p} \tag{5.16}$$

Hence, system utilization increases by 36.5% on average.

It can also be seen that Π_1 has a higher utilization than the standard policy $(\Pi_2, q = 0)$ as the PUs are aware of the SUs. This is also consistent with our previous analysis and discussion in terms of blocked and dropped probabilities of Π_1 as it has the lowest dropped probability and a blocked probability comparable to the standard policy $(\Pi_2, q = 0)$. We also note that even when we change the q value of Π_2, Π_1 still has the highest utilization. This is because the dropped probability of Π_2 for all values of q is higher than the dropped probability of Π_1. The blocked probability is also higher than the blocked probability of Π_2 when $q > 1$.

Imperfect sensing

To evaluate the considered system in the imperfect sensing scenario, we used $P_{fa} = 0.1$ and SNR=-20 dB. The rest of the simulation parameters are the same as in the perfect sensing case. We plotted the results on the same figure, i.e. Fig. 5.9, for comparison. It can be see that the sensing errors which are represented by the events E_1, E_3, E_4 considerably reduce system utilization. On the other hand, policy Π_1 still has a higher utilization compared to policy Π_2. This also provides concrete evidence of the correctness of the presented model.

5.6 Conclusion

In this chapter, we have presented a complete continuous Markov chain model of the two nonstandard access policies for a DSA system with imperfect sensing results. We have also introduced a complete mathematical analysis for both policies using reasonable assumptions. In addition, we showed

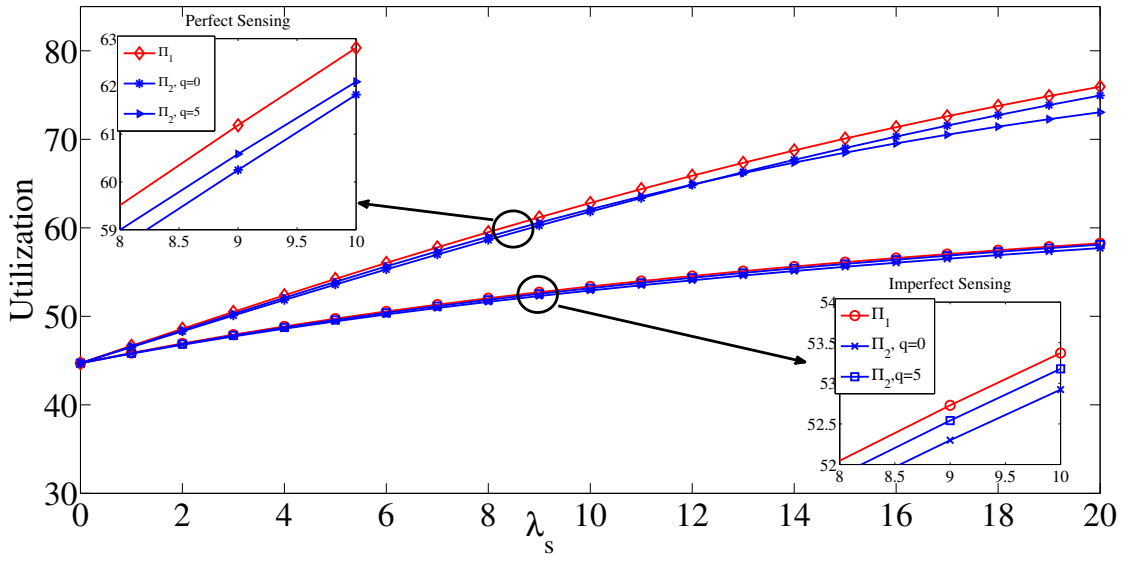

Figure 5.9: System utilization in perfect/imperfect sensing, with $C = 10$, $\lambda_p = 2.26$, $\mu_p = 0.5$, $\mu_s = 5$,$P_{fa} = 0.1$ and SNR=-20 dB

that the standard policy is a special case of the proposed policy Π_2 when $q = 0$. Finally, for both presented policies, we analyzed three performance metrics based on the continuous Markov chain model; namely the blocked probability, the dropped probability and spectrum utilization. Spectrum utilization captures the effect of blocked and dropped probabilities and quantifies their degradations. An extensive simulation was conducted to evaluate and analyze the effect of sensing errors on the considered system. On one hand, our results showed that these polices slightly improved spectrum utilization under imperfect sensing. However, although such an improvement is beneficial and assists in reducing sensing complexity, the results demonstrate the usefulness of a reliable sensing function for the effective utilization of SHs. Our mathematical modeling may be considered as a basic milestone for further analysis and investigation. We conclude that a secondary radio system employing a dynamic, controllable, manageable and easy to configure access policy based on an initial agreement with the primary system can enhance overall system utilization even with severe sensing errors. Our results suggest that, as sensing errors are inevitable, DSA performance can be enhanced by adopting a suitable policy. With the proposed policies, an improvement in the system utilization can still be observed even with severe sensing errors and the GoS requirements for both PUs and SUs can still be satisfied.

Chapter 6

Proposed Future Works

6.1 Challenges in Practical Designs of a CRN

The proposed ideas and their mathematical analysis, which are presented in the previous chapters, cause the reader to think about the many unexplored areas that still need to be extensively studied. For example, although cooperative sensing outperforms local sensing in terms of detection probability, the tradeoffs between the achieved detection gain when cooperative sensing is employed and the complexity of the cognitive network need to be considered. The tradeoffs between the increased complexity and/or power consumption and the main objective to be achieved (spectrum utilization) should also be considered. Other questions may arise and need further studies. For example, what if the sensing layer has a bi-protocol for detecting a PU (local and cooperative)? Does that assure full cognition for a CR user? If so, what factors need to be considered so that either one can be invoked? For example, should the position of PU, channel between the PU and the SU, power available on the SUs side or the SU's ability to cooperate be considered? All of these questions need to be fully investigated and analyzed before a CRN can be considered to be a practical solution to reliably increase spectrum utilization.

In chapter 3, the optimal number of CRs of the centralized cooperative sensing is derived based on the assumption that the CRs decisions are sent to the FC using hard decision combining scheme. Although this scheme is more popular as it is easy to implement and avoids bandwidth expansion of the feedback channel. However, soft combining may also be used and the result can be extended to this case. But the tradeoffs between the bandwidth expansion, the power used to forward a local decision statistic such as, the log-likelihood ratio or any suitable sufficient statistic, and the achieved gain need to be studied, analyzed and compared with the hard case. In addition, other factors that influence decisions when choosing between hard or soft combining should also be studied. For

example, is the bandwidth of the feedback channel the only limiting factor for deciding on hard or soft combining? What about the position of the PU? If the false alarm probability of the individual SUs is not the same, should the weighing of the local decisions to maximize the detection probability at the FC should consider only their detection probabilities or their false alarms? Answering these questions is not a trivial task and it may lead to the discovery of new optimization techniques to solve other existing problems.

Moreover, the thesis is focused on two aspects of CRs, that is, observation and adaptation. The observe portion is represented by work on sensing which has been discussed in chapter 2 and 3, and the adapt portion, that is, when the radio performs channel access and policy selection which has been studied in chapter 4 and 5.[1]. However, other aspects of CR for example reasoning and learning should also be studied. Such aspects may help the CRs to reduce the sensing periodicity and therefore lower the power consumption. For example, researchers may investigate prediction methods or use hidden Markov chain to predict the behavior of the PUs and then identify the SHs.

Once answers to all of the previous questions have been found, the spectrum holes can now be reliably detected but *not* efficiently accessed? This leads to another set of questions that also require further studies to find out the system parameters that affect the access efficiency. For example, What about the sensing periodicity which may considered as a cross layer optimization problem? What if the time remaining after perfectly sensing a PU channel is not sufficient to transmit the smallest data packet size of an SU, should the SU ignore that time or utilize it for other purposes?

Further, in chapter 4 and 5, the proposed access policies are analyzed to study the effect of sensing errors on the system. But, does the model itself perfectly reflect a practical scenario? Are the assumptions that have been made appropriate for the mathematical model? Determining the appropriate values to assign to the parameters of the model (one value per parameter) is both a critical and a challenging part of the model-building process. Determining parameter values for real problems requires gathering relevant data and gathering accurate data is frequently difficult. Therefore, the value assigned to a parameter often is, of necessity, only a rough estimate and can cause a sensitivity analysis problem, i.e. for a mathematical model with specified values for all its parameters, the models sensitive parameters are the parameters whose value cannot be changed without changing the optimal solution. This is because with the uncertainty about the true value of the parameter, it is important to analyze how the solution derived from the model would change (if at all) if the value assigned to the parameter were changed to other plausible values.

[1]The CR may perform other tasks in the adaptation aspect, for example power, topology control, adaptive modulation and coding, or some combination thereof [87]

In addition, there are pitfalls to be avoided when mathematical models are used. Such a model is necessarily an abstract idealization of the problem, so approximations and simplifying assumptions are generally required if the model is to be tractable. The proper criterion for judging the validity of a model is whether the model predicts the relative effects of the alternative courses of action with sufficient accuracy to permit a sound decision. Consequently, it is not necessary to include unimportant details or factors that have approximately the same effect for all the alternative courses of action considered. It is not even necessary that the absolute magnitude of the measure of performance be approximately correct for the various alternatives, provided that their relative values (i.e., the differences between their values) are sufficiently precise. Thus, all that is required is that there be a high correlation between the prediction by the model and what would actually happen in the real world. To ascertain whether this requirement is satisfied, it is important to do considerable testing and consequent modifying of the model.

There are still many challenges ahead, especially in the physical and MAC layers. These are the most important layers that may require modification to build a reliable CRN or to be represented by a perfect mathematical model. Designing and implementing a CRN also requires that hardware limitations and cost implementations should be taken into account.

6.2 Practical and Experimental Studies

The utilization of the spectrum needs to be studied. However, this should not be limited only to theoretical works, simulation models or mathematical models; more effort should be given to experimental studies to see how these ideas can be efficiently combined together to build a reliable CR system that is capable of exploiting the white spaces in the spectrum. All of the above questions can be answered if the results of such a model are compared to a simple practical design. If the model happens to represent the real system reasonably well, then its solution is also optimal for the real situation. Some mathematical models may be so complex that it is impossible to solve them by any of the available optimization algorithms. In such cases, it may be necessary to abandon the search for the optimal solution and simply seek a good solution using heuristics or rules of thumb.

One way to have a suitable comparison is to use a more pragmatic approach, that is, to collect data under various channel and system conditions, and then compare the theoretical works to real time data and see well it fits the theory. In addition, various parameters can be optimized for full spectrum utilization and the implementation of various searching and optimization algorithms under practical scenarios can be studied.

Bibliography

[1] J. Mitola, "The software radio architecture," *Communications Magazine, IEEE*, vol. 33, no. 5, pp. 26 –38, May 1995.

[2] S. Haykin, "Cognitive radio: brain-empowered wireless communications," *IEEE Journal on Selected Areas in Communications*, vol. 23, no. 2, pp. 201 – 220, February 2005.

[3] Q. Zhao and B. Sadler, "A survey of dynamic spectrum access," *IEEE Signal Processing Magazine*, vol. 24, no. 3, pp. 79–89, 2007.

[4] R. Pinyi, W. Yichen, D. Qinghe, and X. Jing, "A survey of dynamic spectrum access protocols for distributed cognitive wireless networks," *EURASIP Journal on Wireless Communications and Networking*, vol. 2012, no. 60, pp. 1687–1499, 2012.

[5] I. F. Akyildiz, W.-Y. Lee, M. C. Vuran, and S. Mohanty, "Next generation/dynamic spectrum access/cognitive radio wireless networks: A survey," *Computer Networks*, vol. 50, no. 13, pp. 2127 – 2159, 2006.

[6] M. A. McHenry, D. McCloskey, D. Roberson, and J. T. MacDonald, "Spectrum occupancy measurements chicago, illinois," IIT Wireless Interference Lab-Illinois Institute of Technology and Shared Spectrum Company, 2005, project: NeTS-ProWIN: Wireless Interference: Characterization and Impact on Network Performance.

[7] I. Akyildiz, W.-Y. Lee, M. C. Vuran, and S. Mohanty, "A survey on spectrum management in cognitive radio networks," *IEEE Communications Magazine*, vol. 46, no. 4, pp. 40–48, 2008.

[8] F. Digham, M.-S. Alouini, and M. K. Simon, "On the energy detection of unknown signals over fading channels," in *IEEE International Conference on Communications, 2003*.

[9] A. Annamalai, O. Olabiyi, S. Alam, O. Odejide, and D. Vaman, "Unified analysis of energy detection of unknown signals over generalized fading channels," in *International Wireless Communications and Mobile Computing Conference (IWCMC)*, July, pp. 636–641.

[10] N. Reisi, M. Ahmadian, and S. Salari, "Performance analysis of energy detection-based spectrum sensing over fading channels," in *6th International Conference on Wireless Communications Networking and Mobile Computing (WiCOM)*, Septemper 2010, pp. 1 –4.

[11] D. Horgan and C. Murphy, "Fast and accurate approximations for the analysis of energy detection in nakagami-m channels," *IEEE Communications Letters*, vol. 17, no. 1, pp. 83–86, January 2012.

[12] H. Urkowitz, "Energy detection of unknown deterministic signals," *Proceedings of the IEEE*, vol. 55, no. 4, pp. 523 – 531, April 1967.

[13] H.-S. Chen, W. Gao, and D. Daut, "Signature based spectrum sensing algorithms for IEEE 802.22 WRAN," in *IEEE International Conference on Communications*, June 2007, pp. 6487 –6492.

[14] S. M. Kay, *Fundamentals of Statistical Signal Processing, Volume 2: Detection Theory.* Prentice Hall, 1998.

[15] P. Sutton, K. Nolan, and L. Doyle, "Cyclostationary signatures in practical cognitive radio applications," *IEEE Journal on Selected Areas in Communications*, vol. 26, no. 1, pp. 13 –24, January 2008.

[16] K.-L. Du and W. H. Mow, "Affordable cyclostationarity-based spectrum sensing for cognitive radio with smart antennas," *IEEE Transactions on Vehicular Technology*, vol. 59, no. 4, pp. 1877 –1886, May 2010.

[17] V. I. Kostylev, "Characteristics of energy detection of quasideterministic radio signals," in *Radiophys. Quantum Electron.*, vol. 43, October 2000, pp. 833 –839.

[18] S. Alam, O. Odejide, O. Olabiyi, and A. Annamalai, "Further results on area under the ROC curve of energy detectors over generalized fading channels," in *2011 34th IEEE, Sarnoff Symposium*, May 2011, pp. 1 –6.

[19] E. Peh, Y.-C. Liang, Y. L. Guan, and Y. Pei, "Energy-efficient cooperative spectrum sensing in cognitive radio networks," in *Global Telecommunications Conference (GLOBECOM 2011)*, December 2011, pp. 1 –5.

[20] D. Shnidman, "The calculation of the probability of detection and the generalized Marcum Q-function," *IEEE Transactions on Information Theory*, vol. 35, no. 2, pp. 389 –400, Mar. 1989.

[21] J. Proakis and M. Salehi, *Digital Communications.* McGraw Hill, 2008.

[22] M. Abramowitz and I. A. Stegun, *Handbook of Mathematical Functions with Formulas, Graphs, and Mathematical Tables*, tenth GPO printing ed. New York: Dover, 1972.

[23] K. Simon, *Probability Distribution involving Gaussian Random Variables: A Handbook for Engineers and Scientists*. Springer, 2002.

[24] F. Digham, M.-S. Alouini, and M. Simon, "On the energy detection of unknown signals over fading channels," *IEEE Transactions on Communications*, vol. 55, no. 1, pp. 21 –24, January 2007.

[25] S. András, Á. Baricz, and Y. Sun, "The generalized marcum q-function: an orthogonal polynomial approach," *ArXiv e-prints*, pp. 1010–3348, October 2010.

[26] J. M. Borwein and P. B. Borwein, "On the complexity of familiar functions and numbers," *SIAM Review*, vol. 30, no. 4, pp. 589–601, December 1988.

[27] S. Gong, P. Wang, and J. Huang, "Robust performance of spectrum sensing in cognitive radio networks," *IEEE Transactions on Wireless Communications*, vol. 12, no. 5, pp. 2217–2227, 2013.

[28] O. Altrad and S. Muhaidat, "A new mathematical analysis of the probability of detection in cognitive radio over fading channels," *EURASIP J. Wireless Commun. Networking*, vol. 2013, no. 1, p. 159, 2013.

[29] S. Tang and B. Mark, "Modeling and analysis of opportunistic spectrum sharing with unreliable spectrum sensing," *IEEE Transactions on Wireless Communications*, vol. 8, no. 4, pp. 1934 – 1943, April 2009.

[30] R. Tandra and A. Sahai, "Fundamental limits on detection in low snr under noise uncertainty," in *International Conference on Wireless Networks, Communications and Mobile Computing*, vol. 1, June 2005, pp. 464 – 469.

[31] T. J. Lim, R. Zhang, Y. C. Liang, and Y. Zeng, "GLRT-based spectrum sensing for cognitive radio," in *GLOBECOM*, December 2008, pp. 1 –5.

[32] A. Sendonaris, E. Erkip, and B. Aazhangl, "User cooperation diversity. part I: System description," *IEEE Trans.commun.*, vol. 51, no. 11, pp. 1927–1938, November 2003.

[33] H. Muhaidat and M. Uysal, "Cooperative diversity with multiple-antenna nodes in fading relay channels," *IEEE Transactions on Wireless Communications*, vol. 7, no. 8, pp. 3036 –3046, August 2008.

[34] K. Zarifi, A. Ghrayeb, and S. Affes, "Distributed beamforming for wireless sensor networks with improved graph connectivity and energy efficiency," *IEEE Transactions on Signal Processing*, vol. 58, no. 3, pp. 1904–1921, 2010.

[35] S. Ikki and M. Ahmed, "Performance of cooperative diversity using equal gain combining (EGC) over Nakagami-m fading channels," *IEEE Transactions on Wireless Communications*, vol. 8, no. 2, pp. 557–562, 2009.

[36] H. Ding, J. Ge, D. da Costa, and Z. Jiang, "Asymptotic analysis of cooperative diversity systems with relay selection in a spectrum-sharing scenario," *IEEE Transactions on Vehicular Technology*, vol. 60, no. 2, pp. 457–472, 2011.

[37] G. de Oliveira Brante, M. Kakitani, and R. Demo Souza, "Energy efficiency analysis of some cooperative and non-cooperative transmission schemes in wireless sensor networks," *IEEE Transactions on Communications*, vol. 59, no. 10, pp. 2671–2677, 2011.

[38] G. G. O. Brante, R. D. Souza, and M. E. Pellenz, "Cooperative partial retransmission scheme in incremental decode-and-forward relaying," *EURASIP Journal on Wireless Communications and Networking*, vol. 2011, pp. 1–13, 2011.

[39] Y. wen Liang, A. Ikhlef, W. Gerstacker, and R. Schober, "Cooperative filter-and-forward beamforming for frequency-selective channels with equalization," *IEEE Transactions on Wireless Communications*, vol. 10, no. 1, pp. 228–239, 2011.

[40] A. Lozano, J. Heath, R., and J. Andrews, "Fundamental limits of cooperation," *IEEE Transactions on Information Theory*, 2013.

[41] Y. Du, H. Li, S. Wu, W. Lin, and X. Wang, "A new cooperative spectrum sensing scheme for cognitive ad-hoc networks," in *Wireless Internet*. Springer Berlin Heidelberg, 2012, vol. 98, pp. 105–116.

[42] G. K. Karagiannidis, C. Tellambura, S. Mukherjee, and A. O. Fapojuwo, "Multiuser cooperative diversity for wireless networks," *EURASIP Journal on Wireless Communications and Networking*, vol. 2006, 2006.

[43] Y. Han, S. H. Ting, and A. Pandharipande, "Cooperative spectrum sharing protocol with selective relaying system," *IEEE Transactions on Communications*, vol. 60, no. 1, pp. 62–67, 2012.

[44] W. Zhuang and M. Ismail, "Cooperation in wireless communication networks," *IEEE Wireless Communications*, vol. 19, no. 2, pp. 10–20, 2012.

[45] T. Aysal, S. Kandeepan, and R. Piesiewicz, "Cooperative spectrum sensing over imperfect channels," in *GLOBECOM*, 2008, pp. 1–5.

[46] S. Astaneh and S. Gazor, "Cooperative spectrum sensing over mixture-Nakagami channels," *IEEE Wireless Communications Letters*, vol. PP, no. 99, pp. 1 –4, 2013.

[47] T. Cui, F. Gao, and A. Nallanathan, "Optimization of cooperative spectrum sensing in cognitive radio," *IEEE Transactions on Vehicular Technology*, vol. 60, no. 4, pp. 1578 –1589, May 2011.

[48] M. Di Renzo, F. Graziosi, and F. Santucci, "Cooperative spectrum sensing in cognitive radio networks over correlated log-normal shadowing," in *Vehicular Technology Conference*, April 2009, pp. 1 –5.

[49] S. Mishra, A. Sahai, and R. Brodersen, "Cooperative sensing among cognitive radios," in *IEEE International Conference on Communications*, vol. 4, June 2006, pp. 1658 –1663.

[50] M. Koulali, A. Kobbane, M. El Koutbi, H. Tembine, and J. Ben-Othman, "Dynamic power control for energy harvesting wireless multimedia sensor networks," *EURASIP Journal on Wireless Communications and Networking*, 158 : 1-8 (2012-06).

[51] G. Xiong and S. Kishore, "Cooperative spectrum sensing with beamforming in cognitive radio networks," *IEEE Communications Letters*, vol. 15, no. 2, pp. 220 –222, February 2011.

[52] Y. Rahulamathavan, K. Cumanan, and S. Lambotharan, "A mixed SINR-balancing and SINR-target-constraints-based beamformer design technique for spectrum-sharing networks," *IEEE Transactions on Vehicular Technology*, vol. 60, no. 9, pp. 4403–4414, 2011.

[53] L. Li, K. Namuduri, and S. Fu, "Cooperative communication based on random beamforming strategy in wireless sensor networks," in *GLOBECOM*, 2012, pp. 4108–4113.

[54] Y.-C. Liang, Y. Zeng, E. Peh, and A. T. Hoang, "Sensing-throughput tradeoff for cognitive radio networks," *IEEE Transactions on Wireless Communications*, vol. 7, no. 4, pp. 1326 –1337, April 2008.

[55] Z. Quan, S. Cui, and A. Sayed, "Optimal linear cooperation for spectrum sensing in cognitive radio networks," *IEEE Journal of Selected Topics in Signal Processing*, vol. 2, no. 1, pp. 28 –40, February 2008.

[56] A. Pandharipande and J.-P. Linnartz, "Performance analysis of primary user detection in a multiple antenna cognitive radio," in *IEEE International Conference on Communications*, June 2007, pp. 6482 –6486.

[57] V. Banjade, N. Rajatheva, and C. Tellambura, "Performance analysis of energy detection with multiple correlated antenna cognitive radio in Nakagami-m fading," *IEEE Communications Letters*, vol. 16, no. 4, pp. 502 –505, April 2012.

[58] J. Tugnait, "On multiple antenna spectrum sensing under noise variance uncertainty and flat fading," *IEEE Transactions on Signal Processing*, vol. 60, no. 4, pp. 1823 –1832, April 2012.

[59] P. Wang, J. Fang, N. Han, and H. Li, "Multiantenna-assisted spectrum sensing for cognitive radio," *IEEE Transactions on Vehicular Technology*, vol. 59, no. 4, pp. 1791 –1800, May 2010.

[60] W. Zhang, R. Mallik, and K. Letaief, "Optimization of cooperative spectrum sensing with energy detection in cognitive radio networks," *IEEE Transactions on Wireless Communications*, vol. 8, no. 12, pp. 5761 –5766, December 2009.

[61] S. Chaudhari, J. Lunden, V. Koivunen, and H. Poor, "Cooperative sensing with imperfect reporting channels: Hard decisions or soft decisions?" *IEEE Transactions on Signal Processing*, vol. 60, no. 1, pp. 18–28, 2012.

[62] D.-C. Oh and Y.-H. Lee, "Cooperative spectrum sensing with imperfect feedback channel in the cognitive radio systems," *Int. J. Commun. Syst*, vol. 23, no. 763, pp. 1326 –1337, March 2010.

[63] J. W. Lee, "Cooperative spectrum sensing scheme over imperfect feedback channels," *IEEE Communications Letters*, vol. 17, no. 6, pp. 1192–1195, 2013.

[64] A. Singh, M. Bhatnagar, and R. Mallik, "Cooperative spectrum sensing in multiple antenna based cognitive radio network using an improved energy detector," *IEEE Communications Letters*, vol. 16, no. 1, pp. 64 –67, January 2012.

[65] I. F. Akyildiz, B. F. Lo, and R. Balakrishnan, "Cooperative spectrum sensing in cognitive radio networks: A survey," *Phys. Commun.*, vol. 4, no. 1, pp. 40–62, 2011.

[66] W.Feller, *An introduction to probability theory and its applications.* John Wiley & Sons, Inc, 1968.

[67] Y. Xing, R. Chandramouli, S. Mangold, and S. N, "Dynamic spectrum access in open spectrum wireless networks," *IEEE Journal on Selected Areas in Communications,*, vol. 24, no. 3, pp. 626 – 637, March 2006.

[68] X. Zhu, L. Shen, and T.-S. Yum, "Analysis of cognitive radio spectrum access with optimal channel reservation," *IEEE Communications Letters*, vol. 11, no. 4, pp. 304 –306, April 2007.

[69] P. K. Tang and Y. H. Chew, "On the modeling and performance of three opportunistic spectrum access schemes," *IEEE Transactions on Vehicular Technology*, vol. 59, no. 8, pp. 4070 –4078, October 2010.

[70] V. Tumuluru, P. Wang, D. Niyato, and W. Song, "Performance analysis of cognitive radio spectrum access with prioritized traffic," *IEEE Transactions on Vehicular Technology*, vol. 61, no. 4, pp. 1895 –1906, May 2012.

[71] I. Suliman, J. Lehtomaki, T. Braysy, and K. Umebayashi, "Analysis of cognitive radio networks with imperfect sensing," in *IEEE 20th International Symposium on Personal, Indoor and Mobile Radio Communications*, 2009, pp. 1616–1620.

[72] S. Tang and Y. Xie, "Performance analysis of unreliable sensing for an opportunistic spectrum sharing system," *International Journal of Communication Networks and Information Security*, vol. 3, December 2011.

[73] Y. Han, H. Jin, W. Tang, and S. Li, "Performance analysis of opportunistic spectrum sharing with unreliable spectrum sensing," in *IEEE International Conference on Intelligent Computing and Intelligent Systems (ICIS)*, vol. 3, October 2010, pp. 299 –304.

[74] F. Capar, I. Martoyo, T. Weiss, and F. Jondral, "Comparison of bandwidth utilization for controlled and uncontrolled channel assignment in a spectrum pooling system," in *Vehicular Technology Conference*, vol. 3, Spring 2002, pp. 1069 – 1073.

[75] G. Bolch, S. Greiner, H. d. Meer, and K. S. Trivedi, *Queueing Networks and Markov Chains*, 2nd ed. Wiley-Interscience, 2006.

[76] "IEEE draft standard for information technology -telecommunications and information exchange between systems - wireless regional area networks WRAN - specific requirements - part 22: Cognitive wireless RAN medium access control MAC and physical layer PHY specifications: Policies and procedures for operation in the TV bands," *IEEE P802.22/D2.0, February 2011*, pp. 1 –698, 2 2011.

[77] B. Wang, Z. Ji, K. Liu, and T. Clancy, "Primary-prioritized Markov approach for dynamic spectrum allocation," *IEEE Transactions on Wireless Communications*, vol. 8, no. 4, pp. 1854 –1865, April 2009.

[78] H. Su and X. Zhang, "Cross-layer based opportunistic MAC protocols for *qos* provisionings over cognitive radio wireless networks," *IEEE Journal on Selected Areas in Communications,*, vol. 26, no. 1, pp. 118–129, 2008.

[79] A. Benslimane, A. Ali, A. Kobbane, and T. Taleb, "A new opportunistic MAC layer protocol for cognitive IEEE 802.11-based wireless networks," in *International Symposium on Personal, Indoor and Mobile Radio Communications*, 2009, pp. 2181–2185.

[80] K. J. Kim, K. S. Kwak, and B. D. Choi, "Performance analysis of opportunistic spectrum access protocol for multi-channel cognitive radio networks," *Journal of Communications and Networks,*, vol. 15, no. 1, pp. 77–86, 2013.

[81] Q. Zhao, L. Tong, and A. Swami, "Decentralized cognitive MAC for dynamic spectrum access," in *First IEEE International Symposium on New Frontiers in Dynamic Spectrum Access Networks*, 2005, pp. 224–232.

[82] V. Tumuluru, P. Wang, and D. Niyato, "A novel spectrum-scheduling scheme for multichannel cognitive radio network and performance analysis," *IEEE Transactions on Vehicular Technology*, vol. 60, no. 4, pp. 1849–1858, 2011.

[83] E. W. M. Wong and C. H. Foh, "Analysis of cognitive radio spectrum access with finite user population," *IEEE Communications Letters*, vol. 13, no. 5, pp. 294–296, 2009.

[84] S. Tang and B. Mark, "Analysis of opportunistic spectrum sharing with markovian arrivals and phase-type service," *IEEE Transactions on Wireless Communications*, vol. 8, no. 6, pp. 3142–3150, 2009.

[85] S. Kannappa and M. Saquib, "Performance analysis of a cognitive network with dynamic spectrum assignment to secondary users," in *IEEE International Conference on Communications*, 2010, pp. 1–5.

[86] K. H. and M. B. L., *System Modeling and Analysis: Foundations of System Performance Evaluation*. Prentice Hall, 2008.

[87] L. Gavrilovska, V. Atanasovski, I. Macaluso, and L. A. DaSilva, "Learning and reasoning in cognitive radio networks," *IEEE Communications Surveys Tutorials*, vol. 15, no. 4, pp. 1761–1777, 2013.